

Rheological properties of minerals and rocks

Shun-ichiro Karato

Yale University

Department of Geology and Geophysics

New Haven, CT 06520, USA

to be published in “*Physics and Chemistry of the Deep Earth*”

(edited by S. Karato)

Wiley-Blackwell

SUMMARY

Plastic deformation in Earth and planetary mantle occurs either by diffusion or by dislocation creep. In both mechanisms, the rate of deformation increases strongly with temperature but decreases with pressure at modest pressures. Addition of water and grain-size reduction enhance deformation. Influence of partial melting is modest for a small amount of melt. Models on the rheological structures of Earth's mantle can be developed by including experimental results on all of these effects combined with models of temperature, water and grain-size distribution. The rheological properties in the upper mantle are controlled mostly by temperature, pressure and water content (locally by grain-size reduction). The strength of the lithosphere estimated from dry olivine rheology for homogeneous deformation is too high for plate tectonics to occur. The influence of orthopyroxene to reduce the strength is suggested. Transition from the lithosphere to the asthenosphere occurs largely by the increase in temperature but partly by the change in the water content. Rheological properties of the transition zone and the lower mantle are controlled by phase transformations. However, a transition to high-density structures does not necessarily increase the viscosity. The grain-size reduction caused by a phase transformation has a stronger effect and weakens the material substantially. The deep mantles of the Moon and Mars are inferred to have low viscosities due presumably to the high water content. Super-Earths' deep mantle may have low viscosities caused by the extremely high pressure (to ~ 1 TPa) that may enhance deformation by the transformation to a compact crystal structure, or the transition in diffusion mechanism from vacancy to interstitial mechanism, and metallization.

INTRODUCTION

Rheological properties and the dynamics and evolution of terrestrial planets

Terrestrial planets are formed hot and they release their energy by mantle convection. Forces associated with mantle convection deform planetary surface and its interior, and convection moves materials to different thermodynamic conditions leading to phase transformations including melting. Consequently, mantle convection is the single most important process on terrestrial planets that dictates their surface tectonics, deep mantle and core dynamics as well as their thermal evolution (e.g., (Schubert *et al.*, 2001)).

Mantle convection is possible because minerals and rocks behave like a viscous fluid at the geological time scale under the mantle conditions but the rheological properties of minerals and rocks change dramatically with a number of parameters including stress (strain-rate), temperature, pressure, water content and grain-size. Consequently rheological properties of planetary materials are the key to the understanding of dynamics and evolution of terrestrial planets.

However, studies of rheological properties are far more complicated than those of other properties such as elastic properties (see Chapters by Murakami, Tsuhciya and Kawai) and electrical conductivity (see a Chapter by Karato and Wang), and consequently there have been only limited constraints on rheological properties including effective viscosities and on deformation microstructures from laboratory or theoretical studies. In these studies, one needs a large extrapolation of laboratory data or of theoretical calculations to infer rheological properties in Earth and planetary interiors. In

order to make appropriate applications (extrapolation) of these data, it is essential to understand the basic physics of plastic deformation. An extensive review on these subjects was presented by (Karato, 2008). In this chapter, I will provide a brief review of the fundamentals of plastic deformation with the emphasis on the recent developments.

Differences between rheological properties and other physical properties

Various physical properties are important in the geophysical studies of Earth and planetary interiors, but the nature of these properties are different that makes important differences in the way materials science studies on these properties should be made in the geophysical context. To highlight some challenges in the studies of rheological properties, let me compare rheological properties with elastic properties and electrical conductivity.

Both elastic and rheological properties are among the various mechanical properties representing the response of a material to applied stress. Elastic deformation occurs when a small stress is applied to a material for a short period (or at high frequencies). In these cases, atoms in a material move their positions only slightly from their stable positions. The new positions of atoms are unstable and when the stress is removed, they go back to the original stable positions immediately. Consequently, elastic deformation is instantaneous (independent of the time scale) and recoverable. The relation between stress and strain is linear in most of elastic deformation. Therefore once the proportional coefficient (elastic constant) is measured or calculated the elasticity is fully characterized. Applications to seismological observations is straightforward with a minor correction for the influence of anelasticity (Karato, 1993).

Atomic processes involved in plastic deformation are different. Plastic deformation occurs by the large atomic displacements over the next stable positions often helped by thermal activation in a stochastic manner. Consequently, plastic deformation is in most cases time-dependent and non-recoverable. This poses important challenges for the study of rheological properties in the geological context. First, time scales (strain-rates) of laboratory experiments are always much shorter (faster strain-rates) than those in Earth. Therefore a large extrapolation is needed to apply laboratory results using a constitutive relationship (a relationship between applied stress and strain-rate). Second, because the constitutive relationship is different among different mechanisms of deformation, the applicability of a constitutive relationship (either determined by lab experiments or calculated by theory) to deformation in Earth's interior needs to be examined. Consequently, one needs to make sure that the mechanism of deformation studied in the lab or by a theoretical study is the same as the mechanism that may operate in Earth and planetary interiors.

Electrical conductivity involves large-scale transport of charged species and has some similarities to plastic deformation. Both plastic deformation and electrical conductivity in minerals occurs via thermally activated motion of atoms or electrons involving crystalline defects (see a Chapter by Karato and Wang). Therefore both of these properties in minerals are sensitive to temperature and in many cases sensitive to impurities such as hydrogen. However, electrical conduction follows a linear relationship and consequently, once conductivity is measured, there are no scaling problems in terms of time scale (or voltage). In plastic properties, the relationship between stress and strain-rate is not always linear. When the constitutive relation is non-linear, then rather than the

proportional coefficient one needs to determine the functional relationship between stress and strain-rate. There is no single-valued viscosity but effective viscosity (defined as a ratio of stress to strain-rate) that depends on the strain-rate (or stress). For instance, if the relationship between stress and strain-rate follows the power-law behavior, viz.,

$$\dot{\epsilon}(T, P, L, C_W) = A(T, P, L, C_W) \cdot \sigma^n \quad (1)$$

where $\dot{\epsilon}$ is strain-rate, T is temperature, P is pressure, L is grain-size, C_W is water content and n is a non-dimensional parameter, then one needs to determine both A and n as a function of various parameters (temperature, pressure, water content, stress, grain-size etc.). And the dependence of these parameters (A and n) on physical/chemical conditions is different among different deformation mechanisms. In the following, rheological properties will be described by the strain-rate at a given stress, or by the effective viscosity ($\eta_{eff} = \frac{\sigma}{\dot{\epsilon}}$), or by the creep strength (i.e., stress needed to deform a material at a given strain-rate).

Similarly, although there is not much transient phenomenon in electrical conductivity (except for the apparent frequency dependence caused by sample-electrode interaction, see a Chapter by Karato and Wang), transient deformation is often important in plastic deformation because the establishment of steady-state driving force and defect concentration requires finite time or strain. Processes that control stress distribution and defect concentrations (densities) need to be understood to formulate the flow laws in plastic deformation.

Fig. 1 illustrates the sensitivity of rheological properties to these variables in a schematic manner. If experimental studies are conducted in a regime where the flow law is different from the one appropriate for deformation in Earth's interior then the experimental results cannot be extrapolated. Identifying the similarity in the mechanisms requires extensive and multifaceted studies, and careful considerations of strategy are needed to make progress in this area.

MECHANISMS OF PLASTIC DEFORMATION AND FLOW LAWS

Fig. 2 illustrates two processes of plastic deformation. In both of them, defects play an important role. These defects include point defects, dislocations and grain boundaries. Plastic deformation in minerals at an appreciable rate is possible only when these defects are present.

Among these defects, point defects are present in any materials at thermochemical equilibrium although point defect concentration is locally modified by the stress. In contrast, both dislocations and grain-boundaries are present as non-equilibrium defects, and their abundance (dislocation density, grain-size) is controlled by the thermo-mechanical history of the material. In most cases, however, it is a good approximation to assume steady-state dislocation density and in these cases, dislocation density can be treated as a parameter that is determined by the magnitude of applied differential stress (e.g., (Poirier, 1985)),

$$\rho \approx b^{-2} \left(\frac{\sigma}{\mu} \right)^2 \quad (2)$$

where ρ is dislocation density (the total length of dislocation per unit volume), b is the length of the Burgers vector (unit displacement associated with a dislocation), σ is the differential stress and μ is the shear modulus.

In contrast, steady-state grain-size can be attained only after long term annealing or after large strain deformation. Transient behavior plays an important role both in dislocation and diffusion creep.

Diffusion creep

Theory and experimental observations are both well established for diffusion creep. Grain-boundaries are weaker than the bulk of the grains, and therefore grain-boundary sliding occurs when deviatoric stress is applied to a polycrystal. Grain-boundary sliding results on the gradient in normal stress among grain-boundaries with different orientations. Gradient in the normal stress establishes the concentration gradient in point defects that requires grain-boundary reactions. This concentration gradient drives diffusion flux. Consequently, the slower of these processes controls the rate of deformation. In most cases, diffusion is the slower process that controls the rate of deformation (Nabarro, 1948, Herring, 1950, Raj and Ashby, 1971). In some cases, reaction at grain-boundaries controls the rate of deformation. This is a case where diffusion occurs through grain-boundary fluids, a case called pressure-solution creep (Spiers *et al.*, 2004).

Diffusion of atoms occurs both inside the grains and along the grain-boundaries. Because the driving force for diffusion creep is the grain-scale heterogeneity in the

normal stress at grain-boundaries, the driving force for diffusional flux is inversely proportional to grain-size. The strain caused by diffusional mass flux is also inversely proportional to grain-size. Therefore the flow law for diffusion creep is written as

$$\dot{\epsilon}_{diff} = A'_{diff} \left(D_V + \frac{3\delta}{L} D_B \right) \frac{\sigma \Omega}{L^2 RT} \quad (3)$$

where A'_{diff} is a non-dimensional parameter, D_V is diffusion coefficient in the grain (volume diffusion coefficient), D_B is diffusion coefficient along grain-boundaries, L is grain-size, δ is the thickness of grain-boundary ($\sim b$), Ω is the molar volume ($\sim b^3$). In this case, the strain-rate is linearly proportional to stress, and the viscosity ($\eta = \frac{\sigma}{\dot{\epsilon}}$) is independent of stress or strain-rate, but depends on grain-size and temperature (and pressure). When grain-size reduction occurs, then viscosity will be reduced. Diffusion coefficients depend on temperature and pressure as $D = D_o \exp\left(-\frac{E_D^* + PV_D^*}{RT}\right)$ (E_D^* : activation energy for diffusion, V_D^* : activation volume for diffusion) and therefore the strain-rate corresponding to diffusion creep depends on temperature, pressure, grain-size and stress as

$$\dot{\epsilon}_{diff} = A_{diff} \cdot \left(\frac{L}{b}\right)^{-2} \cdot \exp\left(-\frac{E_{VD}^* + PV_{VD}^*}{RT}\right) \cdot \frac{\sigma}{\mu} \quad \text{for volume diffusion} \quad (4a)$$

$$\dot{\epsilon}_{diff} = A_{diff} \cdot \frac{3\delta}{b} \cdot \left(\frac{L}{b}\right)^{-3} \cdot \exp\left(-\frac{E_{BD}^* + PV_{BD}^*}{RT}\right) \cdot \frac{\sigma}{\mu} \quad \text{for boundary diffusion} \quad (4b)$$

with $A_{diff} = A'_{diff} \cdot \frac{D_o \mu \Omega}{RTb^2}$ is a constant with a dimension of s^{-1} , $E_{VD(BD)}^*$, $V_{VD(BD)}^*$ are the activation energy and volume for volume or grain-boundary diffusion.

In a compound, the diffusion coefficient in equation (3) or (4) must be a combination of diffusion coefficients of various species. For olivine, there are at least three species (Mg (Fe), Si and O) to consider. Usually diffusion of Si is the slowest and diffusion coefficient of Si is used to calculate creep rate by diffusion from diffusion coefficients (e.g., (Shimojuku *et al.*, 2004, Yamazaki *et al.*, 2000)). However this assumption may not be valid in some cases. First, in many oxides, slow diffusion species in the bulk tends to have high diffusion coefficients along grain-boundaries but the diffusion of fast diffusion species (in the bulk) is not much enhanced along grain-boundaries (Gordon, 1973). In these cases, the net diffusion coefficient of a species that has the faster bulk diffusion can become slower than the diffusion of other species. In these cases, a species that has a fast volume diffusion coefficient could become the rate-limiting step. Second, in (Mg,Fe)SiO₃ perovskite, (Holzapfel *et al.*, 2005) showed that Mg (Fe) diffusion is the slowest in the bulk ((Xu *et al.*, 2011) showed that diffusion coefficients of Si and Mg are similar in perovskite).

A subtle but an important point in diffusion creep is that the rate of deformation depends on the gradient in point defect concentration that depends on the stress state at grain-boundaries. The stress state at grain-boundary is in turn controlled by deformation because deformation relaxes stress concentration. This point was elegantly studied by (Raj and Ashby, 1971). Upon the application of stress to a specimen, stress concentration will occur at grain corners (weak grain-boundaries are assumed). High stress concentration enhances diffusional flow, and reduces the stress concentration.

Consequently, stress distribution will be modified, and at steady-state, smooth distribution of stress is achieved. A faster strain-rate is observed in the initial transient period (see also (Lifshitz and Shikin, 1965)). Such a transient creep behavior is potentially important in the analysis of post-glacial rebound (Karato, 1998a) and in anelastic energy dissipation (see a Chapter by Takei). In calculating strain-rate for diffusion creep, heterogeneous stress distribution and resultant diffusional mass flux must be solved self-consistently to obtain correct steady-state strain-rate.

Dislocation creep

Plastic deformation occurs also by a collective motion of atoms such as the migration of crystal dislocations. A dislocation is defined as a propagation front line of a slip that is characterized by the slip plane and slip direction. A combination of a slip plane and slip direction defines a slip system. The flow law by dislocation creep can be described by the Orowan equation (e.g., (Poirier, 1985, Karato, 2008, Orowan, 1940)),

$$\dot{\epsilon}_{dist} = b\rho v \quad (5)$$

where b is the length of the Burgers vector (the unit displacement associated with a dislocation), ρ is the dislocation density (the total length of dislocations per unit volume) and v is the dislocation velocity. Using equation (2), this equation leads to,

$$\dot{\epsilon}_{dist}(\sigma, T, P; X) \approx b^{-1} \left(\frac{\sigma}{\mu} \right)^2 \cdot v(\sigma, T, P; X) \quad (6)$$

where X is a set of parameters representing chemical environment such as water fugacity and oxygen fugacity. In general the dislocation velocity increases with applied stress and therefore, the rate of deformation by dislocation creep is a non-linear function of stress. If one defines effective viscosity by $\eta_{eff} = \frac{\sigma}{\dot{\epsilon}}$, then the effective viscosity is not a constant but it decreases with stress or strain-rate.

At high temperatures (relative to the melting temperature (T_m), i.e., $T/T_m > 0.5$), dislocation motion is thermally activated, and at low stresses, the dislocation velocity is a linear function of stress. In these cases, the dislocation velocity can be written as

$$v = Bb\sigma = b \cdot B_o \cdot \exp\left(-\frac{E_{disl}^* + PV_{disl}^*}{RT}\right) \cdot \sigma \quad (7)$$

where B is the mobility (B_o is a constant) and E_{disl}^* is the activation energy and V_{disl}^* is the activation volume for dislocation motion and equation (6) becomes,

$$\dot{\epsilon}_{disl} \approx B_o \cdot \mu \cdot \left(\frac{\sigma}{\mu}\right)^3 \cdot \exp\left(-\frac{E_{disl}^* + PV_{disl}^*}{RT}\right). \quad (8)$$

Such a power-law dependence, i.e., $\dot{\epsilon} \propto \sigma^n$ ($n=3$), is often seen in laboratory studies at modest stress levels, $\frac{\sigma}{\mu} < 10^{-3}$ (e.g., (Weertman, 1975, Karato, 2008)), but more generally

$$\dot{\epsilon}_{pl} = A_{pl} \cdot \exp\left(-\frac{E_{pl}^* + PV_{pl}^*}{RT}\right) \cdot \left(\frac{\sigma}{\mu}\right)^n \quad (9)$$

with $A_{pl} = B_o \mu$ and $n=3-5$ (the suffix *pl* means “power-law”) (Weertman, 1975, Weertman, 1999, Karato, 2008, Poirier, 1985).

For simple materials such as metals, the activation energy and volume (E_{pl}^*, V_{pl}^*) agree with those of diffusion (E_D^*, V_D^*) and this is interpreted by a model where the rate of high-temperature creep is controlled by diffusion-controlled dislocation climb (Weertman, 1968, Weertman, 1975, Weertman, 1999, Karato, 2008, Kohlstedt, 2006) (see **Fig. 3a**). However, in oxides and silicates the activation energy and volume often include some extra-term caused by the high energy of dislocations in these crystals (Karato, 2008)¹. The extra-term in dislocation climb is the concentration of jogs (steps on a dislocation line that help dislocation climb, see two steps on a dislocation line in **Fig. 3a**) (e.g., (Poirier, 1985, Karato, 2008)). In oxides or silicates, chemical bonding is strong and the unit cell tends to be large. Consequently, the dislocation energy is large and hence the formation of these steps (jogs in case of dislocation climb) is difficult. In these cases, the formation of these steps requires thermal activation. Therefore, equation (9) is modified to

$$\dot{\epsilon}_{pl} = A'_{pl} \cdot \exp\left(-\frac{(E_D^* + E_j^*) + P(V_D^* + V_j^*)}{RT}\right) \cdot \left(\frac{\sigma}{\mu}\right)^n \quad (10)$$

¹ Kohlstedt (2006) argued that dislocation creep in olivine is directly controlled by diffusion-controlled dislocation climb similar to deformation of metals. However, this model is inconsistent with the presence of large plastic anisotropy in olivine as discussed by (Karato, 2010a).

where E_j^* and V_j^* are the formation energy and volume of a jog respectively. Formation of a step such as a jog requires the distortion of a dislocation line and consequently, the formation energy and the density of these steps are anisotropic, providing a source for large plastic anisotropy.

At high stresses, the activation enthalpy may become stress dependent. This is the case when the rate-controlling process is thermally activated motion of dislocation glide over the Peierls potential (potential energy of a dislocation in a crystal). Dislocation motion over the Peierls potential involves the formation of a kink pair and their migration. **Fig. 3b** shows a saddle point configuration of formation of a pair of kinks where $\Delta A(\sigma)$ is an area swept by a dislocation. Because the force exerted by the external stress on the unit length of a dislocation is σb (e.g., (Poirier, 1985)), the stress does an extra work, $-\Delta A(\sigma) \cdot \sigma b$. Therefore, the activation enthalpy for dislocation glide is

$$H_{glide}^* = H_o^* - \Delta A(\sigma) \cdot b \cdot \sigma \quad (11)$$

and hence activation energy depends strongly on stress. Also the activation area $\Delta A(\sigma)$ itself depends on the shape of a dislocation at the saddle point that depends on the stress, and this leads to various formulae of the activation enthalpy. The flow law for such a mechanism of dislocation motion is given by

$$\dot{\epsilon}_{glide} = A_{glide} \cdot \left(\frac{\sigma}{\mu}\right)^2 \cdot \exp\left[-\frac{H_{glide}^*}{RT} \left\{1 - \left(\frac{\sigma}{\sigma_p}\right)^q\right\}^s\right] \quad (12)$$

where A_{glide} is a constant with the dimension of s^{-1} , H_{glide}^* is the activation enthalpy for dislocation glide at zero stress, σ_P is the Peierls stress (a critical stress for dislocation glide at $T=0$ K), q and s are constants ($0 < q \leq 1$, $1 \leq s \leq 2$)² (Kocks *et al.*, 1975). This mechanism of deformation is often referred to as the Peierls mechanism. Note that this relation implies that deformation at finite strain-rate is possible even at $T=0$ K if stress approaches the Peierls stress, σ_P .

When the flow law described by equation (12) operates (high stress and/or low temperatures), the temperature dependence of creep strength comes mainly from the stress dependence of activation enthalpy and

$$\frac{\sigma}{\sigma_P} \approx \left[1 - \left(\frac{T}{T_o} \right)^{\frac{1}{s}} \right]^{\frac{1}{q}} \quad (13)$$

where T_o is a reference temperature that depends on strain-rate and activation enthalpy at zero stress. The temperature dependence of creep strength corresponding to this mechanism is weaker than that of power-law creep ($\sigma \propto \exp\left(\frac{E_{pl}^* + PV_{pl}^*}{nRT}\right)$). The Peierls stress corrected for temperature is equivalent to the concept of “yield stress” often used in geodynamic modeling (e.g., (Tackley, 1998, Richards *et al.*, 2001)).

² Strictly speaking, the rate of reverse motion of a dislocation needs to be added to equation (12) (see Karato (2008)), but this term is not important at high stresses. The reverse motion term is important when this equation is used at low stresses.

Plastic anisotropy and the relation between single crystal and polycrystal deformation

Flow laws such as those given by equations (9) (or (1)) or (12) apply to deformation by each slip system. In a given crystal, there are several slip systems and a crystal has plastic anisotropy, i.e., the resistance for deformation depends on the orientation of a crystal with respect to the applied stress. In the homogeneous deformation of a polycrystalline aggregate, each grain needs to be deformed to arbitrary geometry. This requires five independent slip systems to be present (the von Mises criterion). Consequently, the rate of deformation of a polycrystalline aggregate is, in most cases, controlled by the rate of the most difficult slip system (Kocks, 1970). This is in contrast to the case of lattice-preferred orientation where the easiest slip system makes the most important contribution.

Anisotropy in deformation for individual grains leads to plastic anisotropy of a rock if the distribution of crystallographic orientation of grains is not random. In these cases, rheological properties must be treated as anisotropic properties (effective viscosity becomes a fourth-rank tensor same as elastic constants). Influence of plastic anisotropy on geodynamic processes has been studied by (Saito and Abe, 1984, Honda, 1986, Lev and Hager, 2008), but plastic anisotropy of rocks has not been studied extensively. In case of olivine, where rheological properties have been studied extensively, a comparison on rheological properties for tri-axial compression and simple shear shows that plastic anisotropy is only modest. However, for highly anisotropic crystal such as *hcp* metals (e.g., zinc and ϵ -iron in the inner core), plastic anisotropy of an aggregate can be very

large (Frost and Ashby, 1982). This may have an important effect on the dynamics of the inner core.

(Karato, 2010a) discussed the influence of anisotropic diffusion on the strength of a polycrystalline aggregate. For diffusion creep, it is the diffusion along the slowest orientation that controls the overall rate of deformation (see also (Lifshitz, 1963)). For dislocation creep controlled by dislocation climb, which is in turn controlled by diffusion, the rate controlling diffusion coefficient is the intermediate diffusion coefficient. This is because the rate of dislocation climb is controlled by diffusion in the direction normal to the dislocation line, and the rate-controlling step of deformation of a polycrystalline aggregate is deformation by the hardest slip system³.

The role of grain-boundary sliding

Deformation of a polycrystalline material can occur by grain-boundary sliding (Langdon, 1975, Langdon, 1994). However, grain-boundary sliding creates gaps and overlaps of grains and therefore some processes must operate to remove gaps or overlaps. Processes of accommodation include diffusion creep and dislocation creep.

Grain-boundary sliding accommodated by diffusion creep is a typical example. (Raj and Ashby, 1971) presented a theoretical analysis of the interplay between grain-boundary sliding and diffusion creep. They showed that these processes must operate simultaneously and therefore a more difficult process controls the overall rate of

³ One compares $\frac{D_{11}+D_{22}}{2}$, $\frac{D_{11}+D_{33}}{2}$, $\frac{D_{22}+D_{33}}{2}$ (D_{ii} : diffusion coefficient along the i -th direction), and the smallest one controls the rate of deformation of a polycrystal.

deformation. In many cases, grain-boundary sliding is easier than diffusional mass transport and the flow law is essentially the same as the diffusion creep.

When dislocation processes are involved in the intra-granular deformation, somewhat different flow law may arise. When accommodation by dislocation creep is much more difficult than grain-boundary sliding, a flow law similar to dislocation creep will apply (e.g., (Chen and Argon, 1979)). However, there is a narrow parameter space where dislocation creep rate can be affected by the stress concentration at grain-boundaries. In these cases, a non-linear, grain-size dependent flow law will be obtained, viz.,

$$\dot{\epsilon}_{gbs} = A_{gbs} \cdot \exp\left(-\frac{E_{gbs}^* + PV_{gbs}^*}{RT}\right) \cdot \left(\frac{\sigma}{\mu}\right)^n \cdot \left(\frac{b}{L}\right)^m \quad (14)$$

where A_{gbs} is a constant with the dimension of s^{-1} , $n=2-3$ and $m=1-3$ (e.g., (Nieh *et al.*, 1997)), and E_{gbs}^* and V_{gbs}^* are the activation energy and activation volume respectively (**Table 1**). (Nieh *et al.*, 1997) listed a number of examples of such a rheological behavior in metals and ceramics. A similar rheological behavior is also reported in geological materials (Goldsby and Kohlstedt, 2001, Hiraga *et al.*, 2010, Hansen *et al.*, 2011). It is sometimes suggested that this mechanism is crucial for shear localization (Warren and Hirth, 2006, Precigout *et al.*, 2007). However, the parameter space in which this mechanism dominates is limited and its importance in geological processes is unclear. Various flow laws are summarized in **Table 1**.

Deformation of multi-phase mixtures

Generalities

Rocks are in general made of various minerals. Let us consider deformation of a two-phase mixture. For simplicity, let us assume these two phases have isotropic plastic properties but their strengths are different. How is the strength of such a mixture related to the strength of each phase? Obviously, the strength of such an aggregate is determined by the strengths of each phase and their volume fraction, but it also depends on the geometry of each phase. Predicting the average strength of a mixture is difficult because the strength of a mixture depends strongly on how stress and strain are distributed among co-existing phases. Two end-member cases can be considered, one with homogeneous stress and another with homogeneous strain. The former gives the upper limit for the actual strength, and the latter does the lower limit.

A key point is that the stress-strain distribution among co-existing phases evolves with strain and it is frequently observed that the strain partitioning changes with strain in such a way that a weaker phase will accommodate a larger fraction of strain at larger strains (e.g., (Bloomfield and Covey-Crump, 1993)). When the weaker phase is interconnected then a sudden strength drop could occur leading to shear localization. The lower mantle of Earth is a region where this type of strain localization may occur because it is made of 20-30% of a weaker phase ((Mg,Fe)O) together with a stronger phase ((Mg, Fe)SiO₃ perovskite) (e.g., (Yamazaki and Karato, 2001)).

Influence of partial melting

Partially molten material is a typical case of a two-phase mixture. When the volume fraction of a liquid phase exceeds a certain limit (~20-30%), then such an aggregate behaves like a liquid with some solid suspensions. If the volume fraction is less than this limit, an aggregate deforms like a solid but its resistance to plastic deformation is modified by the presence of a liquid phase. Various processes may affect the plastic properties of such a solid-liquid mixture including (i) chemical reaction between solid and liquid (dissolution-precipitation), (ii) fast diffusional mass transport through liquid phase, and (iii) stress concentration.

The influence of chemical reaction (dissolution-precipitation) has been studied extensively in relation to so-called “pressure-solution” creep (e.g., (Rutter, 1976, Shimizu, 1994, Spiers *et al.*, 2004)). This mechanism is essentially the same as grain-boundary diffusion creep (Coble creep), but because diffusion is fast in the liquid, the rate of deformation is often controlled by the rate of chemical reaction at the grain-liquid interface (Spiers *et al.*, 2004). The influence of processes (ii) and (iii) were analyzed by (Cooper and Kohlstedt, 1986, Kohlstedt, 2002). They showed that the presence of partial melt has only modest influence on creep rate (see a later part of this Chapter). In contrast, (Takei and Holtzman, 2009a, Takei and Holtzman, 2009b, Takei and Holtzman, 2009c) presented a more sophisticated analysis of stress states at grain-boundaries and concluded that the influence of partial melting is stronger, a factor of ~5 reduction in viscosity even at a small melt fraction, 10^{-3} % (see a Chapter by Takei). The reason for this discrepancy is not well understood. Modeling diffusion creep is complicated because the stress state and diffusional flux have strong interaction and these two must be solved self-consistently as shown by (Raj and Ashby, 1971). For dislocation creep, there is no

mechanism to enhance creep significantly at a small melt fraction. The same is true for diffusion creep controlled by volume diffusion. In some Earth science literatures, boundary diffusion controlled diffusion creep is exclusively considered (e.g., (Mei and Kohlstedt, 2000a, Hirth and Kohlstedt, 1995a, Kohlstedt, 2002)). However, interplay between volume and boundary diffusion is complicated in ionic solids and both boundary diffusion-controlled and volume diffusion-controlled creep behaviors are found in many oxides depending on the grain-size and temperature (e.g., (Cannon and Coble, 1975, Gordon, 1973, Li *et al.*, 1996))).

Deformation mechanism map

Because of the presence of multiple mechanisms of plastic deformation, it is convenient to use some diagrams to illustrate the parameter space where one mechanism dominates over others. Such a diagram is called a deformation mechanism map (Frost and Ashby, 1982). In many cases, the competing mechanisms are independent, so these diagrams simply show the mechanisms with the largest strain-rate under various conditions. Because strain-rate depends on a number of parameters (temperature (T), pressure (P), grain-size (L), stress (σ), water content (C_W)), such a diagram must in general be presented in a multi-dimensional space. However, a two-dimensional diagram is easy to use for practical purposes, and therefore in most cases, such a diagram is usually constructed on a two-dimensional space keeping other parameters fixed. An example of deformation mechanism map is shown in **Fig. 4** where I chose grain-size and stress as independent parameters for a particular set of temperature and pressure. Similar diagrams have been constructed for other minerals including plagioclase (anorthite)

(Rybacki and Dresen, 2000), (Mg,Fe)O and perovskite (Karato, 1998b) and ringwoodite (Karato *et al.*, 1998). For most of mantle minerals, the dominant deformation mechanism in the typical hot mantle is diffusion creep or power-law dislocation creep. However, in a cold subducted lithosphere, the Peierls mechanism also plays an important role (Karato *et al.*, 2001).

Shear localization

The discussions so far are all for “steady-state” deformation. This is a convenient assumption that makes the formulation of flow laws easy. However, the validity of steady-state deformation is questionable in some cases. Particularly important is deformation of the lithosphere. Under low temperature conditions, non-steady deformation likely occurs leading to strain localization that reduces the strength of the lithosphere substantially.

The essence of the conditions for shear localization is the presence of a process of positive feedback, i.e., a process wherein the increase in strain (or strain-rate) leads to the reduction in the creep strength. In these cases, regions that are deformed more become easier to deform so that the runaway instability will occur. Such a positive feedback is, however, not common. In most cases, materials show work-hardening (strain-hardening), and the resistance to deformation increases with strain-rate, leading to a negative feedback that stabilizes deformation.

However, there are several mechanisms that lead to a positive feedback. Two processes of such instability are well documented. One is the thermal runaway instability where deformation-induced heating leads to runaway instability, and another is the

instability caused by grain-size reduction. In both cases, instability will occur under limited conditions.

Consider thermal runaway instability. Deformation produces heat and therefore a region of more deformation will have a higher temperature and the increased temperature enhances deformation. If this positive feedback is more efficient than the work-hardening (strain-hardening) that will stabilize the system, then thermal runaway will occur. The magnitude of positive feedback is proportional to the rate of heat generation by mechanical work and inversely proportional to the rate of heat diffusion that is sensitive to the space scale of deformation. Consequently, this instability occurs when the rate of heating, i.e., the energy dissipation rate, exceeds a certain value (e.g., (Argon, 1973)),

$$\sigma\dot{\epsilon} > (\sigma\dot{\epsilon})_c = \frac{\pi^2 h C_p \kappa R T^2}{H^* L^2} \quad (15)$$

where $h = \frac{\partial \log \sigma}{\partial \log \epsilon}$ (~ 1) is the coefficient of work-hardening, C_p is the specific heat, κ is the thermal diffusivity, H^* is the activation enthalpy, and L is the length scale. Note that the conditions for instability depend strongly on the space scale, L . Because the energy dissipation rate per unit volume is given by $\sigma\dot{\epsilon} = \eta(T, P) \cdot \dot{\epsilon}^2$, this instability occurs when viscosity exceeds a certain value that depends on the space scale. For a typical strain-rate of $\sim 10^{-15} \text{ s}^{-1}$, and a space scale of $\sim 100 \text{ km}$, the critical viscosity is $\sim 10^{23} \text{ Pa s}$. Consequently, we conclude that this mechanism of shear localization occurs at low temperatures where viscosity is high.

Grain-size reduction could also lead to shear localization but again only at low temperatures. Let us consider the grain-size reduction caused by deformation (dynamic recrystallization). Dynamic recrystallization occurs when a material deforms by dislocation creep. Small grains are formed along the pre-existing grain-boundaries (**Fig. 5a**). The size of recrystallized grains is inversely proportional to stress, $\frac{L_r}{b} = A_r \left(\frac{\sigma}{\mu}\right)^{-a}$ (L_r : the size of recrystallized grains, A_r and a : constants) (Karato, 2008, Poirier, 1985, Derby, 1991). If the size of these grains is small enough, grain-size sensitive creep such as diffusion creep will operate there and these regions will be softer than the initial material. Then the load is transferred to coarse-grained regions (cores in **Fig 5a**) that promotes further deformation and the generation of small grains, leading to the runaway instability. The necessary condition for this localization mechanism to operate is that the size of dynamically recrystallized grain is smaller than that of a critical size for the transition between diffusion and power-law dislocation creep, and is given by

$$A_r \left(\frac{A_{pl}}{A_{diff}}\right)^{\frac{1}{m}} < \left(\frac{\sigma}{\mu}\right)^{a-\frac{n-1}{m}} \exp\left(\frac{H_{pl}^* - H_D^*}{mRT}\right). \quad (16)$$

Because $a - \frac{n-1}{m} > 0$ and $H_{pl}^* - H_D^* > 0$ for most materials, this condition means that shear localization likely occurs at high stresses and low temperatures.

This is the necessary condition for shear localization. In order for substantial deformation to occur by this mechanism, the growth rate of newly formed grains must be small enough. Low temperature favors slow growth rate, but for pure material such as pure olivine aggregates, growth rate is still so fast (Karato, 1989b) that substantial shear

localization does not occur. The presence of a secondary phase that retards grain-growth rate is needed to achieve substantial shear localization (Karato, 2008). I will come back to this issue later in this Chapter when I discuss the deformation of the lithosphere.

Localized deformation due to stress-induced melt migration was studied by (Holtzman *et al.*, 2003a, Holtzman *et al.*, 2003b). Such a process is likely important near mid-ocean ridges where extensive partial melting occurs. However, importance of these processes in the asthenosphere far from ridges is unclear.

EXPERIMENTAL METHODS IN DEFORMATION STUDIES

Because plastic deformation involves a number of processes as discussed above and also because defects involved in plastic deformation have low symmetry, theoretical modeling is difficult and it is essential to obtain experimental results. Even in the case of diffusion creep where theory is well established, the interplay of grain-boundary and bulk diffusion of various diffusing species makes the application of diffusion data complicated (e.g., (Gordon, 1973, Gordon, 1985)). In fact, there have been no theoretical studies on the creep strength of any geological materials that predicted the plastic properties including the creep strength and the dominant slip systems correctly. Consequently, experimental studies play the most important role in our understanding of the rheological properties of Earth and planetary interiors.

Plastic properties depend on a number of parameters and many of which change plastic properties (e.g., strain-rate for a given stress) by several orders of magnitude. Therefore a careful control and characterization of chemical environment and

microstructures, and a choice of appropriate method of experiments (or the development of new methods when needed) are critical in the study of plastic properties. Important factors that need to be characterized or controlled include the water content (water fugacity) and the grain-size. The importance of controlling or characterizing water content must be emphasized because the water effects are large and water may be lost or added to the sample during an experiment. Water content of a sample must be measured both before and after each experiment. Similarly grain-size must be measured both before and after each experiment when a polycrystalline sample is used. Although effects are relatively small, oxygen fugacity and oxide activity must also be controlled.

The choice of an apparatus must be made based on the proper understanding of theory of plastic deformation and of thermodynamic properties of materials under high-pressure and temperature conditions. If a necessary apparatus does not exist, then one should design a new one to achieve the scientific goal⁴. Key aspects in choosing or developing deformation apparatus or methods are (i) the range of pressure and temperature in which the machine can be operated and (ii) the resolution of mechanical measurements. A common trade-off is that a high-resolution testing machine such as a gas-medium deformation apparatus has a limited pressure range of operation ($P < 0.5$ GPa), whereas apparatus that can be operated to higher pressures tend to have lower resolution in mechanical measurements.

⁴ Unfortunately, the value of developing new techniques is often not appreciated in the community (my first proposal to develop a rotational Drickamer apparatus (RDA) was declined). However, it should be emphasized that without developing new techniques, one cannot conduct truly pioneering experimental studies.

Let us consider a case of high-resolution, low-pressure deformation apparatus versus high-pressure, low-resolution deformation apparatus. In the late-1960s to early 1970s, a large number of pioneering experimental studies were conducted at UCLA using a solid-medium deformation apparatus designed by David Griggs (Griggs, 1967). Most of the basic concepts on the rheological properties of rocks such as (i) non-linear constitutive relationship, (ii) water weakening, (iii) development of lattice-preferred orientation (and its implications for seismic anisotropy) and (iv) dynamic recrystallization (and its possible implications for shear localization) were established by their classic studies (for a summary of these studies see (Heard *et al.*, 1972)). With this apparatus, one can conduct deformation experiments to $P \sim 2$ GPa (T to ~ 1600 K), but the uncertainties in stress measurements are large due to the large influence of friction (errors in stress measurements sometimes exceed 100 % (Gleason and Tullis, 1993)).

In 1960s to 1980s, Mervyn Paterson at the Australia National University developed a gas-medium deformation apparatus (Paterson, 1970, Chopra and Paterson, 1981, Paterson, 1990) with which high-resolution mechanical tests can be made to $P \sim 0.3$ GPa and $T \sim 1600$ K (stress resolution ~ 1 MPa). A key element in this apparatus is the use of an internal load cell for load (stress) measurements. Because the load cell is located in the pressure vessel, there is no need for the correction for friction and the load (stress) measurements can be made as precisely as at room pressure. This apparatus was used extensively in the Paterson's lab at ANU (e.g., (Chopra and Paterson, 1981, Chopra and Paterson, 1984, Karato *et al.*, 1986, Mackwell *et al.*, 1985)). In particular, (Karato *et al.*, 1986) introduced a new method of deformation experiments where high-resolution mechanical tests are conducted on synthetic samples with controlled grain-size and water

content. Also (Zhang and Karato, 1995) developed a shear deformation technique using the high-resolution gas-medium apparatus. Similarly (Paterson and Olgaard, 2000) developed a torsion apparatus that can be operated to ~ 0.3 GPa. Subsequently, these methods were used extensively in a few groups (e.g., (Mei and Kohlstedt, 2000a, Mei and Kohlstedt, 2000b, Hirth and Kohlstedt, 1995a, Hirth and Kohlstedt, 1995b, Holtzman *et al.*, 2003b, Rybacki and Dresen, 2004, Rybacki *et al.*, 2006, Bystricky *et al.*, 2001)). The applications of these low-pressure, high-resolution apparatus under carefully controlled chemical environment were critical in establishing the rigorous bases of mineral and rock deformation studies (for an excellent review on the low-pressure studies see (Kohlstedt, 2009)).

However, the maximum pressure of experimentation with this apparatus is low, $P < 0.5$ GPa (corresponding to a depth of ~ 15 km) (most experiments were conducted at $P \leq 0.3$ GPa). This pressure range is small compared to the actual pressures in Earth's mantle (~ 2 - 10 GPa in the asthenosphere, ~ 13 GPa at 410-km, ~ 24 GPa at 660-km). Therefore applications of low-pressure data need a large extrapolation in pressure. For such an extrapolation, pressure dependence of creep strength needs to be known precisely. However, it is difficult to determine the pressure dependence of deformation from low-pressure experiments. In addition, many minerals are stable only under high-pressure conditions (e.g., orthopyroxene ($13 \text{ GPa} > P > 1 \text{ GPa}$), wadsleyite ($17 \text{ GPa} > P > 14 \text{ GPa}$), perovskite ($120 \text{ GPa} > P > 24 \text{ GPa}$)). Rheological properties of these minerals cannot be studied using these low-pressure apparatus. Furthermore, the functional form of pressure dependence of deformation likely changes at around $P \sim 0.5$ GPa when water is present in the system (Karato, 2008). This means that the results on the influence of water

obtained below $P \sim 0.5$ GPa cannot be extrapolated to higher pressures even qualitatively (see the later section on the water effect). Consequently, results from low-pressure (< 0.5 GPa) experiments have limited applicability to the regions deeper than ~ 20 km (in Earth). Consequently, the rheological properties of more than 99% of the mantle cannot be investigated by these low-pressure studies.

Recognizing these limitations, a group of scientists initiated a coordinated effort to develop new techniques of quantitative studies of plastic properties at high pressures exceeding ~ 10 GPa (Karato and Weidner, 2008). These new developments include the design of new types of deformation apparatus (**Fig. 6c, d**) and the use of synchrotron X-ray facilities to measure the stress and strain *in-situ* (e.g., (Weidner, 1998, Karato and Weidner, 2008)). In these new methods, stress is not measured by a load cell as has been the case of low-pressure apparatuses but by X-ray diffraction.

Theories of stress measurements using X-ray diffraction were developed by (Singh, 1993, Karato, 2009). (Singh, 1993) considered only elastic deformation, and in this theory, the anisotropy in lattice strain (strain in crystalline lattice) is caused by the anisotropy in the elastic constants. But this theory does not explain observed highly anisotropic lattice strain in plastically deformed materials (e.g., (Weidner *et al.*, 2004, Chen *et al.*, 2006a)). (Karato, 2009) developed a new theory in which the influence of plastic deformation to re-distribute stress among grains is included for non-linear constitutive relationship. In this theory, anisotropy in lattice strain is caused both by elastic and plastic anisotropy. Plastic anisotropy is usually much larger than elastic anisotropy and this theory explains the observed large anisotropy in lattice strain. When

elastic anisotropy is known, this theory provides a way to infer plastic anisotropy from observed anisotropy in lattice strain.

At the time of this writing (February 2012), quantitative deformation experiments have been conducted to $P \sim 23$ GPa and $T \sim 2200$ K using the rotational Drickamer apparatus (RDA) with the resolution of stress measurements of ~ 10 MPa (Hustoft *et al.*, 2011, Weidner *et al.*, 2010). The resolution of stress measurements is not as good as that in the gas-medium, low-pressure apparatus, but this resolution is high enough to characterize rheological properties in most cases (the resolution of stress is ~ 10 MPa).

Deformation experiments at much higher pressures were conducted using a diamond anvil cell (DAC) (e.g., (Meade and Jeanloz, 1988, Sung *et al.*, 1977, Kinsland and Bassett, 1977, Wenk *et al.*, 2004, Merkel *et al.*, 2006, Merkel *et al.*, 2007, Miyagi *et al.*, 2011)). However, in most studies with DAC, temperature was low (some are at room temperature) and in all cases, strain rates are unknown. Consequently, the applicability of these results to deformation in hot Earth's interior is highly questionable.

It must be remembered that simply conducting some poorly characterized deformation experiments under high-pressures does not help our understanding of rheological properties of the deep interior of Earth. Many issues learned by low-pressure experiments (e.g., control or characterization of water content and grain-size, identification of deformation mechanisms) need to be carefully examined in order to obtain results that can be applied to Earth's deep interior. The lack of such an analysis is the main source of confusions as shown by (Karato, 2010b) for olivine. A combination of careful experimentation with technical developments toward high-pressure studies is essential to make further progress in this area.

Fig. 7 shows a range of pressure and temperature conditions in which deformation experiments were performed using various apparatus.

BASIC EXPERIMENTAL OBSERVATIONS

Influence of temperature, stress and grain-size

Fig. 8 illustrates some of the experimental data on plastic deformation of some minerals showing the evidence of various deformation mechanisms discussed above. Transition from diffusion to dislocation creep as stress increases (or grain-size increases) is well documented (**Fig. 8b**), and non-linear flow law is also well established at relatively high stresses. Most experimental results show strongly temperature-dependent rheology. However, there are limited data that indicate the operation of highly non-linear, relatively temperature insensitive deformation mechanism such as the Peierls mechanism (**Fig. 8d**) at low temperatures and high stresses.

The results summarized in **Fig. 8** are obtained at low pressures ($P < 0.3$ GPa) at which high-resolution mechanical measurements are possible. Therefore as far as the dependence of plastic deformation on temperature, stress and grain-size (and oxygen fugacity) are concerned, these are well-established solid data sets. However, the applicability of these data to Earth's interior is limited to the depth of ~ 15 km. But most of plastic deformation in Earth occurs below 20 km. In the past, these low-pressure results were often extrapolated to high pressures using poorly constrained parameters such as the activation volume (e.g., (Karato and Wu, 1993, Hirth and Kohlstedt, 1996, Hirth and Kohlstedt, 2003)). A recent review by (Karato, 2010b) showed that the

uncertainties in activation volume were so large (see **Fig. 10** below) that conclusions in these previous papers have weak basis.

To make further advance in our understanding of dynamics of Earth's deep interior, the influence of pressure and water on rheological properties needs to be well-characterized by high-pressure experimentation. In addition, most minerals undergo a series of phase transformations. The influence of phase transformation must also be evaluated. These are important issues (some of these factors can change the effective viscosity by several orders of magnitude), but due mainly to the technical difficulties, there is not much consensus as to the influence of these factors.

In the following, I will review some of the important observations and their interpretations related to these issues, which is the frontier in the study of rheological properties of Earth materials.

Effect of pressure

Pressure can have a large effect on rheological properties. This is seen from the relationship (9): a positive activation volume reduces strain-rate exponentially with pressure. The importance of activation volume is shown in **Fig. 9**. The values of activation volume for typical oxides or minerals range from ~ 3 to ~ 20 cm³/mol, and this range of V^* makes a large difference in the estimated depth variation in viscosity.

However, the precise determination of pressure effects on rheological properties is challenging. To appreciate this, take a look at **Fig. 10** which shows that there was nearly 10 orders of magnitude difference in the viscosity in the deep upper mantle calculated from the results of different experimental studies (**Fig. 10**). Challenges here

include (i) the precise measurements of pressure effects and (ii) the correction for other effects such as water content and grain-size. As can be seen from relation (9), the influence of pressure on viscosity (or creep strength) is exponential, so the pressure effect is small at low pressures but increases exponential with pressure. Therefore although a low-pressure apparatus such as the Paterson apparatus has high resolution in stress (and strain-rate) measurements, pressure effect can be estimated better from high-pressure measurements even though these methods have lower resolution in stress measurements. For instance, if the activation volume is $10 \text{ cm}^3/\text{mol}$, then if one changes the pressure by 0.3 GPa, one will see the change in strain-rate by $\sim 25 \%$ (at 1600 K) (if strain-rate is fixed then a change in stress is $\sim 7 \%$). To determine the activation volume with 10% error, it will be necessary to measure the difference in strain-rate by $\sim 2-3 \%$ error (or stress by $\sim 0.7 \%$ error). Measuring the change in strain-rate (or stress) with this resolution is difficult particularly when grain-size affects the strength. In contrast, if pressure difference of 10 GPa is used, then the change in strain-rate will be a factor of ~ 1800 (a factor of ~ 9 change in stress)). Even with less precise mechanical measurements under high-pressure environment, changes in properties by high-pressure are so large that much more precise determination of pressure effects can be made if one uses a high-pressure deformation apparatus.

Also critical is the influence of water. In many previous studies, substantial amounts of water were dissolved in the samples particularly at high pressures, but water contents were not well characterized. Because the water reduces the effective viscosity (the creep strength) dramatically, dissolved water can lead to misleading interpretation of the results. For more details on these issues, see (Karato, 2010b).

Using a newly developed deformation apparatus, RDA (rotational Drickamer apparatus) at the synchrotron X-ray facility, (Kawazoe *et al.*, 2009) performed deformation experiments on olivine aggregates to ~10 GPa (to ~1900 K) for nearly water-free (dry) samples. The water content and microstructures (grain-size, dislocation structures) were carefully examined and the evidence for power-law creep involving dislocation recovery was found at high temperatures. Samples show low water contents (below the detection limit) and the data represent the creep strength of dry olivine. The data from (Kawazoe *et al.*, 2009) corresponding to the power-law creep regime are summarized in **Fig. 11**. These data were obtained under the conditions down to the depth of ~300 km in the mantle, so there is no need for large extrapolation in terms of pressure to estimate the creep strength in the deep upper mantle. Extrapolation in strain-rate is still needed but the uncertainties in this extrapolation are small because the stress exponent is well constrained ($n=3-4$). When the relationship (9) is used, we obtain $V^*=15-20$ cm³/mol.

Diffusion coefficients are easier to measure at high pressures than creep strength. Consequently, a relatively large number of data are available on diffusion coefficients measured at high pressures than those on creep strength. For instance, the diffusion coefficient of silicon (and oxygen) in MgSiO₃ perovskite (Yamazaki *et al.*, 2000) and the diffusion coefficient of magnesium and oxygen in MgO (Van Orman *et al.*, 2003) were measured at lower mantle pressures. Similarly, (Shimojuku *et al.*, 2004, Shimojuku *et al.*, 2009) measured the silicon and oxygen diffusion coefficient in wadsleyite and applied these results to high-temperature creep in wadsleyite.

In the relation (9), the activation volume V^* is assumed to be independent of pressure. This is a good approximation at low pressures ($P / K_0 < 0.1$, K_0 : zero-pressure bulk modulus ($K_0 = 120$ GPa for olivine)). However at pressures comparable to or larger than K_0 , such a linear approximation (i.e., $H^* = E^* + PV^*$ with a constant V^*) is no longer valid, and generally V^* decreases with pressure (Poirier and Liebermann, 1984, Karato, 2011a). Because of this non-linear effect, the effective viscosity at very high-pressures will not be as high as one would expect from the relation (9) with a constant V^* . Possible implications of this effect will be discussed later in relation to the rheological properties of the deep interiors of planets such as super-Earths.

Effect of water

David Griggs and his coworkers discovered that the creep strength of silicates such as quartz and olivine decreases strongly with water content (Griggs, 1967, Blacic, 1972). This early notion was confirmed by the later studies using improved experimental techniques (Kronenberg and Tullis, 1984, Post *et al.*, 1996, Chopra and Paterson, 1984, Karato *et al.*, 1986, Mei and Kohlstedt, 2000a, Karato and Jung, 2003). These studies also showed that a finite amount of hydrogen is dissolved in these minerals and that the degree to which materials weaken depends on the amount of dissolved hydrogen. **Fig. 12** shows some examples of experimental observations on water weakening effects.

The precise atomistic mechanisms by which dissolved hydrogen may weaken minerals are not well understood. Based on the theoretical models described in the previous section, one can imagine a few possibilities. (1) Dissolved water may enhance diffusion that in turn enhances diffusion-controlled creep (diffusion creep, dislocation

creep controlled by dislocation climb). (2) Dissolved water may increase the concentration of jogs along the dislocation that enhances dislocation climb and hence deformation. (3) Dissolved water may increase the concentration of kinks (see **Fig. 3b**) and hence enhances dislocation glide.

Using olivine for which the most detailed studies have been performed, I will review some observations. (Costa and Chakraborty, 2008) reported that the addition of water (hydrogen) to olivine enhances diffusion of silicon and oxygen ((Hier-Majumder *et al.*, 2005) reported the enhanced Mg-Fe diffusion by hydrogen). The magnitude of enhancement is roughly same as the amount of enhancement in strain-rate. Therefore, enhancement of diffusion is clearly a cause of weakening (e.g., (Kohlstedt, 2006)). However, the enhancement of diffusion alone cannot explain the marked anisotropy of water weakening effects reported by (Mackwell *et al.*, 1985) because the diffusion coefficient under water-rich conditions is nearly isotropic (Costa and Chakraborty, 2008). (Katayama and Karato, 2008b) reported that plastic deformation of olivine in the Peierls mechanism is enhanced by water and concluded that the Peierls stress is reduced by the addition of water.

Based on these observations, I conclude that the enhanced deformation in olivine is due at least to two factors: (i) enhanced diffusion and (ii) reduced dislocation energy such as the Peierls potential. The reduction of the Peierls potential is likely anisotropic, and it also increases the jog and kink density. Such a model explains the observed anisotropic enhancement of creep and resultant fabric transitions in olivine (Karato *et al.*, 2008) and also predicts that the influence of water is stronger for dislocation creep than for diffusion creep. In both cases, because the amount of hydrogen dissolved in minerals

is proportional to some power of water fugacity, the strain-rate under hydrous conditions can be written as (Karato, 1989a),

$$\dot{\epsilon}_{wet} \propto f_{H_2O}^r(P, T) \cdot \exp\left(-\frac{E_{wet}^* + PV_{wet}^*}{RT}\right) \quad (17)$$

where f_{H_2O} is the fugacity of water. It should be noted that both the water fugacity term, $f_{H_2O}^r(P, T)$, and the exponential term, $\exp\left(-\frac{E_{wet}^* + PV_{wet}^*}{RT}\right)$, depend strongly on pressure (and temperature) but changes with pressure differently. Consequently the determination of two parameters, r and V_{wet}^* , is a key to obtain a formula from which one can estimate the influence of water under a broad range of conditions.

However, if one uses a high-resolution but low-pressure apparatus such as the gas-medium apparatus, one cannot determine any of these parameters uniquely. The reason is as follows. The contributions of these two terms (the fugacity term and the exponential term) are similar in magnitude under low-pressure conditions (see **Fig. 13**). But with a small pressure range, one cannot determine two parameters precisely enough. Consequently, (Mei and Kohlstedt, 2000a, Mei and Kohlstedt, 2000b) tried to determine only one parameter, r , for olivine (because the value of r provides a clue as to the atomistic processes of deformation) assuming a range of V_{wet}^* . But the influence of V_{wet}^* on the inferred r for a plausible range of V_{wet}^* (0-30 cm³/mol) is too large to make any useful conclusions as to the microscopic mechanisms of deformation (an error in r is ± 0.3 -0.4). Besides, with an unconstrained V_{wet}^* , extrapolation of these results to the depth deeper than ~20 km has large uncertainties, and the magnitude of influence of

water under these conditions is essentially unconstrained by these low-pressure studies (see **Fig. 13**). Because most of plastic deformation in Earth occurs below ~ 20 km, the applicability of these studies is highly limited. A more complete analysis was made by (Karato and Jung, 2003) based on the data from the pressure range spanning from 0.1 to 2.0 GPa by which the two key parameters (r and V_{wet}^*) were well constrained (**Fig. 13, 14**).

So far, sufficiently detailed studies on the influence of water on plastic deformation have been made only for olivine. But even from less detailed studies, one can see a general trend that the water weakening effect is stronger for more SiO₂-rich minerals (Karato, 2008). For instance, $r \sim 1$ for olivine but $r \sim 2$ for garnet (Katayama and Karato, 2008a) and $r \sim 3$ for clinopyroxene (in the dislocation creep regime; (Chen *et al.*, 2006b)). Therefore the rheological contrast among these minerals changes with water fugacity (water content).

Effect of crystal structure and bonding

In Earth and planetary interiors, nature of chemical bonding and crystal structures undergo many changes due to the variation in pressure (and temperature). Therefore it is important to understand how these changes may affect rheological properties. (Ashby and Brown, 1982) and (Frost and Ashby, 1982) conducted extensive studies to classify plastic properties of solids. In many cases, materials with the same crystal structure and bonding form an isomechanical group where when plastic properties are compared at the same normalized conditions, all the data converge to a well-defined master curve. For instance,

when strain-rate is normalized by the Debye frequency^{5,6}, ν_D , temperature by melting temperature, T_m , and stress by shear modulus, μ , then most of the data fall into a master curve,

$$\frac{\dot{\epsilon}(T,P,\sigma)}{\nu_D} = F\left(\frac{T}{T_m(P)}, \frac{\sigma}{\mu(P)}\right) \quad (18)$$

Examples were shown for B1 (NaCl structure) (Ashby and Brown, 1982) and garnet (Karato *et al.*, 1995a) (see **Fig. 15a,b**). (Karato, 1989c) extended such a study to oxides and silicates and noted that there is a large variation in plastic properties among oxides and silicates even after the normalization ((Ashby and Brown, 1982) treated oxides as a single group). In particular, this study showed that a transition to a dense structure does not necessarily lead to a high resistance to plastic deformation. (Karato, 2011a) extended such an analysis to include the influence of transition to the metallic state and the influence of the B1 \rightarrow B2 transition (**Fig. 15c**).

Such an analysis shows that unlike elasticity where a phase transformation to a denser structure leads to a higher elastic constant with a minor correction for the influence of coordination (the Birch's law; (Liebermann, 1982)), density does not play an important role in high-temperature plasticity. The Birch's law of correspondent state does

⁵ Normalization of strain-rate is not essential because Debye frequency changes only modestly among different materials.

⁶ Ashby and Brown (1982) used $D(T_m)/b^2$ ($D(T_m)$: diffusion coefficient at melting temperature), but, this normalization is not practical for our purpose because $D(T_m)$ is unknown for many materials.

not work for plastic properties. In many cases, a change in crystal structure has only a modest effect. An increase in melting temperature, therefore, will increase the effective viscosity modestly. Also, if a transition to metallic state occurs in the deep mantle of super-Earths (~ 1 TPa), then a substantial reduction in effective viscosity will occur.

Influence of partial melting

Fig. 16 summarizes the experimental observations on the influence of partial melting on plastic deformation of olivine aggregates (Kohlstedt, 2002). Deformation experiments were performed both for the diffusion creep and dislocation creep regimes. The influence of partial melting is stronger in the diffusion creep regime than in the dislocation creep regime. This is due to the fact that in the diffusion creep regime, fast diffusion in the melt as well as stress concentration enhances deformation whereas in the dislocation creep regime only stress concentration enhances deformation. They proposed an empirical formula to explain these results,

$$\dot{\epsilon}(\phi) = \dot{\epsilon}(0) \cdot \exp(\alpha\phi) \quad (19)$$

where ϕ is the melt fraction and α is a non-dimensional constant ($\sim 20-30$ ($\alpha \approx 25$ for diffusion creep and $\alpha \approx 30$ for dislocation creep))⁷. With 1 % of melt, strain-rate is enhanced by $\sim 30\%$.

⁷ This is an empirical formula without strong theoretical basis. The asymptotic behavior for $\phi \rightarrow 0$ does not agree with a model of equilibrium melt geometry reviewed by Kohlstedt (2002), and the another asymptotic formula for $\phi \rightarrow 1$ does not make sense

Recently, new results on clean olivine aggregates were published showing substantially different creep strength (Faul and Jackson, 2007). In these clean samples, prepared by the sol-gel synthesis process from oxides, the rate of deformation by diffusion creep is substantially lower than that in San Carlos olivine. It is possible that this difference is caused by a small amount of melt that exists in nominally “melt-free” San Carlos olivine aggregates as suggested by (Takei and Holtzman, 2009a). However, other factors such as the impurity content may also be the cause for such a difference.

Markedly different results were published by (Jin *et al.*, 1994) who reported that the addition of a few % of basaltic melt reduces the creep strength by more than one order of magnitude (this corresponds to the enhancement of strain-rate by more than three orders of magnitude). The reason for this large discrepancy is not understood. (Jin *et al.*, 1994) proposed that the melt topology under their deformation experiments is different from the equilibrium geometry. However, the cause for the different results is not well understood.

Table 2 summarizes the flow laws of typical minerals. Nearly complete data set is available for olivine including the influence of temperature, pressure, water and grain-size. The influence of partial melting may be included by applying a correction using the relation (19). Although less complete, extensive data sets are available for quartz, plagioclase and clinopyroxene (diopside). In contrast, experimental data on deep mantle minerals are limited.

because, at that limit, the strain-rate must agree with that of a viscous fluid but this formula does not have the viscosity of liquid (see Karato, 2008).

THEORETICAL STUDIES

Due to the rapid progress in the computational science, a number of computational studies have been published on the physical properties of minerals. For instance, computational approach has played an important role in understanding elasticity and phase relationships in minerals under the extremely high-pressure conditions (see a chapter by Tsuchiya and Kawai). Similar studies have been made on plastic properties (for a recent review see (Walker *et al.*, 2010)). However, the contributions from theoretical studies are limited in the area of plasticity compared to elasticity and phase relationships. The main reasons are (1) defects involved in plastic deformation have low symmetry and theoretical calculations of relevant properties are challenging, (2) defect-related properties are sensitive to impurities such as hydrogen or oxygen (oxygen fugacity) that are difficult to calculate, and (3) in many cases, plastic deformation involves multiple aspects and in order to understand the whole picture, one needs a comprehensive study in which the interactions of many steps are treated appropriately.

For example, (Durinck *et al.*, 2005, Oganov *et al.*, 2005) calculated the resistance to homogeneous shear in olivine and post-perovskite respectively without the concept of a dislocation and discussed the slip systems. (Carrez *et al.*, 2007) calculated the Peierls stress of lower mantle minerals based on the theory of crystal dislocations, and they inferred the dominant slip systems *directly* from these results. These procedures are incorrect. Firstly, one needs a concept of crystal dislocations to calculate the resistance for deformation, and secondly, even if one uses a concept of a dislocation and calculated some key parameter such as the Peierls stress, one needs to consider the role of such a parameter (e.g., the Peierls stress) in high-temperature creep. For instance, if one uses a

classic model of diffusion-controlled high-temperature creep (e.g., (Weertman, 1968, Weertman, 1999)), then the creep rate at high-temperature has nothing to do with the Peierls stress. In order to infer the dominant slip systems, one needs to evaluate the strain-rate for each slip system that is controlled by the interplay of several processes including dislocation glide and climb. (Cordier *et al.*, 2012) presented a more sophisticated analysis of deformation of MgO where they calculated the effective viscosity at geological strain-rates under the lower mantle conditions from the dislocation velocity using a model of dislocation glide over the Peierls barrier. However, in order to calculate the creep strength from dislocation glide velocity, they used unconventional models. For example, they argued that the effective viscosity cannot be defined for a recovery-controlled regime (“athermal regime” in their terminology) because the flow stress is independent of strain-rate. Such a notion is not supported by the experimental observations nor by the theoretical models as discussed in this chapter (equation (9); see also (Frost and Ashby, 1982, Weertman, 1999, Weertman, 1968, Karato, 2008, Poirier, 1985)). Consequently, the validity of their conclusions is highly questionable.

In these studies, it is essential to demonstrate the validity of the method one uses by comparing the results on some materials for which detailed experimental studies are available. For example, if one wants to predict the dominant slip system of post-perovskite through computational studies, one should apply such a method to a material for which the dominant slip systems are well known (e.g., olivine at low pressures). Unfortunately, this important step is often ignored.

The more promising and important role of theory is to provide some guide to interpret and extrapolate experimental data. For example, there is an important issue of

the interpretation of X-ray diffraction to determine the stress. One needs a theory to apply this technique to determine stress acting on a sample (e.g., (Karato, 2009)). Also, the development of lattice-preferred orientation (LPO) during deformation is an important topic but conducting deformation experiments with a broad range of deformation geometry is difficult. Theoretical modeling of LPO development plays an important role in this area (e.g., (Kaminski *et al.*, 2004)). Shear localization is an important process to control the strength of the lithosphere. However, experimental studies on shear localization are limited partly by the limitation of a sample size. Theoretical considerations will help guide experimental studies on shear localization.

SOME APPLICATIONS

In this section, I will illustrate how the knowledge on rheological properties of minerals and rocks and the models of temperature, water distribution may be integrated to understand rheological properties and dynamics of Earth's interior.

Lower crust

Is the lower crust weak?

Deformation of the continental lower crust makes important contributions to the tectonics of the continents including rifting and deformation associated with continental collisions. An important question that has been asked is either the lower crust and the upper mantle are well coupled or not. If the lower crust is significantly weaker than the upper mantle, then the crust and mantle will be decoupled mechanically. The rheological

properties of the continental lower crust can be estimated by the analyses of some geophysical observations including post-seismic crustal deformation, topography and gravity and the results suggest a large regional variation (e.g., (Bürgmann and Dresen, 2008)).

The dominant minerals of the continental lower crust include ortho- and clinopyroxenes, plagioclase and garnet (these minerals make a mafic rock such as gabbro) and they have substantially higher FeO and SiO₂ content than the upper mantle (Rudnick and Fountain, 1995). Experimental data on these minerals or rocks are limited but the results on diabase (basaltic rock), plagioclase and clinopyroxene show that under truly dry conditions, the lower continental crust will have the strength that is not too different from that of the (dry) upper mantle (Mackwell *et al.*, 1998, Rybacki and Dresen, 2004, Bystricky and Mackwell, 2001). However, the influence of water is stronger for SiO₂-rich minerals (or rocks) (e.g., (Chen *et al.*, 2006b, Katayama and Karato, 2008a, Post *et al.*, 1996)) and therefore when the continental lower crust has some water, its creep strength will be lowered substantially. I conclude that the strength contrast at the crust-upper mantle boundary will vary from one region to another particularly due to the heterogeneity in the water content.

Upper mantle

How strong is the lithosphere? Or why does plate tectonics operate on Earth?

Viscosity of minerals and rocks depends strongly on temperature and therefore viscosity is high in regions near the surface. Brittle fractures reduces the strength in the shallow regions, but if one uses a simple model of strength profile using the friction law

for the shallow region and the ductile flow law (corresponding to power-law creep of dry olivine), then one will have a strong oceanic lithosphere with a peak strength exceeding 500 MPa ((Kohlstedt *et al.*, 1995) **Fig. 17**).

In order for plate tectonics to occur, the strength of the lithosphere must be smaller than ~ 100 MPa on average (e.g., (Richards *et al.*, 2001, Tackley, 2000)). For a strong oceanic lithosphere such as shown in **Fig. 17**, the style of convection should be “stagnant lid convection” where a near surface strong layer remains stagnant and convection occurs only in the deep interior of planets (e.g., (Solomatov and Moresi, 1997)) (such a style of convection occurs in most of other terrestrial planets such as the Moon, Venus, Mars and Mercury (Schubert *et al.*, 2001)).

Because plate tectonics occurs on Earth, there must be some mechanisms by which the strength of the oceanic lithosphere becomes less than the model shown in **Fig. 17**. Indeed, the magnitude of deviatoric stress in the lithosphere inferred from recrystallized grain-size seldom exceeds ~ 100 MPa (e.g., (Nicolas, 1978, Avé Lallemant *et al.*, 1980)). One obvious way to reduce the strength is to include a high-stress deformation mechanism such as the Peierls mechanisms as first suggested by (Goetze and Evans, 1979), but its effect is only modest. Grain-size sensitive mechanism is another option but the majority of the lithosphere has coarse grain-size (e.g., (Avé Lallemant *et al.*, 1980)) and deforms by dislocation creep judging from the presence of seismic anisotropy. Therefore this mechanism cannot reduce the strength of the major portion of the lithosphere homogeneously.

How about the contributions from minerals other than olivine? The lithosphere is made of ~ 40 - 60 % of olivine, but other phases such as orthopyroxene (~ 20 - 30 %) also

exist. Orthopyroxene (with some orientations) is much weaker than olivine particularly at low temperatures (Ohuchi *et al.*, 2011). However, with the assumption of homogeneous deformation, the presence of a small fraction of a weak phase does not affect the strength so much (e.g., (Handy, 1994)).

However, deformation may occur heterogeneously. Indeed, geological observations of deformation of the lithosphere strongly suggest that most of the lithosphere deformation occurs in the narrow shear zones (e.g., (Handy, 1989, Drury *et al.*, 1991)). And theory suggests that plastic deformation at relatively low temperatures is often localized as discussed before.

Several mechanisms of shear localization have been discussed, but the best documented mechanism is shear localization associated with grain-size reduction (e.g., (Handy, 1989, Jin *et al.*, 1998)). However, there are two issues in this model of shear localization. First, dynamic recrystallization occurs only after certain finite strain, so if a material is too strong then initiation of shear instability will be difficult. Second, even if fine olivine grains are formed, grain-growth will terminate the instability quickly if grain-growth is fast. (Karato, 2008) showed that for pure olivine grain-growth kinetics is too fast to realize shear localization. The effect of secondary phases to slow down the grain-growth kinetics may be needed as suggested by (Warren and Hirth, 2006). It is possible that the secondary mineral, orthopyroxene, solves these problems simultaneously. Orthopyroxene with certain orientations are much softer than olivine under lithospheric conditions (Ohuchi *et al.*, 2011). Therefore these orthopyroxene grains will be deformed and recrystallized. The recrystallized grains of orthopyroxene are much smaller than those of olivine (e.g., (Skemer and Karato, 2008)) and hence mobile, and they might

penetrate into regions of recrystallized olivine grain to stabilize small grain-size and hence promote shear localization (e.g., (Farla *et al.*, 2011)). Further experimental studies are needed to clarify these processes.

The remaining issue is to develop a theoretical framework to include the influence of shear localization in large-scale modeling. In most of modeling studies, the influence of grain-size reduction is investigated through the analysis of competition between grain refinement and grain growth. In evaluating the grain refinement by deformation, it is often assumed that the effective viscosity is sensitive to grain-size (e.g., (Kameyama *et al.*, 1997, Landuyt and Bercovici, 2009)). However such a formulation is physically unsound because grain-size sensitive creep such as diffusion creep does not cause dynamic recrystallization. Simultaneous operation of dynamic recrystallization and weakening by grain-size sensitive creep is a key to shear localization. Co-existence of dynamic recrystallization and diffusion creep is a natural consequence of heterogeneous microstructure as depicted in **Fig. 5a**. Geodynamic modeling on shear localization must include this aspect of physics if the variation in the degree of shear localization among different planets were to be investigated through such modeling.

Also, if the Earth's lithosphere is weak enough to allow the operation of plate tectonics, one should ask why plate tectonics does not operate on other planets such as Venus. Nearly complete absence of water on Venus and the presence of some water on Earth (the lithosphere is "dry" but has some water particularly in pyroxenes) might be an explanation. Alternatively, the higher near surface temperatures in Venus than Earth could be the reason because shear localization is favored at low temperatures.

How has the continental lithosphere survived against convectational erosion?

The continental roots have survived for ~ 3 Gyrs against convective erosion. This is demonstrated by the age distribution of xenoliths from the continents showing nearly the same age throughout the sampling depth interval (to ~ 200 km) (e.g., (Carlson *et al.*, 2005)). In order for continental roots to have survived for ~ 3 Gyrs, they must have a high resistance for plastic deformation. (Shapiro *et al.*, 1999, Lenardic and Moresi, 1999) showed that in order for the deep continental roots to survive, their viscosity must be higher than surrounding mantle by a factor of $\sim 10^3$. In a model of the strength of the continental lithosphere by (Kohlstedt *et al.*, 1995), the deep continental mantle is assumed to be “wet” (water-saturated). In these cases, the deep continental roots will be softer than or have similar viscosity as the surrounding mantle, and the continental roots would not have survived.

(Karato, 2010b) revisited a hypothesis originally proposed by (Pollack, 1986) that the long-term stability of the continental roots might be due to the removal of water by deep partial melting. A key to evaluate this model is to calculate the viscosity ratio,

$$\xi = \frac{\eta_{dry}(P,T)}{\eta_{wet}(P,T)} = \frac{\dot{\epsilon}_{wet}(P,T)}{\dot{\epsilon}_{dry}(P,T)} \quad (20)$$

under the deep upper mantle conditions ($P \sim 10$ GPa, $T \sim 1700$ K) where $\eta_{dry,wet}(P,T)$ is the effective viscosity at dry (wet) conditions (at pressure P and temperature T) ($\dot{\epsilon}_{dry,wet}(P,T)$ is corresponding strain-rate) (wet viscosity is for the surrounding mantle and dry viscosity for the continental roots). Such a calculation is now possible due to the laboratory studies on the influence of water and pressure on deformation of olivine as

discussed before. **Fig. 18** shows that indeed, if a large degree of water depletion occurs as suggested by geochemical observations (e.g., (Carlson *et al.*, 2005)), then the experimental results on rheological properties of olivine explain the stability of the continents.

Continental lithosphere (at least many of them) have survived for ~3 Gyrs. At the same time, many continental lithosphere have rifted. For rifting to occur, the lithosphere cannot be so strong (e.g., (Huisman *et al.*, 2005)). How can we explain both the long-term stability of the continental lithosphere against convective erosion and the frequent occurrence of rifting? There are several possibilities. First, the stress magnitude is different between convective erosion and rifting. Convective erosion is due to convection in the asthenosphere and therefore stress is low (~0.1-1 MPa). In contrast, the stress levels associated with rifting is larger, ~10-50 MPa. Rheological properties are often highly non-linear and the effective viscosity is lower at higher stress than at lower stress. This provides an explanation. Second, at lower temperatures, deformation is often localized. As a result the resistance for deformation is smaller. Rifting involves deformation in the cold lithosphere and would involve localized deformation (e.g., (Huisman and Beamont, 2003)). Third, rifting is often associated with magmatism (e.g., (Sengör and Burke, 1978)). Magmatism will provide heat and volatiles to the lithosphere and will weaken it locally. Such a weakened region may help rifting to initiate.

Why is the asthenosphere weak and chemically homogeneous?

Below the lithosphere is a weak layer called the asthenosphere (Barrell, 1914). The presence of such a weak layer is in large part due to high temperature. If temperature

increases from 900 K to 1600 K, then the viscosity will decrease by ~ five orders of magnitude. Even if the influence of high pressure is included, still temperature effects dominate at relatively shallow regions and viscosity decreases with depth (**Fig. 19**).

In addition to the influence of temperature and pressure, a variation in other factors such as water content will affect the viscosity-depth profile. A case of oceanic lithosphere is shown in **Fig. 19** where the influence of a sharp change in water content at ~70 km is included as proposed by (Karato, 1986) and (Hirth and Kohlstedt, 1996). (Karato, 2012, Karato and Jung, 1998) proposed that the layered water content can also explain a sharp and large velocity reduction at ~70 km. The influence of grain-size is small because the dominant deformation mechanism in most of the upper mantle is likely dislocation creep judged from the presence of seismic anisotropy.

Partial melting is frequently invoked to explain a weak (a low seismic wave velocity, and low viscosity) layer in Earth (e.g., (Lambert and Wyllie, 1970, Kawakatsu *et al.*, 2009)). However, the influence of partial melting on rheological properties is rather modest particularly when deformation occurs by dislocation creep. Laboratory studies showing this point are reviewed by (Kohlstedt, 2002, Kohlstedt and Zimmerman, 1996). Recently (Takei and Holtzman, 2009a, Takei and Holtzman, 2009b, Takei and Holtzman, 2009c) presented a new analysis of deformation of a partially molten material and suggested that partial melting reduces viscosity by an order of magnitude in the diffusion creep regime. The predicted amount of enhanced deformation is larger than the results reported by (Kohlstedt, 2002, Kohlstedt and Zimmerman, 1996) and the reason for this discrepancy is not well understood. Takei-Holtzman's analysis includes more detailed treatment of the stress distribution in a deforming partially molten material and the

diffusion path and the stress distribution are different from a simpler model by (Kohlstedt, 2002) (see a Chapter by Takei). In any case, the enhancement of strain-rate in their model is only modest for diffusion creep (a factor of $\sim 5-10$), and in case of dislocation creep, enhancement of deformation will be less. The presence of strong seismic anisotropy suggests that dislocation creep dominates in the asthenosphere, and therefore partial melting unlikely has a large direct effect on rheological properties. Rather, the main role of partial melting is its indirect effect through the redistribution of water (Karato, 1986).

The asthenosphere is also characterized by the homogeneous and modestly depleted chemical composition. In a model of chemical evolution proposed by (Hofmann, 1988), he assumed that highly depleted components and undepleted components have been well mixed to explain the homogeneous and modestly depleted nature of the asthenosphere. However, mixing is difficult if two components have largely different viscosity (Manga, 1996). Depleted and undepleted components have largely different water contents and hence different viscosity in the upper mantle (Karato, 2010b). Therefore mixing is likely to be inefficient at least in the upper mantle. Other mechanisms of homogenization need to be considered. Mixing of materials with different composition is often studied assuming the homogeneous viscosity (e.g., (Christensen and Hofmann, 1994, van Keken *et al.*, 2002)). Influence of viscosity contrasts needs to be included in more realistic studies. (Karato, 2012) proposed that the asthenosphere is made of the residual of partial melting at 410-km and homogeneous and modestly depleted composition is due to partial melting.

Transition zone

Is the 410-km and/or 660-km discontinuity a rheological barrier for mantle convection?

Some geodynamic observations strongly suggest that mantle viscosity increases substantially at around the transition zone. Viscosity below that depth is higher than that above (the depth at which viscosity increases is not well constrained). Seismological observations show the presence of seismic anisotropy in the transition zone (Trampert and van Heijst, 2002, Visser *et al.*, 2008) suggesting that dislocation creep dominates in this region. However, currently available mineral physics observations do not provide robust explanation for this rheological layering. This is due mostly to the very limited quantitative experimental data on minerals in these regions.

However, some new experimental observations are becoming available. According to (Nishihara *et al.*, 2008, Kawazoe *et al.*, 2010), the creep strength of wadsleyite in the power-law creep regime is comparable to that of olivine compared at the similar pressure and temperature (and water content). Water content in the transition zone is generally higher than that of the upper mantle and varies significantly from one region to another (Karato, 2011b). It is likely that the 410-km is not a strong rheological barrier for convection but the viscosity contrast at the 410-km discontinuity will depend on the water content.

Not much can be said about the rheological contrast at the 660-km discontinuity. Firstly, there is strong evidence that a majority of the lower mantle except for the D'' layer deforms by diffusion creep (see the later section on the lower mantle). If so the viscosity depends on the grain-size that is not well constrained. Secondly, currently there is no experimental data on the water effects on rheological properties on lower mantle

minerals. In addition there are no observational constraints on the water distribution in the lower mantle (Karato, 2011b). The inferred large viscosity increase at around 660-km from the geodynamic studies (e.g., (Hager, 1984, Nakada and Lambeck, 1989)) could be due to the variation in water content, grain-size and/or diffusion coefficients.

Why do cold slabs deform in the transition zone?

According to the high-resolution seismic tomography, subducted slabs are highly deformed in the western Pacific (e.g., (Fukao *et al.*, 1992, Fukao *et al.*, 2009)), but not much in the eastern Pacific (Kárason and van der Hilst, 2000, Grand *et al.*, 1997). This is a puzzling observation because slabs in the western Pacific are colder than those in the eastern Pacific. Not only this apparent paradoxical correlation, but also the deformation of a slab in the deep mantle itself is a puzzle in the first place because a cold slab in the deep mantle (high pressure) should have a high viscosity. These observations suggest that there must be some mechanisms by which a cold slab becomes weaker than a warm slab in the transition zone. In order to address these questions, one needs to understand the rheological properties of minerals under the transition zone conditions.

Direct measurements of rheological properties of transition zone minerals (wadsleyite, ringwoodite and majorite) have been made only recently. Early measurements used stress relaxation tests (Chen *et al.*, 1998, Xu *et al.*, 2003, Karato *et al.*, 1998) and powder samples were used in some of them (Chen *et al.*, 1998, Xu *et al.*, 2003). In stress relaxation tests, there is no guarantee if the results correspond to steady-state flow law. Furthermore, when powder samples are used, crushing and resultant creation of high density of dislocations affect the mechanical properties and stress

measurements. Consequently, the usefulness of these results is questionable. Better-defined results have been obtained for wadsleyite and ringwoodite under constant strain-rate (to ~ 23 GPa and ~ 2100 K) using RDA operated at the synchrotron facility (Nishihara *et al.*, 2008, Kawazoe *et al.*, 2010, Hustoft *et al.*, 2011). Also semi-quantitative results were obtained on ringwoodite by (Karato *et al.*, 1998).

These results showed that, in the dislocation creep regime, transition zone minerals are stronger than olivine (at a similar water content), but grain-size sensitive mechanisms become important when grain-size is less than $\sim 1 \mu\text{m}$ at laboratory conditions ($\sim 10^{-4}$ - 10^{-5} s^{-1} , $T=1500$ - 2000 K, $P=14$ - 20 GPa). When extrapolated, these results suggest that diffusion creep would become important at geological strain-rates for the grain-size less than ~ 1 mm that is consistent with the estimate from the diffusion coefficients (Shimojuku *et al.*, 2009) (**Fig. 20**). Because the grain-size in the shallow lithosphere is several mm (Avé Lallemant *et al.*, 1980), and the subducted lithosphere are at high pressures, low temperatures and dry (e.g., (Kubo *et al.*, 2009)), these results imply that the subducted slabs will have much higher viscosity than the surrounding mantle (at least by several orders of magnitude) and hence will not deform if grain-size remains the same.

Due to the poor constraints on the influence of water on deformation and diffusion of wadsleyite, a robust estimate of the strength difference between olivine and wadsleyite (or ringwoodite) cannot be made at this time. However, a conservative estimate of a viscosity of the cold slab is possible based on the similarity in the creep strength in the power-law creep regime between olivine and wadsleyite. Because the pressure is high (~ 20 GPa) and temperature is low in the central portions of a cold slab

($T \sim 1000$ K), the viscosity there will exceed $\sim 10^{30}$ Pa s if the rheological properties of dry wadsleyite (or ringwoodite) in the power-law creep regime is used. Consequently, without any weakening effects, a cold slab will not deform appreciably. In contrast to this expectation, subducted cold slabs in the western Pacific are deformed in the transition zone. A possible explanation of this puzzling observation is the weakening caused by the grain-size reduction after a phase transformation in a slab. When a subducted slab penetrates into the transition zone, a series of phase transitions will occur that will modify the grain-size. (Riedel and Karato, 1997) studied the influence of temperature on the size of newly formed grains in a slab. They found that the grain-size after a phase transformation depends strongly on the temperature and the grain-size is small when the transformation occurs at low temperatures (**Fig. 21**). When a cold slab subducts, then the grain-size reduction is significant and the small grain-size will persist (because of slow grain-growth), leading to substantial weakening (Riedel and Karato, 1997, Karato *et al.*, 2001). For instance, the grain-size after the phase transformation in a cold slab is estimated to be on the order of $1 \mu\text{m}$. Using the critical grain-size for the transition to diffusion creep of ~ 1 mm and the initial grain-size of several mm, I conclude that the viscosity reduction will be ~ 6 - 9 orders of magnitude ($\eta / \eta_o = (L / L_o)^2$, $(L / L_o)^3 = 10^6$ - 10^9 , η : viscosity, L : grain-size). In contrast, a warm slab will not weaken because the grain-size after a phase transformation will be large. This causes a regional variation in the slab strength, and provides a possible explanation for the observed paradoxical correlation between the slab deformation and slab temperatures (Karato *et al.*, 2001) (**Fig. 22**).

The lower mantle

What is the deformation mechanism in the lower mantle, and how does viscosity change with depth in the lower mantle?

Very little experimental data are available for the rheological properties of the lower mantle minerals. Quantitative deformation experiments under lower mantle conditions have not been performed at the time of this writing (September, 2011). Low-temperature deformation experiments at unknown strain-rate were performed at lower mantle pressures (e.g., (Merkel *et al.*, 2003, Cordier *et al.*, 2004, Merkel *et al.*, 2006, Merkel *et al.*, 2007, Miyagi *et al.*, 2011)). But, the relevance of these results to deformation in the lower mantle is questionable, because deformation mechanisms are likely high-stress mechanism such as the Peierls mechanism that is irrelevant for most of the hot mantle.

Based on the absence of seismic anisotropy, (Karato *et al.*, 1995b) proposed that the majority of the lower mantle deforms by grain-size sensitive creep such as diffusion creep although dislocation creep dominates in some regions of the D'' layer. Given this notion, some useful conclusions can be obtained on the rheological properties from the measurements of diffusion coefficients. (Yamazaki and Karato, 2001) conducted such a study and concluded that the depth variation in viscosity is modest because both activation energy and volume of lower mantle minerals (perovskite and (Mg,Fe)O) are small. This provided a simple explanation of the inferred modest variation in viscosity in the lower mantle (**Fig. 23**). They also noted that (Mg,Fe)O is likely weaker than perovskite, and consequently, strain softening and resultant shear localization likely occur in the lower mantle. If shear localization occurs, then much of deformation in the lower

mantle is in narrow regions and a large portion of the lower mantle is isolated from the large-scale material circulation. Recently, (Xu *et al.*, 2011) determined the diffusion coefficients of Si and Mg in MgSiO₃ perovskite. They used theoretical models of diffusion creep and dislocation creep to discuss the deformation mechanisms. They found that the contribution from diffusion creep is comparable to that of dislocation creep in the lower mantle. However, a model of dislocation creep is not well established and the conclusions based on a model has large uncertainties.

A possible role of spin transition on diffusion and rheological properties was discussed by (Wentzcovitch *et al.*, 2009). Using the elastic strain energy model of activation energy (Keyes, 1963), they suggest that the spin transition may enhance plastic deformation. However, such a conclusion is highly speculative because the elastic strain energy model is a crude model for the activation energy for diffusion and the appropriate elastic constants to be used in this model is not well known.

When deformation occurs by diffusion creep, then viscosity depends strongly on grain-size. However, the grain-size in the lower mantle is poorly constrained. There is no sample from the lower mantle except for small inclusions in diamond (e.g., (Harte, 2010)). (Yamazaki and Karato, 2001) estimated the average grain-size from the comparison of the diffusion coefficients with geodynamically inferred viscosity. (Yamazaki *et al.*, 1996) showed slow grain-growth kinetics. (Solomatov *et al.*, 2002) investigated the grain growth kinetics through numerical modeling and concluded substantially faster grain-growth kinetics. Much remains to be investigated on the grain-size evolution and rheological properties on the lower mantle minerals and their assemblages.

Is the D'' layer weak?

(Ammann *et al.*, 2010) calculated the point defect mobility in lower mantle minerals including post-perovskite. They found large anisotropy in point defect mobility in post-perovskite, and assuming that the diffusion coefficient along the fastest direction controls the creep rate by dislocation creep they concluded that post-perovskite is weaker than co-existing minerals when deformed by diffusion-controlled dislocation creep. However, their conclusion is not valid because (i) no constraints are available for defect concentration and (ii) the averaging scheme of anisotropic diffusion used by (Ammann *et al.*, 2010) is incorrect (Karato, 2010a). Currently no experimental studies are available on plastic deformation of post-perovskite that can be applied to deformation in the D'' layer. There are a number of papers reporting deformation of post-perovskite as cited above, but none of these results are applicable to D'' layer because all of these experiments were conducted at low temperatures at unknown strain rates (and stress in most cases). (Hunt *et al.*, 2009) conducted deformation experiments on post-perovskite analogue (CaIrO_3) and concluded that there is weakening associated with transformation from perovskite to post-perovskite phase and suggested that this is evidence for a weak post-perovskite phase. However, the validity of their conclusion is questionable because weakening during a phase transformation is observed in many materials caused by the internal stress (or strain) (e.g., (Zamora and Poirier, 1983)) and such an observation does not necessarily mean that a new phase is weak.

Even though the notion of weak post-perovskite is questionable, the D'' layer is likely to be weak compared to the regions above. This is simply because of high

temperature (the D'' layer is a thermal boundary layer where temperature increases by ~ 1000 K, (Lay *et al.*, 2008)). Geodynamic evidence for a weak D'' layer is presented by (Cadek and Fleitout, 2006, Nakada and Karato, 2011).

SOME SPECULATIONS ON THE RHEOLOGICAL PROPERTIES OF OTHER PLANETS

Physical conditions in the planets such as the Moon, Venus, Mars and Mercury are largely the same as those in Earth with somewhat lower pressures than Earth. Also the major element compositions are also similar (except for modest difference in iron content). Therefore inferring rheological properties in these planets does not require any new experimental data.

Most critical is the knowledge of water distribution in these planets (or satellites). Although observations relevant to the rheological properties in these planets are scarce, some observations such as tidal energy dissipation provide some constraints. For example, tidal Q of the Moon is ~ 40 -50 (Williams *et al.*, 2001), and that of Mars is ~ 80 (Lainey *et al.*, 2007, Bills *et al.*, 2005). Because tidal dissipation occurs mostly in the deep mantle (e.g., (Peale and Cassen, 1978)), these observations imply that deep mantles of these planets have relatively low viscosity (tidal Q of Earth due to solid Earth is ~ 280 (Ray *et al.*, 2001)). Q and viscosity scale as $Q/Q_o = (\eta/\eta_o)^\alpha$ with $\alpha \approx 0.3$ (Karato, 2008) (see also a Chapter by Takei). If such a relation is used, then the viscosity of the deep mantle of the Moon is estimated to be $\sim 10^{19}$ Pa s and that of Mars is $\sim 10^{20}$ Pa s. A plausible cause for these low viscosities is a large amount of water (hydrogen) in the deep mantles of these planets (or satellites) (for water in the Moon see (Hauri *et al.*, 2011)).

Electrical conductivity measurements by remote sensing (electromagnetic induction) on these planets will provide additional data to estimate the water contents (see a Chapter by Karato and Wang).

Some of the near surface tectonics on a planet depends on the lithosphere thickness. One major factor controlling the lithosphere thickness is the temperature-depth profile that depends critically on the mode of heat transfer (plate tectonics versus stagnant lid convection, e.g., (Breuer and Moore, 2009)). The lithosphere thickness is also controlled by the depth at which dehydration hardening occurs (Karato, 1986, Hirth and Kohlstedt, 1996). The depth at which dehydration hardening occurs is determined by the depth at which the adiabat (during the process of crust formation) cuts the dry solidus. This depth is inversely proportional to the gravity, and is large for a small planet. The inferred thick lithosphere on Mars (Phillips *et al.*, 2008) may be partly due to the role of dehydration hardening.

Recently a large number of planets have been discovered outside of the solar system (see a Chapter by Valencia). These exoplanets include Earth-like planets but some of their mass exceeds that of Earth (to $\sim 10 M_{\oplus}$). Given a broad range of planets with a similar composition but different total mass, plausible evolution and dynamics of these planets have been studied as a function of mass (e.g., (Tachinami *et al.*, 2011, Valencia and O'Connell, 2009, Papuc and Davies, 2008, Kite *et al.*, 2009)). Because the convective heat transfer controls the evolution of planets, rheological properties of these planets are the key to understand their evolution. However, because the pressures in these planets reach ~ 1 TPa, it is difficult to make reliable estimates of their rheological properties. (Papuc and Davies, 2008) and (Tachinami *et al.*, 2011) used a model of a constant V^* ,

whereas (Karato, 2011a) discussed that at pressures around ~ 1 TPa, several processes will make materials weaker and that a model of constant V^* is not valid under these conditions. At such a pressure range, deviations from the conventional formulation such as equation (9) occurs including (i) transition in diffusion mechanisms, (ii) transition to a weaker phase ($B1 \rightarrow B2$), (iii) dissociation of a post-perovskite phase and (iv) transition to metallic state. All of these processes reduce viscosity. Therefore viscosity in the deep interior of a super-Earth is likely lower than that of the lower mantle of Earth (**Fig. 24**).

In modeling the dynamics of super-Earths, pressure dependence of viscosity needs to be included in addition to the temperature dependence. This means that one needs to use at least three parameters to characterize the rheological structure of super-Earths: mean viscosity, temperature dependence of viscosity (viscosity near the surface), and pressure dependence of viscosity (deep mantle viscosity). In addition, when one evaluates whether plate tectonics occurs on these planets or not, one should also consider the dependence of lithosphere thickness on planetary size.

SUMMARY AND CONCLUSIONS

Plastic deformation (rheological properties) of minerals and rocks plays a crucial role in controlling the dynamics and evolution of terrestrial planets. However because of the presence of multiple mechanisms of deformation, sensitivity to many parameters and also because of non-linear rheological behavior (in most cases), reliable quantitative studies of rheological properties is difficult. I summarized some basics of rheological properties that will guide a reader to make a good judgment when he/she applies

laboratory data or results of computational studies to understand the dynamics of Earth and planets.

High-resolution mechanical data obtained at low pressures (<0.5 GPa) contributed to understand the microscopic processes of deformation. However, the applicability of these results is limited to less than ~ 20 km depth in Earth. Robust experimental results applicable to Earth's interiors below ~ 20 km, where most of plastic deformation occurs, can be obtained only from experiments at pressures above ~ 1 GPa or higher. The existing experimental data and seismological observations strongly suggest that power-law dislocation creep and diffusion creep are the dominant mechanisms of deformation in most regions of Earth's (and planetary) interior. Rheological properties of minerals and rocks are highly sensitive to temperature, pressure, water (hydrogen) content and grain-size. Characterizing the influence of these parameters on rheological properties is challenging but new methods have been developed (or being developed) by which these properties can be constrained under deep Earth (planet) conditions. When the influence of these factors are well characterized by experiments, then one can develop models of rheological properties by combining these results with models of temperature, hydrogen and grain-size distribution in Earth and planets.

Well-established flow laws are now available for some of the crustal and upper mantle minerals based on the experimental studies at high pressures (see **Table 2**). Quantitative results on deep mantle minerals are currently limited, but using new methods of high-pressure rheological studies, important results on the rheological properties of deep mantle minerals are expected to come soon. The use of analogue materials will be still valuable in some cases. Important topics to be studied using

analogue materials include deformation and deformation fabrics (LPO) in post-perovskite and deformation of materials with the B2 (CsCl) structure. The results of carefully conducted studies on analogue materials at low pressures will be more useful than low-temperature deformation experiments under high-pressures at unknown strain-rates.

In the theoretical side, more efforts must be directed to establish a theoretical framework for interpreting experimental data rather than calculating the creep strength. An important case is a theory for shear localization. Currently a very crude phenomenological approach is used in this area (e.g., (Landuyt and Bercovici, 2009)). Such a model does not capture some essence of shear localization including the microscopic processes of load transfer leading to the runaway instability.

In many cases, modeling rheological structures in Earth and planets involves feedbacks: a temperature-depth profile depends strongly on the temperature and pressure dependence of rheological properties. These studies are crucial in developing our understanding of the dynamics and evolution of Earth and other terrestrial planets.

ACKNOWLEDGMENTS

This work is supported partly by the grants from NSF. The work summarized here is based on my long-term collaborations with many colleagues including Mervyn Paterson, Dave Kohlstedt, Zhichao Wang, Mike Riedel, Haemyeong Jung, Daisuke Yamazaki, Yousheng Xu, Don Weidner, Yu Nishihara, Phil Skemer, Takaaki Kawazoe, Tomohiro Ohuchi, Kazuhiko Otsuka, Justin Hustoft, Lowell Miyagi, and Robert Farla. Yasuko Takei and Daisuke Yamazaki provided helpful comments on the manuscript. I thank them all.

REFERENCES

- Ammann, M.W., Brodhlot, J.P., Wookey, J. & Dobson, D.P., 2010. First-principles constraints on diffusion in lower-mantle minerals and a weak D" layer, *Nature*, 465, 462-465.
- Argon, A.S., 1973. Stability of plastic deformation. in *The Inhomogeneity of Plastic Deformation*, pp. 161-189, ed. Reed-Hill, R. E. American Society of Metals, Metals Park, OH.
- Ashby, M.F. & Brown, A.M., 1982. Flow in polycrystals and the scaling of mechanical properties. in *Deformation of Polycrystals: Mechanisms and Microstructures*, pp. 1-13, eds. Hansen, N., Horsewell, A., Leffers, T. & Lilholt, H. RISØ National Laboratory, Roskilde.
- Avé Lallemant, H.G., Mercier, J.-C.C. & Carter, N.L., 1980. Rheology of the upper mantle: inference from peridotite xenoliths, *Tectonophysics*, 70, 85-114.
- Barrell, J., 1914. The strength of the crust, Part VI. Relations of isostatic movements to a sphere of weakness - the asthenosphere, *Journal of Geology*, 22, 655-683.
- Bills, B.G., Neumann, G.A., Smith, D.E. & Zuber, M.T., 2005. Improved estimate of tidal dissipation within Mars from MOLA observations of the shadow of Phobos, *Journal of Geophysical Research*, 110, 10.1029/2004JE002376.
- Blacic, J.D., 1972. Effects of water in the experimental deformation of olivine. in *Flow and Fracture of Rocks*, pp. 109-115, eds. Heard, H. C., Borg, I. Y., Carter, N. L. & Raleigh, C. B. American Geophysical Union, Washington DC.
- Bloomfield, J.P. & Covey-Crump, S.J., 1993. Correlating mechanical data with microstructural observations in deformation experiments on synthetic two-phase aggregates, *Journal of Structural Geology*, 15, 1007-1019.
- Breuer, D. & Moore, W.B., 2009. 9 Dynamics and thermal history of the terrestrial planets, the Moon, and Io. in *Treatise on Geophysics*, pp. 299-348, ed. Spohn, T. Elsevier, Amsterdam.
- Bürgmann, R. & Dresen, G., 2008. Rheology of the lower crust and upper mantle: Evidence from rock mechanics, geodesy, and field observations, *Annual Review of Earth and Planetary Sciences*, 36, 531-567.
- Bystricky, M., Kunze, K., Burlini, L. & Burg, J.-P., 2001. High shear strain of olivine aggregates: rheological and seismic consequences, *Science*, 290, 1564-1567.
- Bystricky, M. & Mackwell, S.J., 2001. Creep of dry clinopyroxene aggregates, *Journal of Geophysical Research*, 106, 13443-13454.
- Cadek, O. & Fleitout, L., 2006. Effect of lateral viscosity variations in the core-mantle boundary region on predictions of the long-wavelength geoid, *Studia Geophysica et Geodetica*, 50, 217-232.
- Cannon, R.M. & Coble, R.L., 1975. Review of diffusional creep of Al₂O₃. in *Deformation of Ceramic Materials*, pp. 61-100, eds. Bradt, R. C. & Tressler, R. E. Plenum Press.
- Carlson, R.W., Pearson, D.G. & James, D.E., 2005. Physical, chemical, and chronological characteristics of continental mantle, *Review of Geophysics*, 43, 10.1029/2004RG000156.
- Carrez, P., Ferre, D. & Cordier, P., 2007. Implications for plastic flow in the deep mantle from modelling dislocations in MgSiO₃ minerals, *Nature*, 446, 68-70.

- Chen, I.W. & Argon, A.S., 1979. Steady state power-law creep in heterogeneous alloys with coarse microstructures, *Acta Metallurgica*, 27, 785-791.
- Chen, J., Inoue, T., Weidner, D.J., Wu, Y. & Vaughan, M.T., 1998. Strength and water weakening of mantle minerals, olivine, wadsleyite and ringwoodite, *Geophysical Research Letters*, 25, 575-578.
- Chen, J., Li, L., Yu, T., Long, H., Weidner, D.J., Wang, L. & Vaughan, M.T., 2006a. Does Reuss and Voigt bounds really bound in high-pressure rheology experiments?, *Journal of Physics: Condensed Matter*, 18, S1049-S1059.
- Chen, S., Hiraga, T. & Kohlstedt, D.L., 2006b. Water weakening of clinopyroxene in the dislocation creep regime, *Journal of Geophysical Research*, 111, 10.1029/2005JB003885.
- Chopra, P.N. & Paterson, M.S., 1981. The experimental deformation of dunite, *Tectonophysics*, 78, 453-573.
- Chopra, P.N. & Paterson, M.S., 1984. The role of water in the deformation of dunite, *Journal of Geophysical Research*, 89, 7861-7876.
- Christensen, U.R. & Hofmann, A.W., 1994. Segregation of subducted oceanic crust in the convecting mantle, *Journal of Geophysical Research*, 99, 19867-19884.
- Cooper, R.F. & Kohlstedt, D.L., 1986. Rheology and structure of olivine-basalt partial melts, *Journal of Geophysical Research*, 91, 9315-9323.
- Cordier, P., Amodeo, J. & Carrez, P., 2012. Modelling the rheology of MgO under Earth's mantle pressure, temperature and strain rates, *Nature*, 481, 177-181.
- Cordier, P., Ungar, T., Zsoldos, L. & Tichy, G., 2004. Dislocation creep in MgSiO₃ perovskite at conditions of the Earth's uppermost lower mantle, *Nature*, 428, 837-840.
- Costa, F. & Chakraborty, S., 2008. The effect of water on Si and O diffusion rates in olivine and implications for transport properties and processes in the upper mantle, *Physics of the Earth and Planetary Interiors*, 166, 11-29.
- Derby, B., 1991. The dependence of grain size on stress during dynamic recrystallization, *Acta Metallurgica Materials*, 39, 955-962.
- Drury, M.R., Vissers, R.L.M., van der Wal, D. & Hoogerduin Strating, E.H., 1991. Shear localization in upper mantle peridotites, *Pure and Applied Geophysics*, 137, 439-460.
- Durinck, J., Legris, A. & Cordier, P., 2005. Pressure sensitivity of olivine slip systems: first-principle calculations of generalised stacking faults, *Physics and Chemistry of Minerals*, 32, 646-654.
- Farla, R., Cai, Z. & Karato, S., 2011. Deformation of olivine-orthopyroxene aggregates: Implications for the strength of the lithosphere, *EOS*.
- Faul, U.H. & Jackson, I., 2007. Diffusion creep of dry, melt-free olivine, *Journal of Geophysical Research*, 112, 10.1029/2006JB004586.
- Frost, H.J. & Ashby, M.F., 1982. *Deformation Mechanism Maps*, edn, Vol., pp. Pages, Pergamon Press, Oxford.
- Fukao, Y., Obayashi, M., Inoue, H. & Nishii, M., 1992. Subducting slabs stagnant in the mantle transition zone, *Journal of Geophysical Research*, 97, 4809-4822.
- Fukao, Y., Obayashi, M., Nakakuki, T. & Group, D.S.P., 2009. Stagnant slab: A review, *Annual Review of Earth and Planetary Sciences*, 37, 19-46.

- Gleason, G.C. & Tullis, J., 1993. Improving flow laws and piezometers for quartz and feldspar aggregates, *Geophysical Research Letters*, 20, 2111-2114.
- Goetze, C., 1978. The mechanisms of creep in olivine, *Philosophical Transaction of Royal Society of London*, A 288, 99-119.
- Goetze, C. & Evans, B., 1979. Stress and temperature in the bending lithosphere as constrained by experimental rock mechanics, *Geophysical Journal of Royal Astronomical Society*, 59, 463-478.
- Goldsby, D.L. & Kohlstedt, D.L., 2001. Superplastic deformation of ice: experimental observations, *Journal of Geophysical Research*, 106, 11017-11030.
- Gordon, R.S., 1973. Mass transport in the diffusional creep of ionic solids, *Journal of the American Ceramic Society*, 65, 147-152.
- Gordon, R.S., 1985. Diffusional creep phenomena in polycrystalline oxides. in *Point Defects in Minerals*, pp. 132-140, ed. Schock, R. N. American Geophysical Union, Washington DC.
- Grand, S.P., van der Hilst, R.D. & Widiyantoro, S., 1997. Global seismic tomography: A snapshot of convection in the Earth, *GSA Today*, 7, 1-7.
- Griggs, D.T., 1967. Hydrolytic weakening of quartz and other silicates, *Geophysical Journal of Royal Astronomical Society*, 14, 19-31.
- Hager, B.H., 1984. Subducted slabs and the geoid: constraints on mantle rheology and flow, *Journal of Geophysical Research*, 89, 6003-6015.
- Handy, M.R., 1989. Deformation regimes and the rheological evolution of fault zones in the lithosphere: the effects of pressure, temperature, grain size and time, *Tectonophysics*, 163, 119-152.
- Handy, M.R., 1994. Flow laws for rocks containing two non-linear viscous phases: a phenomenological approach, *Journal of Structural Geology*, 16, 287-301.
- Hansen, L.N., Zimmerman, M.E. & Kohlstedt, D.L., 2011. Grain boundary sliding in San Carlos olivine: Flow law parameters and crystallographic-preferred orientation, *Journal of Geophysical Research*, 116, 10.1029/2011JB008220.
- Harte, B., 2010. Diamond formation in the deep mantle: the record of mineral inclusions and their distribution in relation to mantle dehydration zones, *Mineralogical Magazine*, 74, 189-215.
- Hauri, E.H., Weinreich, T., Saal, A.E., Rutherford, M.C. & Van Orman, J.A., 2011. High pre-eruptive water contents preserved in lunar melt inclusions, *Science*, 333, 213-215.
- Heard, H.C., Borg, I.Y., Carter, N.L. & Raleigh, C.B., 1972. *Flow and Fracture of Rocks*, edn, Vol. 16, pp. Pages, American Geophysical Union, Washington DC.
- Herring, C., 1950. Diffusional viscosity of a polycrystalline solid, *Journal of Applied Physics*, 21, 437-445.
- Hier-Majumder, S., Anderson, I.M. & Kohlstedt, D.L., 2005. Influence of protons on Fe-Mg interdiffusion in olivine, *Journal of Geophysical Research*, 110, 10.1029/2004JB003292.
- Hiraga, T., Miyazaki, T., Tasaka, M. & Yoshida, H., 2010. Mantle superplasticity and its self-made demise, *Nature*, 468, 1091-1095.
- Hirth, G. & Kohlstedt, D.L., 1995a. Experimental constraints on the dynamics of partially molten upper mantle: deformation in the diffusion creep regime, *Journal of Geophysical Research*, 100, 1981-2001.

- Hirth, G. & Kohlstedt, D.L., 1995b. Experimental constraints on the dynamics of partially molten upper mantle: deformation in the dislocation creep regime, *Journal of Geophysical Research*, 100, 15441-15450.
- Hirth, G. & Kohlstedt, D.L., 1996. Water in the oceanic upper mantle - implications for rheology, melt extraction and the evolution of the lithosphere, *Earth and Planetary Science Letters*, 144, 93-108.
- Hirth, G. & Kohlstedt, D.L., 2003. Rheology of the upper mantle and the mantle wedge: a view from the experimentalists. in *Inside the Subduction Factory*, pp. 83-105, ed. Eiler, J. E. American Geophysical Union, Washington DC.
- Hofmann, A.W., 1988. Chemical differentiation of the Earth: the relationship between mantle, continental crust, and oceanic crust, *Earth and Planetary Science Letters*, 90, 297-314.
- Holtzman, B.K., Groebner, N.J., Zimmerman, M.E., Ginsberg, S.B. & Kohlstedt, D.L., 2003a. Stress-driven melt segregation in partially molten rocks, *Geochemistry, Geophysics, Geosystems*, 4, 10.1029/2001GC000258.
- Holtzman, B.K., Kohlstedt, D.L., Zimmerman, M.E., Heidelbach, F., Hiraga, K. & Hustoft, J., 2003b. Melt segregation and strain partitioning: implications for seismic anisotropy and mantle flow, *Science*, 301, 1227-1230.
- Holzappel, C., Rubie, D.C., Frost, D.J. & Langenhorst, F., 2005. Fe-Mg interdiffusion in (Mg,Fe)SiO₃ perovskite and lower mantle, *Science*, 309, 1707-1710.
- Honda, S., 1986. Strong anisotropic flow in finely layered asthenosphere, *Geophysical Research Letters*, 13, 1454-1457.
- Huisman, R.S. & Beamont, C., 2003. Symmetric and asymmetric lithospheric extension: Relative effects of frictional-plastic and viscous strain softening, *Journal of Geophysical Research*, 108, 10.1029/2002JB002026.
- Huisman, R.S., Buitter, S.J.H. & Beamont, C., 2005. Effect of plastic-viscous layering and strain softening on mode selection during lithospheric extension, *Journal of Geophysical Research*, 110, 10.1029/2004JB003114.
- Hunt, S.A., Weidner, D.J., Wang, L., Walte, N.P., Brodholt, J.P. & Dobson, D.P., 2009. Weakening of calcium iridate during its transformation from perovskite to post-perovskite, *Nature Geoscience*, 2, 794-797.
- Hustoft, J., Amulele, G., Otsuka, K., Du, Z. & Karato, S., 2011. Deformation of wadsleyite and ringwoodite under the transition zone conditions, *Earth and Planetary Science Letters*, submitted.
- Jin, D., Karato, S. & Obata, M., 1998. Mechanisms of shear localization in the continental lithosphere: inference from the deformation microstructures of peridotites from the Ivrea zone, northern Italy, *Journal of Structural Geology*, 20, 195-209.
- Jin, Z.M., Green, H.W., II. & Zhou, Y., 1994. Melt topology in partially molten mantle peridotite during ductile deformation, *Nature*, 372, 164-167.
- Kameyama, M., Yuen, D.A. & Fujimoto, H., 1997. The interaction of viscous heating with grain-size dependent rheology in the formation of localized slip zones, *Geophysical Research Letters*, 24, 2523-2526.
- Kaminski, E., Ribe, N.M. & Browaeys, J.T., 2004. D-rex, a program for calculation of seismic anisotropy due to crystal lattice preferred orientation in the convective upper mantle, *Geophysical Journal International*, 158, 744-752.

- Kárason, H. & van der Hilst, R.D., 2000. Constraints on mantle convection from seismic tomography. *in The History and Dynamics of Global Plate Motions*, pp. 277-288, eds. Richards, M. A., Gordon, R. G. & Hilst, R. D. v. d. American Geophysical Union, Washington DC.
- Karato, S., 1986. Does partial melting reduce the creep strength of the upper mantle?, *Nature*, 319, 309-310.
- Karato, S., 1989a. Defects and plastic deformation in olivine. *in Rheology of Solids and of the Earth*, pp. 176-208, eds. Karato, S. & Toriumi, M. Oxford University Press, Oxford.
- Karato, S., 1989b. Grain growth kinetics in olivine aggregates, *Tectonophysics*, 155, 255-273.
- Karato, S., 1989c. Plasticity-crystal structure systematics in dense oxides and its implications for creep strength of the Earth's deep interior: a preliminary result, *Physics of Earth and Planetary Interiors*, 55, 234-240.
- Karato, S., 1993. Importance of anelasticity in the interpretation of seismic tomography, *Geophysical Research Letters*, 20, 1623-1626.
- Karato, S., 1998a. Micro-physics of post glacial rebound. *in Dynamics of the Ice Age Earth: A Modern Perspective*, pp. 351-364, ed. Wu, P. Trans Tech Publisher, Zürich.
- Karato, S., 1998b. Seismic anisotropy in the deep mantle, boundary layers and geometry of mantle convection, *Pure and Applied Geophysics*, 151, 565-587.
- Karato, S., 2008. *Deformation of Earth Materials: Introduction to the Rheology of the Solid Earth*, edn, Vol., pp. Pages, Cambridge University Press, Cambridge.
- Karato, S., 2009. Theory of lattice strain in a material undergoing plastic deformation: Basic formulation and applications to a cubic crystal, *Physical Review*, B79, 10.1103/PhysRevB.1179.214106.
- Karato, S., 2010a. The influence of anisotropic diffusion on the high-temperature creep of a polycrystalline aggregate, *Physics of the Earth and Planetary Interiors*, 183, 468-472.
- Karato, S., 2010b. Rheology of the deep upper mantle and its implications for the preservation of the continental roots: A review, *Tectonophysics*, 481, 82-98.
- Karato, S., 2011a. Rheological properties of the mantle of super-Earths : Some insights from mineral physics, *Icarus*, 212, 14-23.
- Karato, S., 2011b. Water distribution across the mantle transition zone and its implications for global material circulation, *Earth and Planetary Science Letters*, 301, 413-423.
- Karato, S., 2012. On the origin of the asthenosphere, *Earth and Planetary Science Letters*, in press.
- Karato, S., Dupas-Bruzek, C. & Rubie, D.C., 1998. Plastic deformation of silicate spinel under the transition zone conditions of the Earth, *Nature*, 395, 266-269.
- Karato, S. & Jung, H., 1998. Water, partial melting and the origin of seismic low velocity and high attenuation zone in the upper mantle, *Earth and Planetary Science Letters*, 157, 193-207.
- Karato, S. & Jung, H., 2003. Effects of pressure on high-temperature dislocation creep in olivine polycrystals, *Philosophical Magazine, A*, 83, 401-414.

- Karato, S., Jung, H., Katayama, I. & Skemer, P.A., 2008. Geodynamic significance of seismic anisotropy of the upper mantle: New insights from laboratory studies, *Annual Review of Earth and Planetary Sciences*, 36, 59-95.
- Karato, S., Paterson, M.S. & Fitz Gerald, J.D., 1986. Rheology of synthetic olivine aggregates: influence of grain-size and water, *Journal of Geophysical Research*, 91, 8151-8176.
- Karato, S., Riedel, M.R. & Yuen, D.A., 2001. Rheological structure and deformation of subducted slabs in the mantle transition zone: implications for mantle circulation and deep earthquakes, *Physics of Earth and Planetary Interiors*, 127, 83-108.
- Karato, S., Wang, Z., Liu, B. & Fujino, K., 1995a. Plastic deformation of garnets: systematics and implications for the rheology of the mantle transition zone, *Earth and Planetary Science Letters*, 130, 13-30.
- Karato, S. & Weidner, D.J., 2008. Laboratory studies of rheological properties of minerals under deep mantle conditions, *Elements*, 4, 191-196.
- Karato, S. & Wu, P., 1993. Rheology of the upper mantle: a synthesis, *Science*, 260, 771-778.
- Karato, S., Zhang, S. & Wenk, H.-R., 1995b. Superplasticity in Earth's lower mantle: evidence from seismic anisotropy and rock physics, *Science*, 270, 458-461.
- Katayama, I. & Karato, S., 2008a. Effects of water and iron content on the rheological contrast between garnet and olivine, *Physics of the Earth and Planetary Interiors*, 166, 59-66.
- Katayama, I. & Karato, S., 2008b. Low-temperature high-stress rheology of olivine under water-rich conditions, *Physics of the Earth and Planetary Interiors*, 168, 125-133.
- Kawakatsu, H., Kumar, P., Takei, Y., Shinohara, M., Kanazawa, T., Araki, E. & Suyehiro, K., 2009. Seismic evidence for sharp lithosphere-asthenosphere boundaries of oceanic plates, *Science*, 324, 499-502.
- Kawazoe, T., Karato, S., Ando, J., Jing, Z., Otsuka, K. & Hustoft, J., 2010. Shear deformation of polycrystalline wadsleyite up to 2100 K at 14-17 GPa using a rotational Drickamer apparatus (RDA) *Journal of Geophysical Research*, 115, 10.1029/2009JB007096.
- Kawazoe, T., Karato, S., Otsuka, K., Jing, Z. & Mookherjee, M., 2009. Shear deformation of dry polycrystalline olivine under deep upper mantle conditions using a rotational Drickamer apparatus (RDA), *Physics of the Earth and Planetary Interiors*, 174, 128-137.
- Keyes, R.W., 1963. Continuum models of the effect of pressure on activated processes. in *Solids Under Pressure*, pp. 71-91, eds. Paul, W. & Warschauer, D. M. McGraw-Hills, New York.
- Kinsland, G.L. & Bassett, W.A., 1977. Strength of MgO and NaCl polycrystals to confining pressures of 250 Kbar at 25 C, *Journal of Applied Physics*, 48, 978-985.
- Kite, E.S., Manga, M. & Gaidos, E., 2009. Geodynamics and rate of volcanism on massive Earth-like planets, *The Astrophysical Journal*, 700, 1732-1749.
- Kocks, U.F., 1970. The relation between polycrystal deformation and single crystal deformation, *Metallurgical Transactions*, 1, 1121-1143.

- Kocks, U.F., Argon, A.S. & Ashby, M.F., 1975. Thermodynamics and kinetics of slip, *Progress in Materials Sciences*, 19, 1-288.
- Kohlstedt, D.L., 2002. Partial melting and deformation. in *Plastic Deformation of Minerals and Rocks*, pp. 121-135, eds. Karato, S. & Wenk, H.-R. Mineralogical Society of America, Washington DC.
- Kohlstedt, D.L., 2006. The role of water in high-temperature rock deformation. in *Water in Nominally Anhydrous Minerals*, pp. 377-396, eds. Keppler, H. & Smyth, J. R. Mineralogical Society of America, Washington DC.
- Kohlstedt, D.L., 2009. Properties of rocks and minerals - Constitutive equations, rheological behavior, and viscosity of rocks. in *Treatise on Geophysics*, pp. 389-417, ed. Price, G. D. Elsevier, Amsterdam.
- Kohlstedt, D.L., Evans, B. & Mackwell, S.J., 1995. Strength of the lithosphere: constraints imposed by laboratory measurements, *Journal of Geophysical Research*, 100, 17587-17602.
- Kohlstedt, D.L. & Zimmerman, M.E., 1996. Rheology of partially molten mantle rocks, *Annual Review of Earth and Planetary Sciences*, 24, 41-62.
- Kronenberg, A.K. & Tullis, J., 1984. Flow strength of quartz aggregates: grain size and pressure effects due to hydrolytic weakening, *Journal of Geophysical Research*, 89, 4281-4297.
- Kubo, T., Kaneshima, S., Torii, Y. & Yoshioka, S., 2009. Seismological and experimental constraints on metastable phase transformations and rheology of the Mariana slab, *Earth and Planetary Science Letters*, 287, 12-23.
- Lainey, V., Dehant, V. & Pätzold, M., 2007. First numerical ephemerides of the Martian moons, *Astronomy and Astrophysics*, 465, 1075-1084.
- Lambert, I.B. & Wyllie, P.J., 1970. Low-velocity zone of the Earth's mantle: Incipient melting caused by water, *Science*, 169, 764-766.
- Landuyt, W. & Bercovici, D., 2009. Formation and structure of lithospheric shear zones with damage, *Physics of the Earth and Planetary Interiors*, 175, 115-126.
- Langdon, T.G., 1975. Grain boundary processes during creep. in *Rate Processes in Plastic Deformation of Materials*, pp. 410-433, eds. Li, J. C. M. & Mukherjee, M. K. American Society of Metals, Metals Park, OH.
- Langdon, T.G., 1994. A unified approach to grain boundary sliding in creep and superplasticity, *Acta Metallurgica et Materialia*, 42, 2437-2443.
- Lay, T., Hernlund, J. & Buffett, B.A., 2008. Core-mantle boundary heat flow, *Nature Geoscience*, 1, 25-32.
- Lenardic, A. & Moresi, L.N., 1999. Some thoughts on the stability of cratonic lithosphere: effects of buoyancy and viscosity, *Journal of Geophysical Research*, 104, 12747-12759.
- Lev, E. & Hager, B.H., 2008. Rayleigh-Taylor instabilities with anisotropic lithospheric viscosity, *Geophysical Journal International*, 173, 806-814.
- Li, P., Karato, S. & Wang, Z., 1996. High-temperature creep in fine-grained polycrystalline CaTiO_3 , an analogue material of $(\text{Mg,Fe})\text{SiO}_3$ perovskite, *Physics of Earth and Planetary Interiors*, 95, 19-36.

- Liebermann, R.C., 1982. Elasticity of minerals at high pressure and temperature. *in High Pressure Research in Geosciences*, pp. 1-14, ed. Schreyer, W. Schweizerbart, Stuttgart.
- Lifshitz, I.M., 1963. On the theory of diffusion-viscous flow of polycrystalline bodies, *Soviet Physics JETP*, 17, 909-920.
- Lifshitz, I.M. & Shikin, V.B., 1965. The theory of diffusional viscous flow of polycrystalline solids, *Soviet Physics, Solid State*, 6, 2211-2218.
- Mackwell, S.J., Kohlstedt, D.L. & Paterson, M.S., 1985. The role of water in the deformation of olivine single crystals, *Journal of Geophysical Research*, 90, 11319-11333.
- Mackwell, S.J., Zimmerman, M.E. & Kohlstedt, D.L., 1998. High-temperature deformation of dry diabase with application to tectonics on Venus, *Journal of Geophysical Research*, 103, 975-984.
- Manga, M., 1996. Mixing of heterogeneities in the mantle: effect of viscosity differences, *Geophysical Research Letters*, 23, 403-406.
- Meade, C. & Jeanloz, R., 1988. Yield strength of the B1 and B2 phases of NaCl, *Journal of Geophysical Research*, 93, 3270-3274.
- Mei, S. & Kohlstedt, D.L., 2000a. Influence of water on plastic deformation of olivine aggregates, 1. Diffusion creep regime, *Journal of Geophysical Research*, 105, 21457-21469.
- Mei, S. & Kohlstedt, D.L., 2000b. Influence of water on plastic deformation of olivine aggregates, 2. Dislocation creep regime, *Journal of Geophysical Research*, 105, 21471-21481.
- Merkel, S., Kubo, A., Miyagi, L., Speziale, S., Duffy, T.S., Mao, H.-K. & Wenk, H.-R., 2006. Plastic deformation of MgGeO₃ post-perovskite at lower mantle pressures, *Science*, 311, 644-646.
- Merkel, S., McNamara, A.K., Kubo, A., Speziale, S., Miyagi, L., Meng, Y., Duffy, T.S. & Wenk, H.-R., 2007. Deformation of (Mg,Fe)SiO₃ post-perovskite and D" anisotropy, *Science*, 316, 1729-1732.
- Merkel, S., Wenk, H.-R., Badro, J., Montagnac, G., Gillet, P., Mao, H.-K. & Hemley, R.J., 2003. Deformation of (Mg_{0.9},Fe_{0.1})SiO₃ perovskite aggregates up to 32 GPa, *Earth and Planetary Science Letters*, 209, 351-360.
- Miyagi, L., Kanitpanyacharoen, W., Kaercher, P., Lee, K.K.M. & Wenk, H.-R., 2011. Slip systems in MgSiO₃ post-perovskite: Implications for D" anisotropy, *Science*, 329, 1639-1641.
- Nabarro, F.R.N., 1948. Deformation of crystals by the motion of single ions. *in Report of a Conference on Strength of Solids*, pp. 75-90 The Physical Society of London.
- Nakada, M. & Karato, S., 2011. Low viscosity of the bottom of the Earth's mantle inferred from the analysis of Chandler wobble and tidal deformation, *Physics of the Earth and Planetary Interiors*, in press.
- Nakada, M. & Lambeck, K., 1989. Late Pleistocene and Holocene sea-level change in the Australian region and mantle rheology, *Geophysical Journal International*, 96, 497-517.
- Nicolas, A., 1978. Stress estimates from structural studies in some mantle peridotites, *Philosophical Transaction of Royal Society of London*, A288, 49-57.

- Nieh, T.G., Wadsworth, J. & Sherby, O.D., 1997. *Superplasticity in Metals and Ceramics*, edn, Vol., pp. Pages, Cambridge University Press, Cambridge.
- Nishihara, Y., Tinker, D., Kawazoe, T., Xu, Y., Jing, Z., Matsukage, K.N. & Karato, S., 2008. Plastic deformation of wadsleyite and olivine at high-pressures and high-temperatures using a rotational Drickamer apparatus (RDA), *Physics of the Earth and Planetary Interiors*, 170, 156-169.
- Oganov, A.R., Martonak, R., Laio, A., Raiteri, P. & Parrinello, M., 2005. Anisotropy of Earth's D" layer and stacking faults in the MgSiO₃ post-perovskite phase, *Nature*, 438, 1142-1144.
- Ohuchi, T., Karato, S. & Fujino, K., 2011. Strength of single crystal of orthopyroxene under the lithospheric conditions, *Contributions to Mineralogy and Petrology*, 161, 961-975.
- Orowan, E., 1940. Problems of plastic gliding, *Proceedings of the Physical Society*, 52, 8-21.
- Papuc, A.M. & Davies, G.F., 2008. The internal activity and thermal evolution of Earth-like planets, *Icarus*, 195, 447-458.
- Paterson, M.S., 1970. A high temperature high pressure apparatus for rock deformation, *International Journal of Rock Mechanics and Mining Sciences*, 7, 517-526.
- Paterson, M.S., 1990. Rock deformation experimentation. in *The Brittle-Ductile Transition in Rocks: The Heard Volume*, pp. 187-194, eds. Duba, A. G., Durham, W. B., Handin, J. W. & Wang, H. F. American Geophysical Union, Washington DC.
- Paterson, M.S. & Olgaard, D.L., 2000. Rock deformation tests to large shear strains in torsion, *Journal of Structural Geology*, 22, 1341-1358.
- Peale, S.J. & Cassen, P., 1978. Contribution of tidal dissipation to lunar thermal history, *Icarus*, 36, 245-269.
- Phillips, R.J., Zuber, M.T., Smrekar, S.E., Mellon, M.T., Head, J.W., Tanaka, K.L., Putzig, N.E., Milkovich, S.M., Campbell, B.A., Plaut, J.J., Safaeinili, A., Seu, R., Biccari, D., Carter, L.M., Picardi, G., Orosei, R., Mohit, P.S., Heggy, E., Zurek, R.W., Egan, A.F., Giacomoni, E., Russo, F., Cutigni, M., RPettinelli, E., Holt, J.W., Leuschen, C.J. & Marinangeli, L., 2008. Mars north polar deposits: Stratigraphy, age, and geodynamical response, *Science*, 320, 1182-1185.
- Poirier, J.-P., 1985. *Creep of Crystals*, edn, Vol., pp. Pages, Cambridge University Press, Cambridge.
- Poirier, J.-P. & Liebermann, R.C., 1984. On the activation volume for creep and its variation with depth in the Earth's lower mantle, *Physics of Earth and Planetary Interiors*, 35, 283-293.
- Pollack, H.K., 1986. Cratonization and the thermal evolution of the mantle, *Earth and Planetary Science Letters*, 80, 175-182.
- Post, A.D., Tullis, J. & Yund, R.A., 1996. Effects of chemical environment on dislocation creep of quartzite, *Journal of Geophysical Research*, 101, 22143-22155.
- Precigout, J., Gueydan, F., Gapais, D., Garrido, C.J. & Essaifi, A., 2007. Strain localisation in the subcontinental mantle - a ductile alternative to the brittle mantle, *Tectonophysics*, 445, 318-336.

- Raj, R. & Ashby, M.F., 1971. On grain boundary sliding and diffusional creep, *Metallurgical Transactions*, 2, 1113-1127.
- Ray, R.D., Eanes, R.J. & Lemoine, F.G., 2001. Constraints on energy dissipation in the Earth's body tide from satellite tracking and altimetry, *Geophysical Journal International*, 144, 471-480.
- Richards, M.A., Yang, W.S., Baumgardner, J.R. & Bunge, H.-P., 2001. Role of a low-viscosity zone in stabilizing plate tectonics: Implications for comparative planetology, *Geochemistry, Geophysics, Geosystems*, 2, 10.1029/2000GC000115.
- Riedel, M.R. & Karato, S., 1997. Grain-size evolution in subducted oceanic lithosphere associated with the olivine-spinel transformation and its effects on rheology, *Earth and Planetary Science Letters*, 148, 27-43.
- Rudnick, R.L. & Fountain, D.M., 1995. Nature and composition of the continental lower crust: the lower crustal perspective, *Review of Geophysics and Space Physics*, 33, 267-309.
- Rutter, E.H., 1976. The kinetics of rock deformation by pressure solution, *Philosophical Transaction of Royal Society of London*, A283, 203-219.
- Rybacki, E. & Dresen, G., 2000. Dislocation and diffusion creep of synthetic anorthite aggregates, *Journal of Geophysical Research*, 26017-26036.
- Rybacki, E. & Dresen, G., 2004. Deformation mechanism maps for feldspar rocks, *Tectonophysics*, 382, 173-187.
- Rybacki, E., Gootschalk, M., Wirth, R. & Dresen, G., 2006. Influence of water fugacity and activation volume on the flow properties of fine-grained anorthite aggregates, *Journal of Geophysical Research*, 111, 10.1029/2005JB003663.
- Saito, M. & Abe, Y., 1984. Consequences of anisotropic viscosity in the Earth's mantle, *Journal of the Seismological Society of Japan*, 37, 237-245.
- Schubert, G., Turcotte, D.L. & Olson, P., 2001. *Mantle Convection in the Earth and Planets*, edn, Vol., pp. Pages, Cambridge University Press, Cambridge.
- Sengör, A.M.C. & Burke, K., 1978. Relative timing of rifting and volcanism on Earth and its tectonic implications, *Geophysical Research Letters*, 5, 419-421.
- Shapiro, N., Hager, B.H. & Jordan, T.H., 1999. Stability and dynamics of the continental tectosphere, *Lithos*, 48, 135-152.
- Shimizu, I., 1994. Rock deformation by pressure solution and its implications to the rheology of lithosphere: a review, *Structural Geology*, 39, 153-164.
- Shimajuku, A., Kubo, T., Ohtani, E., Nakamura, T., Okazaki, R., Dohmen, R. & Chakraborty, S., 2009. Si and O diffusion in (Mg,Fe)₂SiO₄ wadsleyite and ringwoodite and its implications for the rheology of the mantle transition zone, *Earth and Planetary Science Letters*, 284, 103-112.
- Shimajuku, A., Kubo, T., Ohtani, E. & Yurimoto, H., 2004. Silicon self-diffusion in wadsleyite: Implication for rheology of the mantle transition zone and subducting slabs, *Geophysical Research Letters*, 31, 10.1029/2004GL020002.
- Singh, A.K., 1993. The lattice strain in a specimen (cubic system) compressed nonhydrostatically in an opposed anvil device, *Journal of Applied Physics*, 73, 4278-4286.
- Skemer, P.A. & Karato, S., 2008. Sheared lherzolite revisited, *Journal of Geophysical Research*, 113, 10.1029/2007JB005286.

- Solomatov, V.S., El-Khozondar, R. & Tikare, V., 2002. Grain size in the lower mantle: constraints from numerical modeling of grain growth in two-phase systems, *Physics of the Earth and Planetary Interiors*, 129, 265-282.
- Solomatov, V.S. & Moresi, L.N., 1997. Three regimes of mantle convection with non-Newtonian viscosity and stagnant lid convection on the terrestrial planets, *Geophysical Research Letters*, 24, 1907-1910.
- Spiers, C.J., De Meer, S., Niemeijer, A.R. & Zhang, X., 2004. Kinetics of rock deformation by pressure solution and the role of thin aqueous films. in *Physicochemistry of Water in Geological and Biological Systems*, pp. 129-158, eds. Nakashima, S., Spiers, C. J., Mercury, L., Fenter, P. A. & M.F. Hochella, J. Universal Academy Press, Inc., Tokyo.
- Sung, C.-M., Goetze, C. & Mao, H.-K., 1977. Pressure distribution in the diamond anvil press and shear strength of fayalite, *Review of Scientific Instruments*, 48, 1386-1391.
- Tachinami, C., Senshu, H. & Ida, S., 2011. Thermal evolution and lifetime of intrinsic magnetic fields of super-Earths in habitable zones, *The Astrophysical Journal*, 726, 10.10188/10004-10637X/10726/10182/10170.
- Tackley, P.J., 1998. Self-consistent generation of tectonic plates in three-dimensional mantle convection, *Earth and Planetary Science Letters*, 157, 9-22.
- Tackley, P.J., 2000. Self-consistent generation of tectonic plates in time-dependent, three dimensional mantle convection simulations, 2. Strain weakening and asthenosphere, *Geochemistry, Geophysics, Geosystems*, 1, 2000GC2000, 2043.
- Takei, Y. & Holtzman, B., 2009a. Viscous constitutive relations of solid-liquid composites in terms of grain boundary contiguity: 1. Grain boundary diffusion control model, *Journal of Geophysical Research*, 114, 10.1029/2008JB005850.
- Takei, Y. & Holtzman, B., 2009b. Viscous constitutive relations of solid-liquid composites in terms of grain boundary contiguity: 2. Compositional model for small melt fractions, *Journal of Geophysical Research*, 114, 10.1029/2008JB005851.
- Takei, Y. & Holtzman, B., 2009c. Viscous constitutive relations of solid-liquid composites in terms of grain boundary contiguity: 3. Causes and consequences of viscous anisotropy, *Journal of Geophysical Research*, 114, 10.1029/2008JB005852.
- Trampert, J. & van Heijst, H.J., 2002. Global azimuthal anisotropy in the transition zone, *Science*, 296, 1297-1299.
- Valencia, D. & O'Connell, R.J., 2009. Convection scaling and subduction on Earth and super-Earth, *Earth and Planetary Science Letters*, 286, 492-502.
- van Keken, P.E., Hauri, E.H. & Ballentine, C.J., 2002. Mantle mixing: the generation, preservation, and destruction of chemical heterogeneity, *Annual Review of Earth and Planetary Sciences*, 30, 493-525.
- Van Orman, J.A., Fei, Y., Hauri, E.H. & Wang, J., 2003. Diffusion in MgO at high pressure: constraints on deformation mechanisms and chemical transport at the core-mantle boundary, *Geophysical Research Letters*, 30, 10.1029/2002GL016343.

- Visser, K., Trampert, J., Lebedev, S. & Kennett, B.L.N., 2008. Probability of radial anisotropy in the deep mantle, *Earth and Planetary Science Letters*, 270, 241-250.
- Walker, A.M., Carrez, P. & Cordier, P., 2010. Atomic-scale models of dislocation cores in minerals: Progress and prospects, *Mineralogical Magazine*, 74, 381-413.
- Warren, J.M. & Hirth, G., 2006. Grain size sensitive deformation mechanisms in naturally deformed peridotites, *Earth and Planetary Science Letters*, 248, 438-450.
- Weertman, J., 1968. Dislocation climb theory of steady state creep, *Transactions of the American Society of Metals*, 61, 681-694.
- Weertman, J., 1975. High temperature creep produced by dislocation motion. in *Rate Processes in Plastic Deformation*, pp. 315-336, eds. Li, J. C. M. & Mukherjee, A. K. American Institute of Metals, Metals Park, OH.
- Weertman, J., 1999. Microstructural mechanisms of creep. in *Mechanics and Materials: Fundamentals and Linkages*, pp. 451-488, eds. Meyers, M. A., Armstrong, R. W. & Kirschner, H. John Wiley & Sons, New York.
- Weidner, D.J., 1998. Rheological studies at high pressure. in *Ultrahigh-Pressure Mineralogy*, pp. 492-524, ed. Hemley, R. J. The Mineralogical Society of America, Washington DC.
- Weidner, D.J., Li, L., Davis, M. & Chen, J., 2004. Effect of plasticity on elastic modulus measurements, *Geophysical Research Letters*, 31, 10.1029/2003GL019090.
- Weidner, D.J., Vaughan, M.T., Wang, L., Long, H., Li, L., Dixon, N.A. & Durham, W.B., 2010. Precise stress measurements with white synchrotron x-rays, *Review of Scientific Instruments*, 81, 013903.
- Wenk, H.-R., Lonardelli, I., Pehl, J., Devine, J.D., Prakapenka, V., Shen, G. & Mao, H.-K., 2004. In situ observation of texture development in olivine, ringwoodite, magnesiowüstite and silicate perovskite at high pressure, *Earth and Planetary Science Letters*, 226, 507-519.
- Wentzcovitch, R.M., Justo, J.F., Wu, Z., da Silva, C.R.S., Yuen, D.A. & Kohlstedt, D.L., 2009. Anomalous compressibility of ferropericlase throughout the iron spin cross-over, *Proceedings of National Academy of Sciences*, 106, 8447-8452.
- Williams, J.G., Boggs, D.H., Yoder, C.F., Ratcliff, J.T. & Dickey, J.O., 2001. Lunar rotational dissipation in solid body and molten core, *Journal of Geophysical Research*, 106, 27933-27968.
- Xu, J., Yamazaki, D., Katsura, T., Wu, X., Remmert, P., Yurimoto, H. & Chakraborty, S., 2011. Silicon and magnesium diffusion in a single crystal of MgSiO₃ perovskite, *Journal of Geophysical Research*, 116, 10.1029/2011JB00844.
- Xu, Y., Weidner, D.J., Chen, J., Vaughan, M.T., Wang, Y. & Uchida, T., 2003. Flow-law for ringwoodite at subduction zone conditions, *Physics of Earth and Planetary Interiors*, 136, 3-9.
- Yamazaki, D. & Karato, S., 2001. Some mineral physics constraints on the rheology and geothermal structure of Earth's lower mantle, *American Mineralogist*, 86, 385-391.
- Yamazaki, D., Kato, T., Ohtani, E. & Toriumi, M., 1996. Grain growth rates of MgSiO₃ perovskite and periclase under lower mantle conditions, *Science*, 274, 2052-2054.

- Yamazaki, D., Kato, T., Toriumi, M. & Ohtani, E., 2000. Silicon self-diffusion in MgSiO₃ perovskite at 25 GPa, *Physics of Earth and Planetary Interiors*, 119, 299-309.
- Zamora, M. & Poirier, J.-P., 1983. Experiments in anisothermal transformation plasticity: the case of cobalt. Geophysical implications, *Mechanics of Materials*, 2, 193-202.
- Zhang, S. & Karato, S., 1995. Lattice preferred orientation of olivine aggregates deformed in simple shear, *Nature*, 375, 774-777.
- Zimmerman, M.E. & Kohlstedt, D.L., 2004. Rheological properties of partially molten lherzolite, *Journal of Petrology*, 45, 275-298.

Fig. 1 Rheological properties (effective viscosities) depend on various parameters

(a) stress dependence of viscosity behavior

Power-law regime in the low stress region and the Peierls mechanism in the high stress region are shown. If lab experiments are done in the same regime as Earth (lab-I), the results can be extrapolated to Earth, but if lab experiments are made in the different regime (lab-II), extrapolation cannot be justified.

(b) temperature dependence (low T versus high T mechanisms)

Similar to (1), lab data can be extrapolated only when experiments are made in the same regime as in Earth (lab-I).

(c) grain-size dependence

A change in the deformation mechanisms with grain-size occurs at different grain-size between geological deformation and laboratory experiments. To simulate, in the lab, how grain-size may affect rheological properties, one should use smaller grain-size than grain-size in Earth.

(d) water content dependence

Water content affects the viscosity of a rock, but the manner in which water affects the viscosity depends on the mechanisms of deformation.

Fig. 2 Cartoons illustrating physical processes of plastic deformation

(a) Diffusion creep

When grain-boundaries are weak, grain-boundary sliding occurs upon applying a stress. This leads to the variation in the normal stress at grain-boundaries with different orientation, which in turn causes the concentration gradient in vacancies. Diffusive mass transport occurs due to this concentration gradient in vacancies that leads to plastic deformation. Diffusional mass transport relaxes stress concentration, and steady-state creep occurs corresponding to the steady-state relaxed stress distribution. Diffusional mass transport occurs both inside of grains and along grain-boundaries.

(b) dislocation creep (\perp indicates a dislocation)

Crystal dislocations are generated in a crystal and the propagation of crystal dislocations results in finite strain of a crystal. The rate of deformation by this mechanism is proportional to dislocation density and its mobility and hence in general a non-linear function of stress. Dislocations move only along certain crystallographic orientations. Therefore plastic deformation by dislocation motion is anisotropic.

Fig. 3 Schematic diagram showing the thermally activated processes in dislocation creep

(a) diffusion-controlled dislocation climb and in (b) dislocation glide over the Peierls potential

Dislocation climb requires diffusion of atoms from or to a jog of the dislocation line. When the density of jog is high, all portions of a dislocation line act as sources or sinks for diffusion, whereas when the density of jog is small, then dislocation climb requires the creation of jogs. The rate of diffusion by thermal

activation assisted by stress will be proportional to

$$\exp\left(-\frac{H_o^* - \sigma\Omega}{RT}\right) - \exp\left(-\frac{H_o^* + \sigma\Omega}{RT}\right) \approx 2 \cdot \frac{\sigma\Omega}{RT} \cdot \exp\left(-\frac{H_o^*}{RT}\right) \left(\frac{\sigma\Omega}{RT} \ll 1\right).$$

Dislocation glide over the Peierls potential involves the formation and migration of a pair of kinks. This figure shows a saddle point configuration for the formation of a pair of kinks. ΔA is the area swept by a dislocation to form the saddle point configuration. Because the force per unit length of a dislocation by the external stress is σb , the extra work done by the stress is $-\Delta A(\sigma) \cdot b \cdot \sigma$. This term $\left(\frac{\Delta A(\sigma) \cdot b \cdot \sigma}{RT}\right)$ is large at high stress, and should be included explicitly leading to the high sensitivity of strain-rate on stress.

Fig. 4 A deformation mechanism map for olivine (after (Karato, 2010b))

P=7 GPa and T=1700 K (~300 km depth), dry condition

Dominant deformation mechanisms in the hot mantle are either diffusion or power-law (dislocation) creep although in the laboratory conditions many mechanisms may compete depending on the precise conditions. A similar conclusion is obtained for other minerals (see (Karato, 1998b)).

Fig. 5 A schematic diagram showing a possible mechanism of shear localization by grain-size reduction due to dynamic recrystallization

(a) A schematic drawing of a microstructure of dynamically deforming rock after a stress pulse

Upon a stress pulse, small dynamically recrystallized grains are formed along pre-existing grain-boundaries

- (b) Deformation mechanism map (on a grain-size versus stress) showing the dominant mechanisms of deformation together with the grain-size versus stress relationship for dynamically recrystallized grains

Upon a stress pulse, small grains are formed (A: initial stress and grain-size, B: grain-size after dynamic recrystallization). If the size of new grains is smaller than the mechanism boundary between diffusion and dislocation creep, then that region is weak and promotes shear localization. At relatively low temperatures, the mechanism boundary moves to high stress, coarse-grain region and shear localization is likely.

Fig. 6 Typical apparatus used for the experimental studies of plastic deformation

- (a) A solid-medium, high-pressure deformation apparatus designed by Griggs in 1960s

This apparatus can be operated to $P < 3$ GPa and $T < 1600$ K. Stress (load) is measured by an external load cell and a correction for friction is needed to determine the stress.

- (b) A gas-medium, low-pressure deformation apparatus designed by Paterson in 1970s

This apparatus can be operated to $P < 0.5$ GPa and $T < 1600$ K. Stress (load) is measured by an internal load cell and stress can be determined by high precision.

- (c) A solid-medium apparatus where hydrostatic compression and uni-axial compression can be separated (D-DIA)

This apparatus can be operated to $P \sim 10$ GPa (or higher) and $T \sim 1600$ K. Stress and strain are measured by X-ray diffraction and imaging respectively.

- (c) A solid-medium apparatus designed in our lab (RDA) where torsion tests can be performed at high P and T

This apparatus has been operated to $P \sim 23$ GPa and $T \sim 2000$ K. Stress and strain are measured by X-ray diffraction and imaging respectively.

Fig. 7 The pressure-temperature range of operation of various deformation apparatus

Fig. 8 (a) Dependence of strain-rate on temperature (CaTiO₃ perovskite data from (Li *et al.*, 1996))

- (b) Dependence of strain-rate on stress (lherzolite (dry), data from (Zimmerman and Kohlstedt, 2004))

At small stresses, strain-rate is linearly proportional to stress, whereas at high stresses, strain-rate is proportional to some power of stress (in this case $\dot{\epsilon} \propto \sigma^4$).

- (c) Dependence of strain-rate on grain-size (CaTiO₃ perovskite, data from (Li *et al.*, 1996))

m is the grain-size sensitivity (see equation (14)). $m \sim 2$ (and stress dependence is linear) suggesting diffusion creep due to volume diffusion.

(d) Dependence of creep strength on temperature (olivine (dry), data from (Goetze, 1978)) showing two regimes of deformation: creep strength is highly sensitive to temperature at high temperature but only weakly sensitive to temperature at low temperatures. Deformation mechanism in the low temperature regime is likely the Peierls mechanism. (Numbers in the figure correspond to $\log_{10} \dot{\epsilon} (s^{-1})$)

Fig. 9 Influence of pressure on effective viscosity for various values of activation volume

$$\eta / \eta_0 = \exp\left(\frac{PV^*}{RT}\right) \text{ is used. } T=2000 \text{ K.}$$

Fig. 10 Viscosity-depth relationships calculated using various experimental results on high-pressure rheological properties of olivine (Karato, 2010b)

Thick curves correspond to results by (Kawazoe *et al.*, 2009) (1) (dry) and (Karato and Jung, 2003) (7,8) ((7): 1,000 ppm H/Si, (8): 10,000 ppm H/Si) where water content was controlled, deformation mechanisms are identified and appropriate thermodynamic formula was used. Other results ((2), (3), (4), (5), (6)) are from studies where unreasonable extrapolations are made or the influence of water content was not examined. For the detailed discussions on these results, see (Karato, 2010b).

Fig. 11 Influence of pressure on the creep strength of olivine (from (Kawazoe *et al.*, 2009))

Different stresses at the same pressure correspond to the stress estimate using different diffracting lattice planes. V^* is activation volume (in cm^3/mol)

Fig. 12 Influence of water fugacity on the creep strength of (a) quartz (Post *et al.*, 1996) and (b) olivine (Mei and Kohlstedt, 2000b)

Stress needed for deformation (creep strength) decreases with water fugacity. In these experiments, water fugacity was changed by changing the confining pressure

Fig. 13 Pressure versus creep strength relationship in a water-saturated system (modified from (Karato, 2010b))

Creep strength (stress) under water-saturated conditions initially decreases with pressure because of the increase in the water content in olivine, but eventually increases with pressure at higher pressures. In the pressure range used by (Mei and Kohlstedt, 2000a, Mei and Kohlstedt, 2000b) the latter effect is not visible and the extrapolation of such data to higher pressures cannot be done with any confidence (errors in the creep strength (viscosity) at ~ 400 km is a factor of $\sim 10^6$). The pressure range used by (Karato and Jung, 2003) covers both regions and the key parameters were well constrained and the results can be extrapolated to higher pressures.

Fig. 14 Analysis of the influence of water on creep strength in olivine under water-saturated conditions (after (Karato and Jung, 2003))

(a) the determination of the water content exponent r

(b) the determination of the activation volume V_{wet}^* (shown as V_w^*)

Fig. 15 Crystal structure-creep strength systematics (normalization of strain-rate is not made in these studies, but the Debye frequency varies only modestly among different materials)

(a) A comparison of creep strength of various garnets as a function of temperature (Karato *et al.*, 1995a)

(b) A comparison of creep strength of garnet after normalization (Karato *et al.*, 1995a)

(c) crystal structure-plasticity systematics (modified from (Karato, 2011a))

Fig. 16 Influence of partial melt on deformation of olivine aggregates (after (Kohlstedt, 2002))

The empirical relation $\dot{\epsilon}(\phi) = \dot{\epsilon}(0) \cdot \exp(\alpha\phi)$ is used to fit the data (ϕ : volume fraction of melt).

Fig. 17 The strength profile of the lithosphere (after (Kohlstedt *et al.*, 1995))

(a) oceanic lithosphere (b) continental lithosphere

In the shallow region, brittle failure controls the strength, whereas in the deep region, plastic flow controls the strength. Kohlstedt *et al.* assumed dry (water-free) oceanic lithosphere and wet (water-saturated) continental lithosphere.

Fig. 18 Effect of removal of water on the change in viscosity under the deep upper mantle (~300 km) conditions (after (Karato, 2010b))

Removal of water from initially water-rich condition (~0.01 wt%) to nearly dry conditions increases viscosity. The degree to which viscosity changes depends on the

viscosity of dry olivine which depends on the activation volume, V^* . The viscosity increases more than 10^3 if the activation volume for dry olivine is larger than $10 \text{ cm}^3/\text{mol}$.

Fig. 19 The depth variation in the effective viscosity in the upper mantle (modified after (Karato and Jung, 2003))

A thick grey curve corresponds to a likely viscosity-depth variation. Thin curves show the viscosity-depth variation for a range of fixed water content. Viscosity changes with depth due to the depth variation in temperature and pressure, and in water content. In this model, the water content changes from nearly “dry” (zero water content) to ~ 1000 ppm H/Si at ~ 70 km.

Fig. 20 Deformation mechanism map for ringwoodite (after (Karato *et al.*, 1998))

T: temperature, T_m : melting temperature, L: grain-size, b: the length of the Burgers vector, σ : stress, μ : shear modulus

The experiments were conducted at $\sigma / \mu \approx 10^{-2}$. In Earth’s interior, $\sigma / \mu \approx 10^{-5} - 10^{-3}$ and the grain-size for the mechanism change will scale as $L / L_o = (\sigma / \sigma_o)^{-\frac{n-1}{m}}$ where n is the stress exponent and m is the grain-size exponent. Therefore at lower stresses in Earth, the transition grain-size will be larger. Results similar to these were obtained by (Kawazoe *et al.*, 2010).

Fig. 21 Influence of temperature on the grain-size of wadsleyite (ringwoodite) formed by transformation from olivine in a slab (after (Riedel and Karato, 1997))

Fig. 22 Rheological properties of subducted lithosphere in the upper mantle and the transition zone (after (Karato *et al.*, 2001))

- (a) A schematic diagram showing a subducted slab (F is the force causing bending)
- (b) Viscosity distribution in subducted slabs (top: a warm slab, bottom: a cold slab)
- (c) The slab strength (measured by the flexural viscosity) versus slab temperature relationship (flexural viscosity is defined by $4h^3 \int_{-1/2}^{1/2} \eta(x) \cdot x^2 \cdot dx$ where h is the thickness of a slab and η is effective viscosity)

The resistance for slab bending is characterized by the flexural viscosity (Karato *et al.*, 2001). The slab strength increases with decreasing temperature in the high-temperature regime, whereas it decreases with decreasing temperature in the low-temperature regime. The former is caused by normal temperature sensitivity of viscosity while the latter is caused by the anomalous temperature sensitivity of viscosity caused by the strong temperature sensitivity of grain-size after a phase transformation (see **Fig. 21**).

Note that the central portion of a cold slab is weakened by grain-size reduction (**Fig. 22b**) that makes slab deformation possible. However, even after weakening, the flexural viscosity is still high (higher than that at trenches ($\sim 10^{37}$ Nms)) suggesting that the energy dissipation by deep slab deformation may control the rate of mantle convection.

Fig. 23 The viscosity-depth profiles for the lower mantle calculated from diffusion coefficients (from (Yamazaki and Karato, 2001))

(a) $dT/dz=0.3$ K/km and (b) $dT/dz=0.6$ K/km

In both cases, the pressure dependence of viscosity was calculated by the elastic strain energy model where the activation free energy is assumed to be proportional to the strain energy. The experimental results on the activation volume are consistent with the strain energy model.

Fig. 24 A schematic diagram showing the depth variation of viscosity in the mantle of super-Earth where the maximum pressure reaches ~ 1 TPa (from (Karato, 2011a))

Under these high-pressure conditions, a commonly held view of higher viscosity at higher pressure will not work. Several processes including (i) a change in diffusion mechanism, (ii) a change to a more compact crystal structure ($B1 \rightarrow B2$, decomposition of post-perovskite) and (iii) transition to metals will weaken the material.

Table 1 Constitutive relationship for several deformation mechanisms

(a) Power-law constitutive relation

This type of flow law works at low stresses ($\sigma / \mu < 10^{-3}$, μ : shear modulus)

$$\dot{\epsilon} = A \left(\frac{\sigma}{\mu} \right)^n \left(\frac{L}{b} \right)^{-m} \exp \left(-\frac{H^*}{RT} \right)$$

<i>mechanism</i>	<i>n</i>	<i>m</i>
Diffusion creep (volume diffusion)	1	2
Diffusion creep (grain-boundary diffusion)	1	3
Diffusion creep (reaction controlled)	1	1
Dislocation creep (power-law creep)	3-5	0
Grain-boundary sliding + dislocation creep	2	2
	2	1
	2	3

(b) Exponential constitutive relation

This type of flow law works at high stresses ($\sigma / \mu > 10^{-3}$, μ : shear modulus)

$$\dot{\epsilon} = B \left(\frac{\sigma}{\mu} \right)^2 \exp \left[-\frac{H^*}{RT} \left\{ 1 - \left(\frac{\sigma}{\sigma_0} \right)^q \right\}^s \right], \quad 0 \leq q \leq 1, \quad 1 \leq s \leq 2$$

<i>mechanism</i>	<i>q</i>	<i>s</i>
Discrete obstacle	1	1
Peierls barrier (low stress)	1/2	1
Peierls barrier (high stress)	1	2

Table 2 Flow laws for power-law creep (including diffusion creep)

The flow law $\dot{\epsilon} = A \cdot f_{H_2O}^r \cdot \sigma^n \cdot L^{-m} \cdot \exp\left(-\frac{E^*+PV^*}{RT}\right)$ is assumed.

units: A ($s^{-1} (MPa)^{-r-n} (\mu m)^m$), E^* (kJ/mol), V^* (cm^3/mol)

	$\log_{10}A$	r	n	m	E^*	V^*	P	T	L	<i>apparatus</i>	<i>Melt, water</i>	<i>ref.</i>
--	--------------	-----	-----	-----	-------	-------	-----	-----	-----	------------------	--------------------	-------------

quartz ¹	-4.0	1	4	-	223	-	1.5	1173-1373	100	liquid-Griggs ²⁰	Melt free	(1)
quartz ¹	-	2 ¹⁹	-	-	-	-	0.71-1.72	1173	100	liquid-Griggs		(2)
feldspar ²	2.6	-	3	-	356	-	0.3	1270-1480	2.7-3.4	Paterson	“wet” (~11500 ppm H/Si)	(3)
feldspar ²	13	-	3	-	648	-	0.3	1370-1480	2.7-3.4	Paterson	“dry” (~640 ppm H/Si)	(3)
feldspar ²	1.7	-	1	3	170	-	0.3	1180-1480	2.7-3.4	Paterson	“wet” (~11500 ppm H/Si)	(3)
feldspar ²	2.6	-	1	3	467	-	0.3	1370-1480	2.7-3.4	Paterson	“dry” (~640 ppm H/Si)	(3)
diopside ³	9.8	-	4.7	-	760	-	0.3-0.43	1373-1523	5.2-330	Paterson	“dry” (<10 ppm H/Si)	(4)
diopside ³	15	-	1	3	560	-	0.3-0.43	1373-1523	5.2-330	Paterson	“dry” (<10 ppm H/Si)	(4)
diopside ⁴	0.09	1.4	1	3	340	14	0.1-0.3	1321-1421	6.6-10.5	Paterson	“wet” (98-216 ppm H/Si)	(5)
diopside ⁵	6.7	3.0	2.7	-	670	-	0.15-0.30	1373-1473	~500	Paterson	“wet” (saturated)	(6)
enstatite ⁶	-2.2	-	2.8	-	270	-	1	1273-1673	~1000	solid-Griggs	“wet” (water from talc)	(7)
enstatite ⁷	8.8	-	2.9	-	600	-	0.45	1473-1523	~10	Paterson	“dry” (see note ¹⁰)	(8)
garnet ⁸	13	-	3.2	-	270	-	4.3-6.8	1113-1573	2-10	D-DIA ²¹	“dry” (<5 ppm H/Si)	(9)
garnet ⁹	7.1	-	2.7	-	530	-	0.0001	1370-1430	-	MTS ²²	dry	(10)
garnet ¹⁰	5.1	-	1.1	2.5	347	-	0.0001	1373-1543	2-6	dead weight	“dry” (~100 ppm H/Si)	(11)
olivine ¹¹	3.2 ¹⁸	1 ¹⁸	3	-	470	20 ¹⁸	0.1-0.45	1393-1573	12-17	Paterson	“wet” (water-saturated)	(18)
olivine ¹¹	4.7 ¹⁸	1 ¹⁸	1.1	3	295	20 ¹⁸	0.1-0.45	1473-1573	12-17	Paterson	“wet” (water-saturated)	(12)
olivine ¹¹	6.8	-	1	3	315	-	0.3	1473-1523	10-14	Paterson	“dry” (<50 ppm H/Si)	(13)
olivine ¹¹	5.8	-	3	-	510	-	0.3	1473-1573	14-18	Paterson	“dry” (<50 ppm H/Si)	(14)
olivine ¹¹	5.0	-	3.5	-	530	15-20	4.9-9.6	1300-1870	~10	RDA ²³	“dry” (<100 ppm H/Si)	(15)
olivine ¹¹	2.9	1.2	3	-	470	24	0.1-2.0	1473	12-40	solid-Griggs	“wet” (water-saturated)	(16)
diabase ¹²	-1.2	-	3.1	-	276	-	0.35-0.45	1073-1273	~50	gas apparatus	“wet” (saturated)	(17)
diabase ¹²	0.92	-	4.7	-	485	-	0.4-0.5	1213-1345	~50	Paterson	“dry” (<10 ppm H/Si)	(18)
eclogite ¹³	3.3	-	3.4	-	480	-	3	1450-1600	30-100	liquid-Griggs	~1000 ppm H/Si	(19)
peridotite ¹⁴	7.6	-	3.5	-	600	-	0.45	1473-1523	~10	Paterson	“dry”	(8)
peridotite ¹⁵	6.1	-	2.2	-	338	-	0.6	1173-1275	1-2	gas-apparatus	“wet” (~0.5 wt%)	(20)
peridotite ¹⁶	8.8	-	1.7	3	538	-	0.0001	1473-1558	8-25	dead weight	dry	(21)
peridotite ¹⁷	9.1	-	1	3	370	-	0.3	1373-1573	8-34	Paterson	“dry” (<30 ppm H/Si)	(22)
peridotite ¹⁷	4.8	-	4.3	-	550	-	0.3	1373-1573	8-34	Paterson	“dry” (<30 ppm H/Si)	(22)

(1): (GLEASON and TULLIS, 1995), (2): (POST et al., 1996), (3): (RYBACKI and DRESEN, 2000), (4): (BYSTRICKY and MACKWELL, 2001), (5): (HIER-MAJUMDER et al., 2005), (6): (Chen et al., 2006), (7): (ROSS and NIELSEN, 1978), (8): (LAWLIS, 1998), (9): (LI et al., 2006), (10): (Karato et al., 1995), (11): (WANG and JI, 2000), (12): (MEI and KOHLSTEDT, 2000b), (13): (MEI and KOHLSTEDT, 2000a), (14): (HIRTH and KOHLSTEDT, 1995), (15): (Kawazoe et al., 2009), (16): (KARATO and JUNG, 2003), (17): (CARISTAN, 1982), (18): (MACKWELL et al., 1998), (19): (JIN et al., 2001), (20): (MCDONNELL et al., 2000), (21): (JI et al., 2001), (22): (ZIMMERMAN and KOHLSTEDT, 2004)

¹: Black Hills quartzite, β -quartz

²: synthetic specimens ($\text{CaAl}_2\text{Si}_2\text{O}_8$)

³: synthetic specimens ($\text{Ca}(\text{Mg}_{0.8}\text{Fe}_{0.2})\text{Si}_2\text{O}_6$)

⁴: synthetic specimens ($\text{Ca}_{0.97}(\text{Mg}_{0.8}\text{Fe}_{0.2})\text{Si}_{1.99}\text{O}_6$)

⁵: $\text{Ca}_{0.98}\text{Mg}_{0.79}\text{Fe}_{0.256}\text{Al}_{0.017}\text{Na}_{0.012}\text{Si}_2\text{O}_6$

⁶: $(\text{Mg}_{0.89}\text{Fe}_{0.8}\text{Ca}_{0.3})\text{SiO}_3$

⁷: synthetic specimens ($(\text{Mg}_{0.94}\text{Fe}_{0.04}\text{Ca}_{0.02})_2\text{Si}_2\text{O}_6$, $(\text{Mg}_{0.906}\text{Fe}_{0.091}\text{Ni}_{0.003})_2\text{Si}_2\text{O}_6$). Water content was not measured.

⁸: synthetic specimens (Py, $\text{Py}_{70}\text{Alm}_{16}\text{Gr}_{14}$)

⁹: A universal flow law based on the results on different garnets

¹⁰: synthetic specimens ($\text{Py}_{88}\text{Alm}_{10}\text{Gr}_2$)

¹¹: synthetic specimens

¹²: Maryland diabase

¹³: synthetic specimens (~50% garnet, ~40% omphacite, ~10% quartz)

¹⁴: synthetic specimens San Carlos olivine + orthopyroxene mixture (60:40), no report on water content.

¹⁵: synthetic specimens forsterite and Mg-enstatite (97:03 to 80:20).

¹⁶: synthetic specimens forsterite + Mg-enstatite (60:40).

¹⁷: lherzolite (62% olivine, 26% orthopyroxene, 10% clinopyroxene, 2% spinel)

¹⁸: A , r , V^* are not determined separately. Assuming $V^*=20\text{ cm}^3/\text{mol}$, A and r were calculated.

¹⁹: $r/n=0.5$ was constrained by the experiments. If $n=4$ then $r=2$.

²⁰: Influence of friction is reduced using a liquid pressure confining medium.

²¹: One type of high-pressure deformation apparatus operated to ~10 GPa.

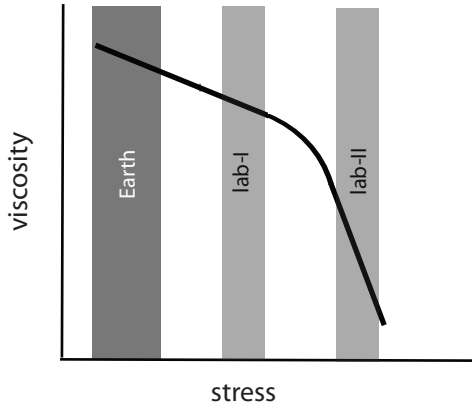
²²: A room pressure deformation apparatus controlled by a servo system.

²³: One type of high-pressure deformation apparatus operated to ~23 GPa.

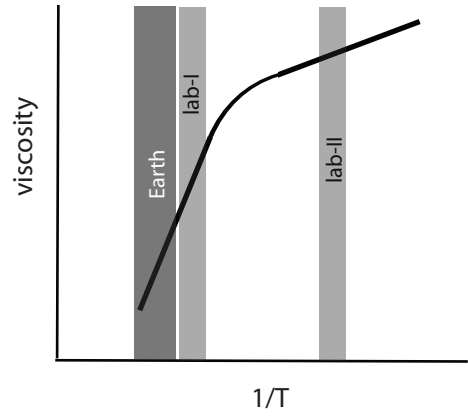
- Bystricky, M. and Mackwell, S.J., 2001. Creep of dry clinopyroxene aggregates. *Journal of Geophysical Research*, 106: 13443-13454.
- Caristan, Y., 1982. The transition from high-temperature creep to fracture in Maryland diabase. *Journal of Geophysical Research*, 887: 6781-6790.
- Chen, S., Hiraga, T. and Kohlstedt, D.L., 2006. Water weakening of clinopyroxene in the dislocation creep regime. *Journal of Geophysical Research*, 111: 10.1029/2005JB003885.
- Gleason, G.C. and Tullis, J., 1995. A flow law for dislocation creep of quartz aggregates determined with the molten salt cell. *Tectonophysics*, 247: 1-23.
- Hier-Majumder, S., Mei, S. and Kohlstedt, D.L., 2005. Water weakening of clinopyroxene in diffusion creep regime. *Journal of Geophysical Research*, 110: 10.1029/2004JB003414.
- Hirth, G. and Kohlstedt, D.L., 1995. Experimental constraints on the dynamics of partially molten upper mantle: deformation in the diffusion creep regime. *Journal of Geophysical Research*, 100: 1981-2001.
- Ji, S., Wang, Z. and Wirth, R., 2001. Bulk flow strength of forsterite-enstatite composites as a function of forsterite content. *Tectonophysics*, 341: 69-93.
- Jin, Z.M., Zhang, J., Green, H.W., II. and Jin, S., 2001. Eclogite rheology: implications for subducting lithosphere. *Geology*, 29: 667-670.
- Karato, S. and Jung, H., 2003. Effects of pressure on high-temperature dislocation creep in olivine polycrystals. *Philosophical Magazine*, A, 83: 401-414.
- Karato, S., Wang, Z., Liu, B. and Fujino, K., 1995. Plastic deformation of garnets: systematics and implications for the rheology of the mantle transition zone. *Earth and Planetary Science Letters*, 130: 13-30.
- Kawazoe, T., Karato, S., Otsuka, K., Jing, Z. and Mookherjee, M., 2009. Shear deformation of dry polycrystalline olivine under deep upper mantle conditions using a rotational Drickamer apparatus (RDA). *Physics of the Earth and Planetary Interiors*, 174: 128-137.
- Lawlis, J.D., 1998. High Temperature Creep of Synthetic Olivine-Enstatite Aggregates. Ph D Thesis, The Pennsylvania State University, 131 pp.
- Li, L., Raterron, P., Weidner, D.J. and Long, H., 2006. Plastic flow of pyrope at mantle pressure and temperature. *American Mineralogist*, 91: 517-525.
- Mackwell, S.J., Zimmerman, M.E. and Kohlstedt, D.L., 1998. High-temperature deformation of dry diabase with application to tectonics on Venus. *Journal of Geophysical Research*, 103: 975-984.
- McDonnell, R.D., Peach, C.J., van Roemund, H.L.M. and Spiers, C.J., 2000. Effect of varying enstatite content on the deformation behavior of fine-grained synthetic peridotite under wet conditions. *Journal of Geophysical Research*, 105: 13535-13553.

- Mei, S. and Kohlstedt, D.L., 2000a. Influence of water on plastic deformation of olivine aggregates, 1. Diffusion creep regime. *Journal of Geophysical Research*, 105: 21457-21469.
- Mei, S. and Kohlstedt, D.L., 2000b. Influence of water on plastic deformation of olivine aggregates, 2. Dislocation creep regime. *Journal of Geophysical Research*, 105: 21471-21481.
- Post, A.D., Tullis, J. and Yund, R.A., 1996. Effects of chemical environment on dislocation creep of quartzite. *Journal of Geophysical Research*, 101: 22143-22155.
- Ross, J.V. and Nielsen, K.C., 1978. High-temperature flow of wet polycrystalline enstatite. *Tectonophysics*, 44: 233-261.
- Rybacki, E. and Dresen, G., 2000. Dislocation and diffusion creep of synthetic anorthite aggregates. *Journal of Geophysical Research*(105): 26017-26036.
- Wang, Z. and Ji, S., 2000. Diffusion creep of fine-grained garnetite: implications for the flow strength of subducting slabs. *Geophysical Research Letters*, 27: 2333-2336.
- Zimmerman, M.E. and Kohlstedt, D.L., 2004. Rheological properties of partially molten lherzolite. *Journal of Petrology*, 45: 275-298.

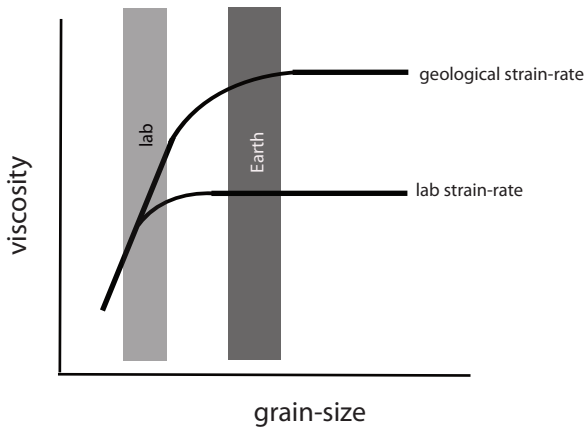
(a) stress dependence



(b) temperature dependence



(c) grain-size dependence



(d) water content dependence

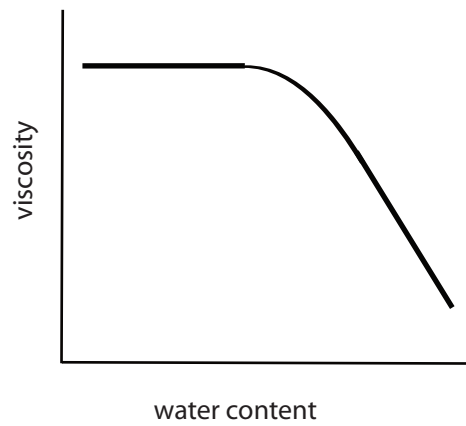
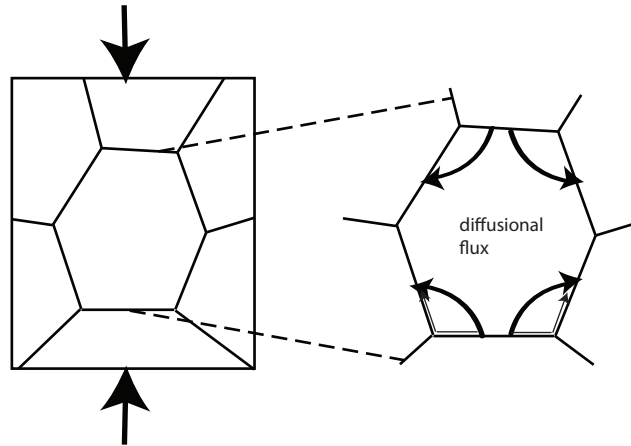


Fig. 1 (Karato-I)

(a) diffusion creep



(b) dislocation creep

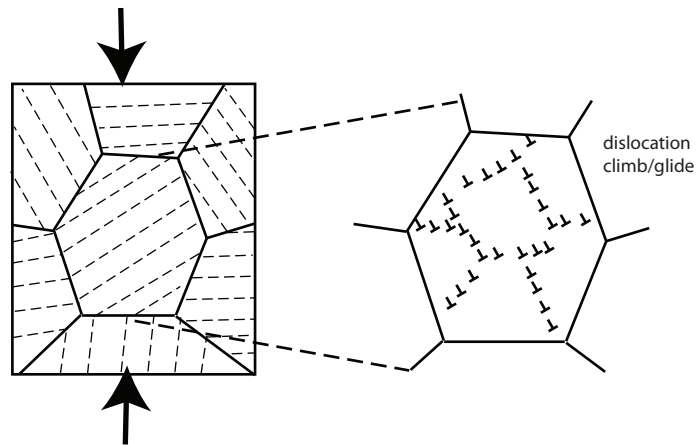
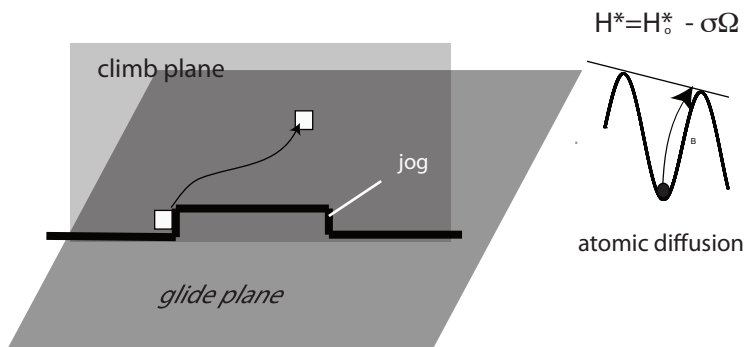


Fig. 2 (Karato-I)

(a) diffusion-controlled dislocation climb



(b) dislocation glide over the Peierls potential

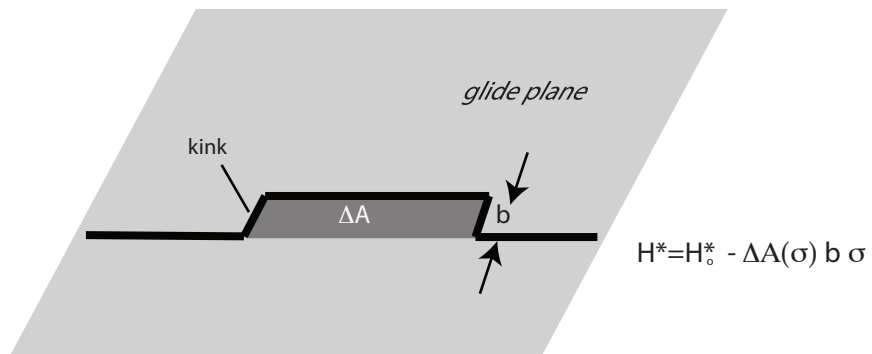


Fig. 3 (Karato-I)

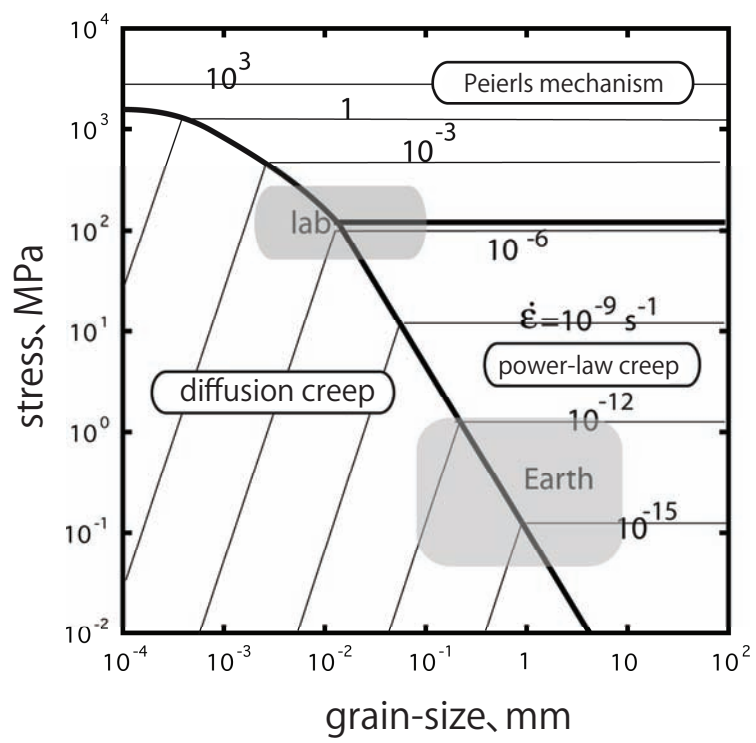
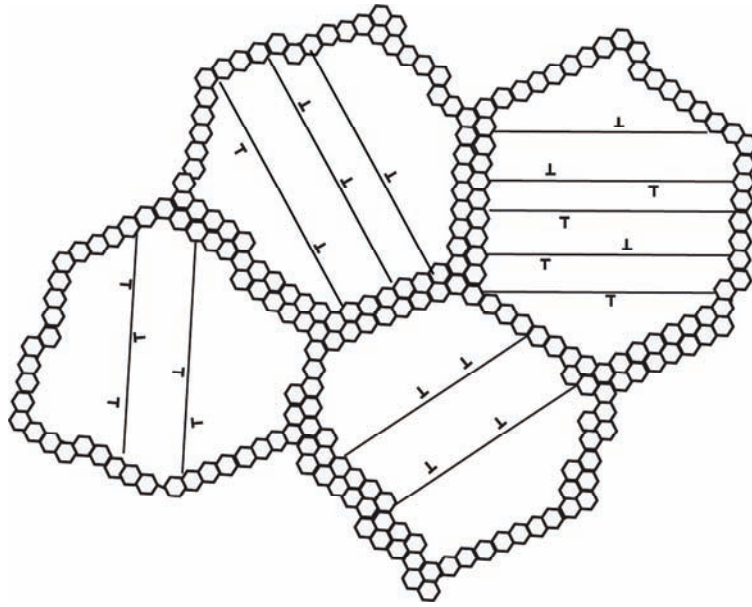


Fig. 4 (Karato-I)

(a)



(b)

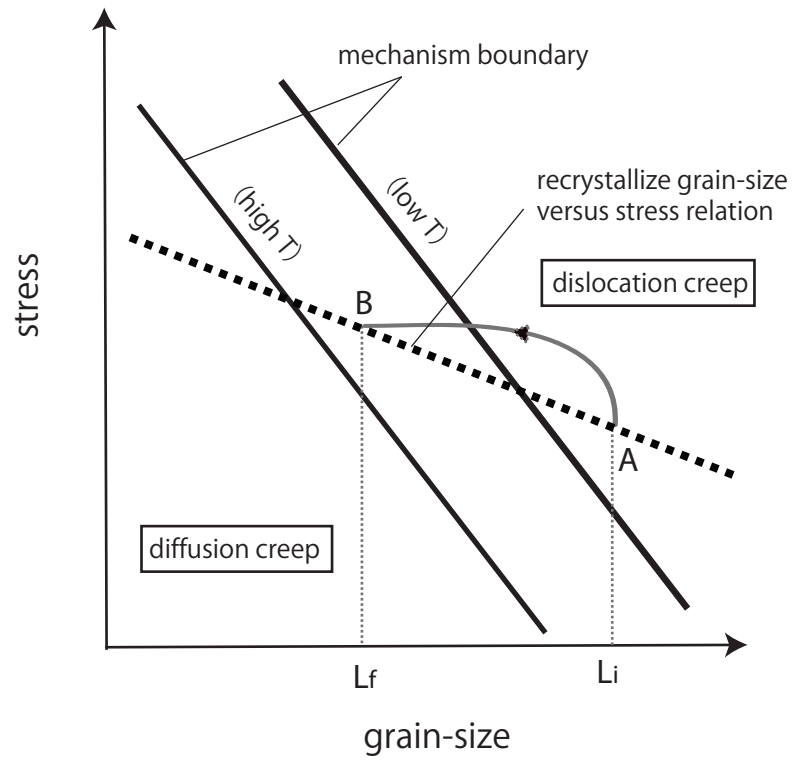


Fig. 5 (Karato-I)

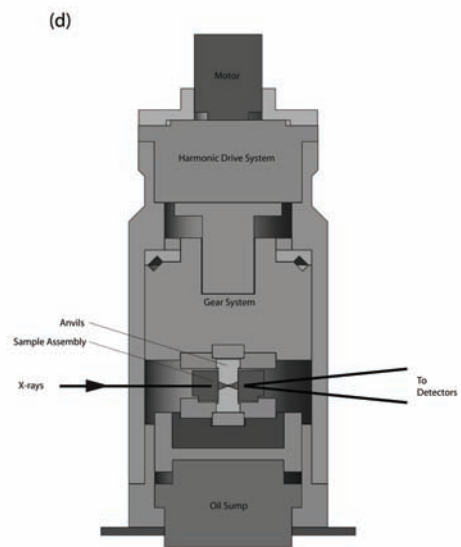
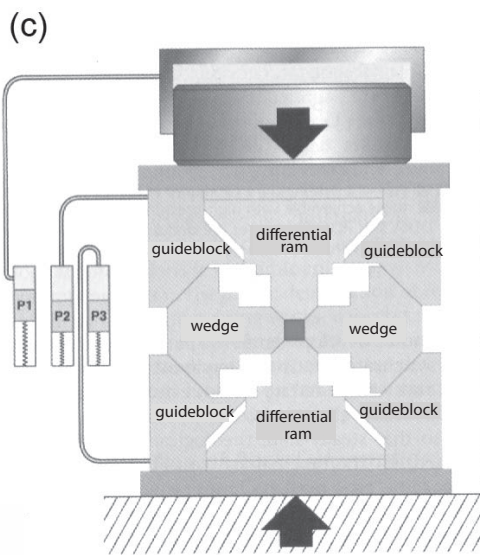
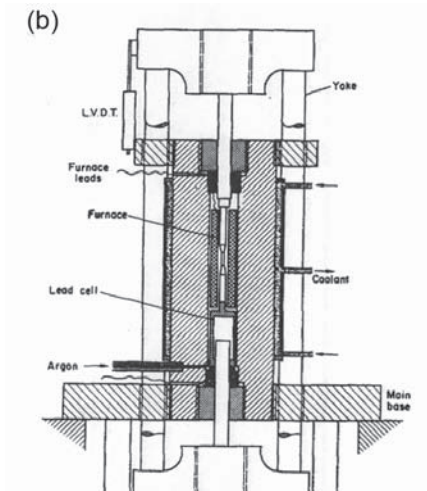
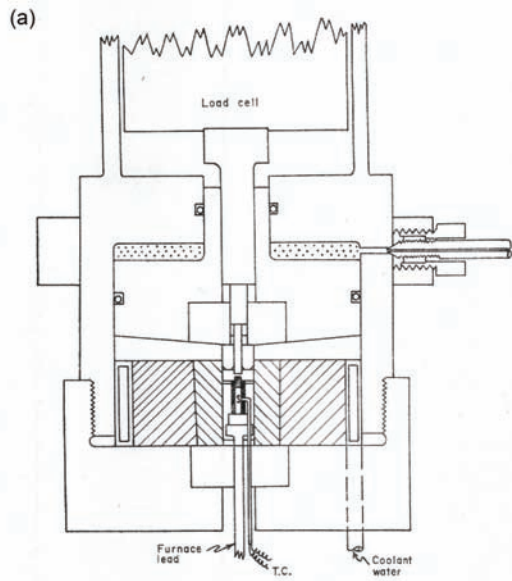


Fig. 6 (Karato-I)

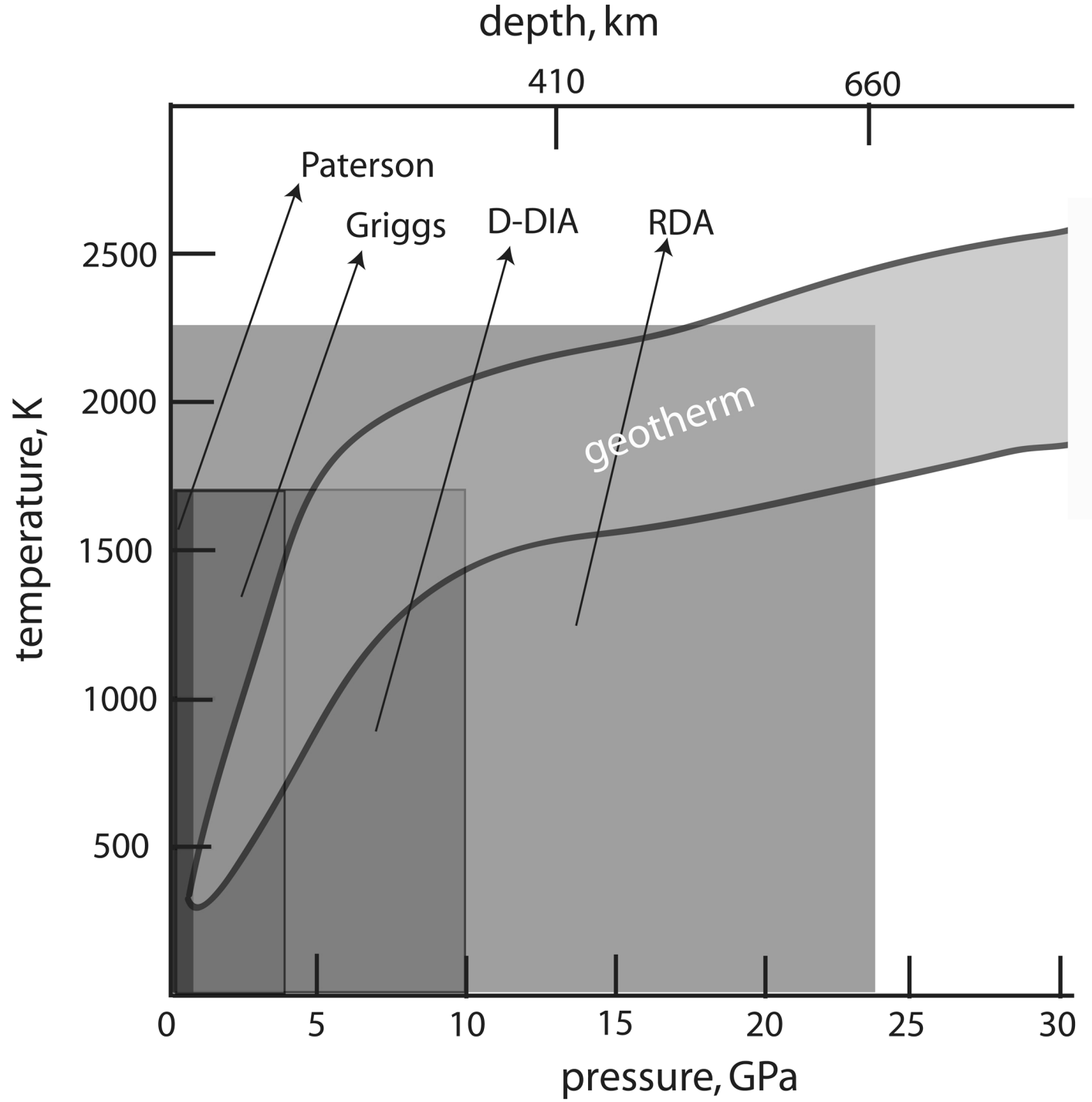
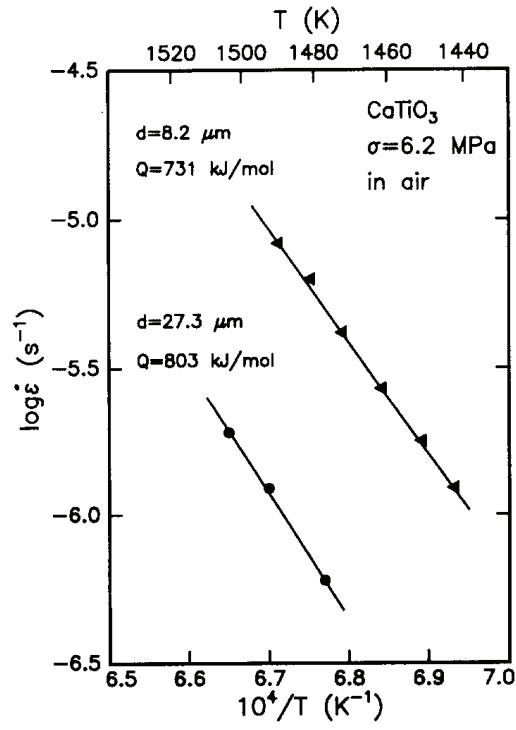


Fig.7 (Karato-I)

(a)



(b)

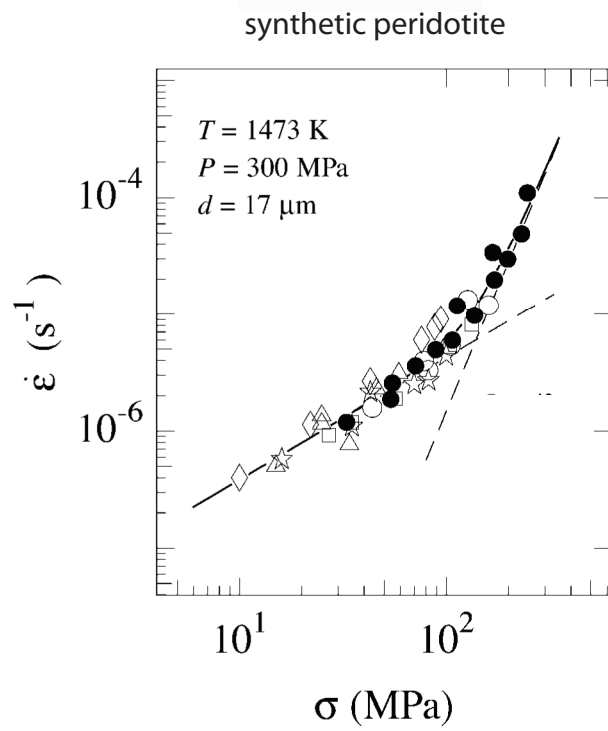
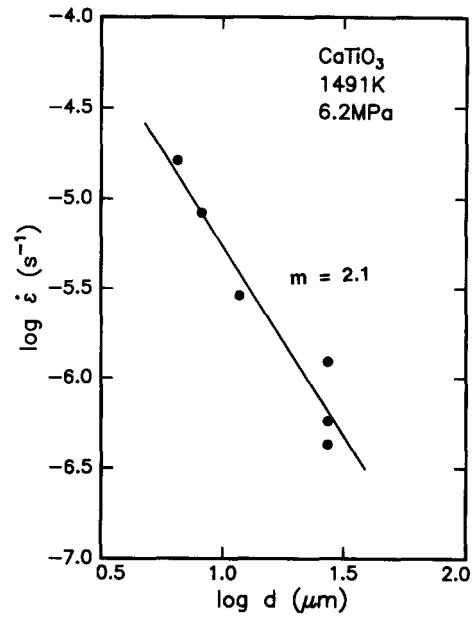


Fig. 8a, b (Karato-I)

(c)



(d)

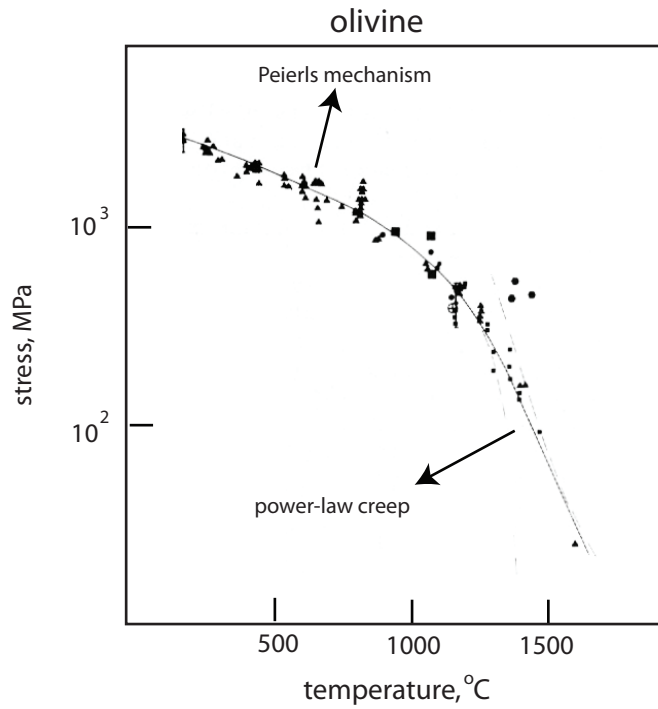


Fig. 8cd (Karato-I)

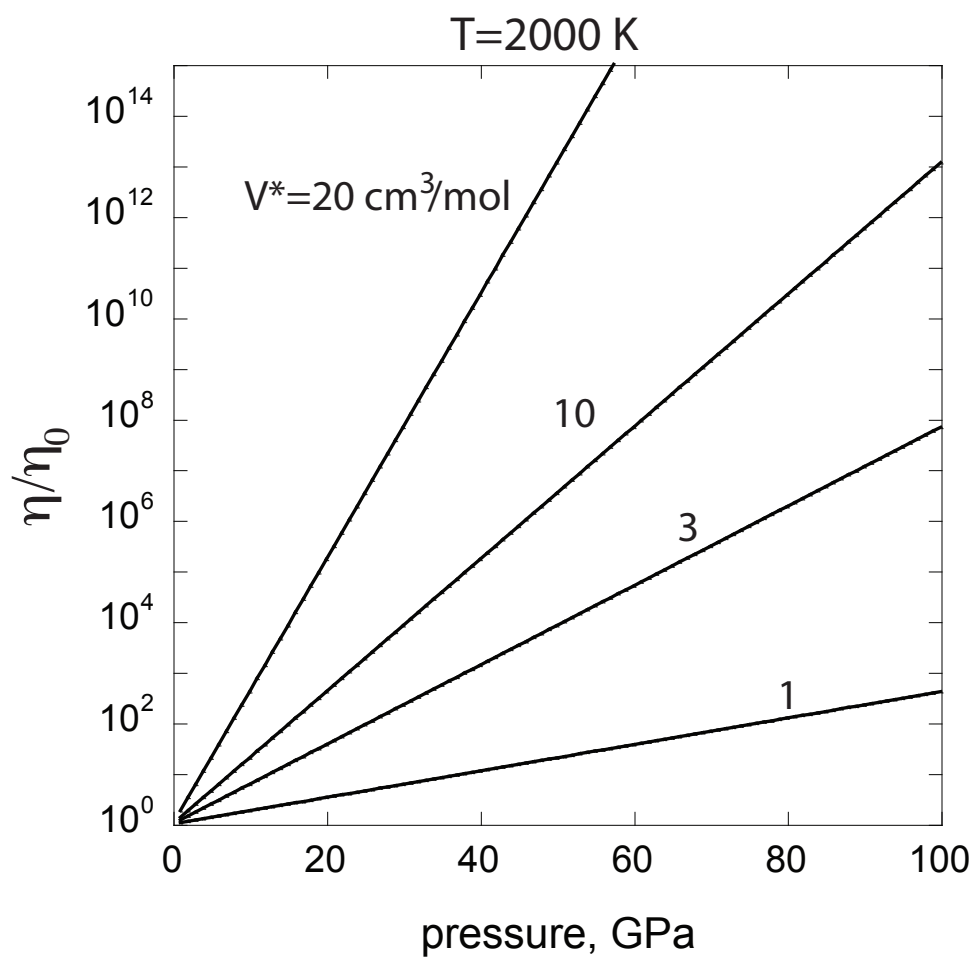


Fig. 9 (Karato-I)

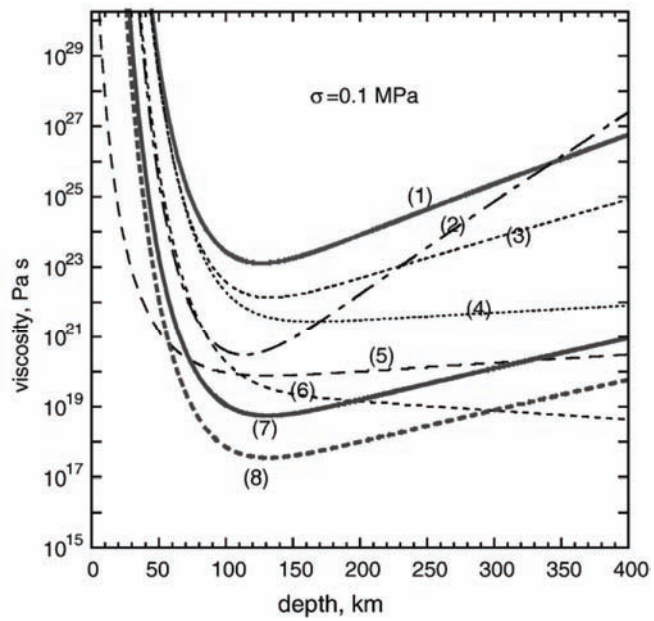


Fig. 10 (Karato-I)

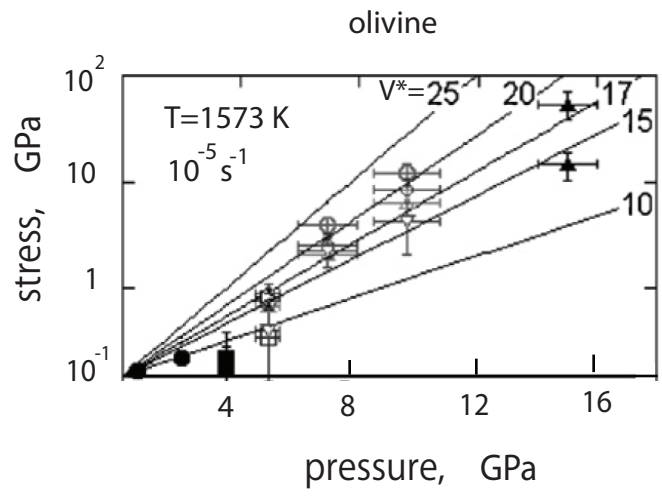
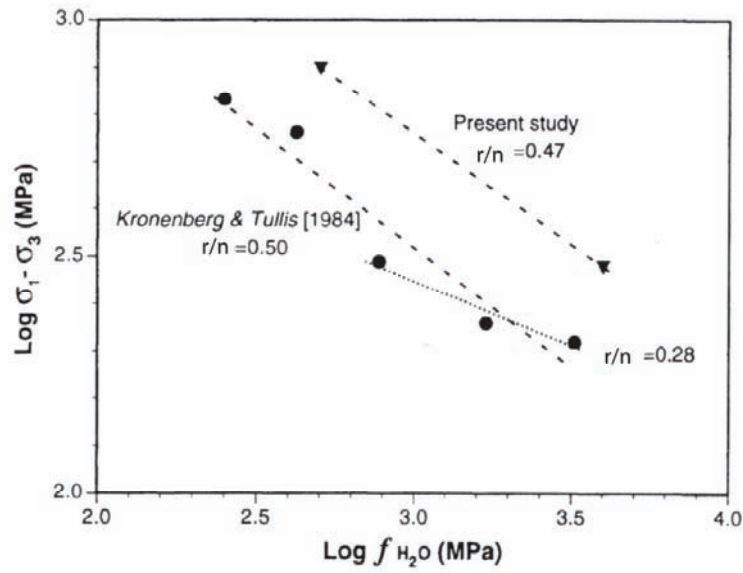


Fig. 11 (Karato-I)

(a)

quartz



(b)

olivine

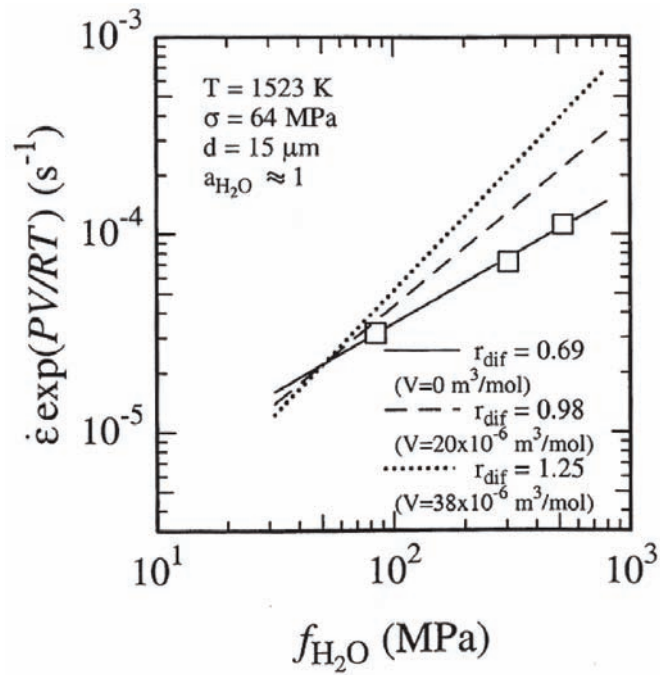


Fig. 12 (Karato-I)

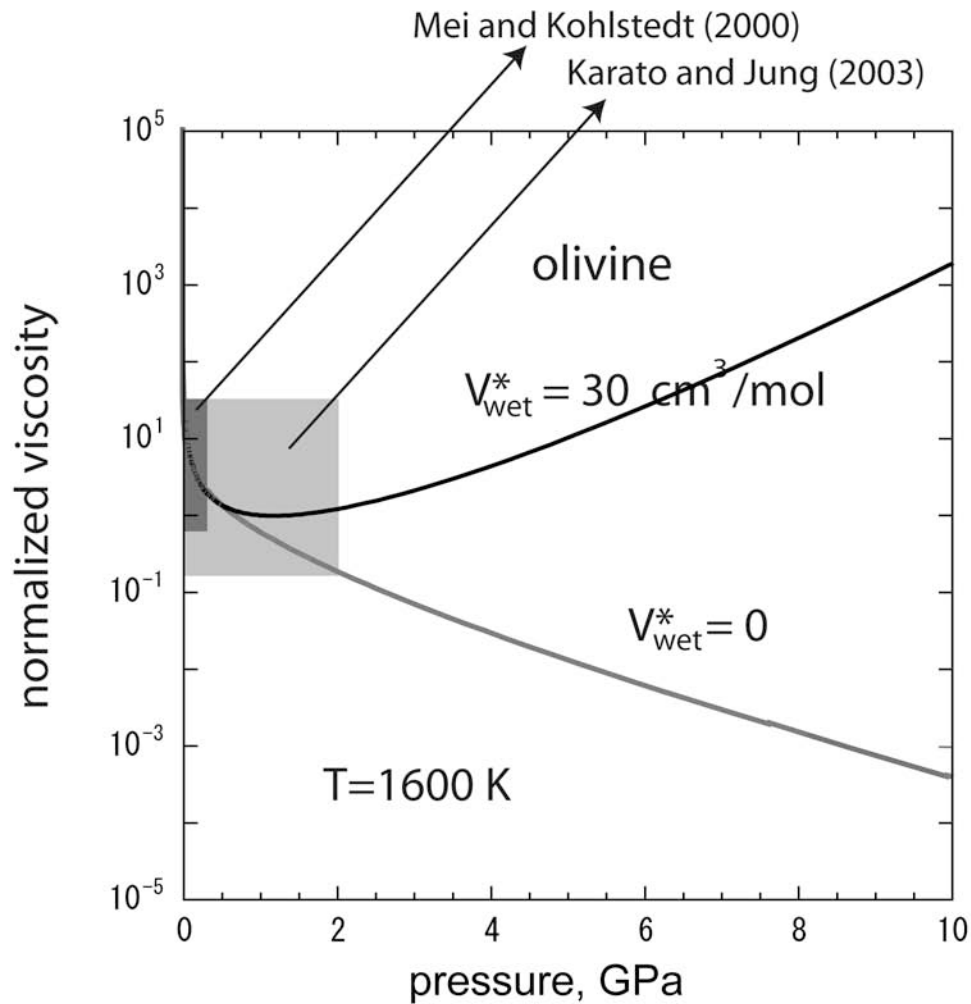


Fig. 13 (Karato-I)

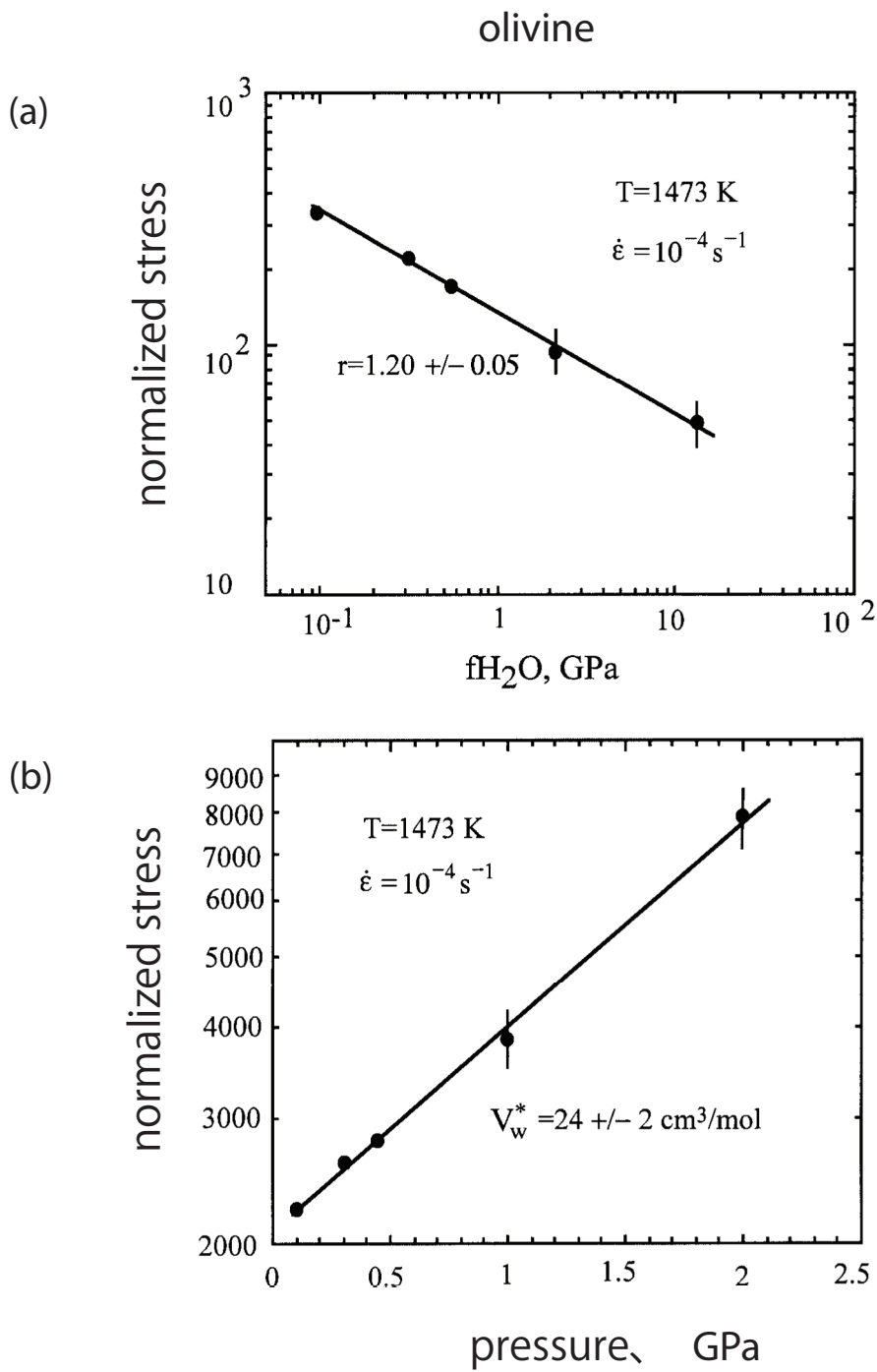
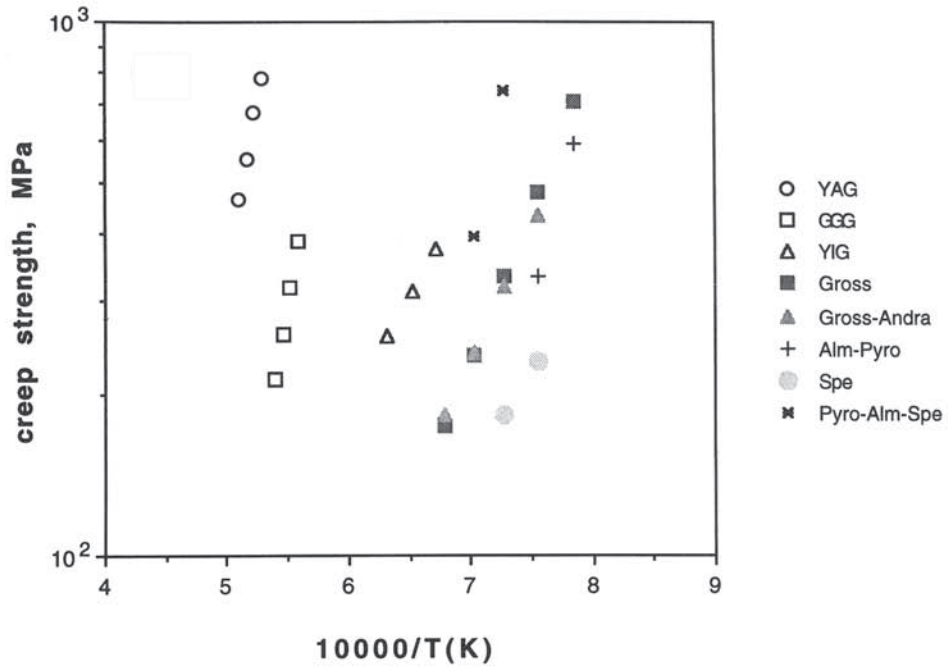


Fig. 14 (Karato-I)

garnet

(a)



(b)

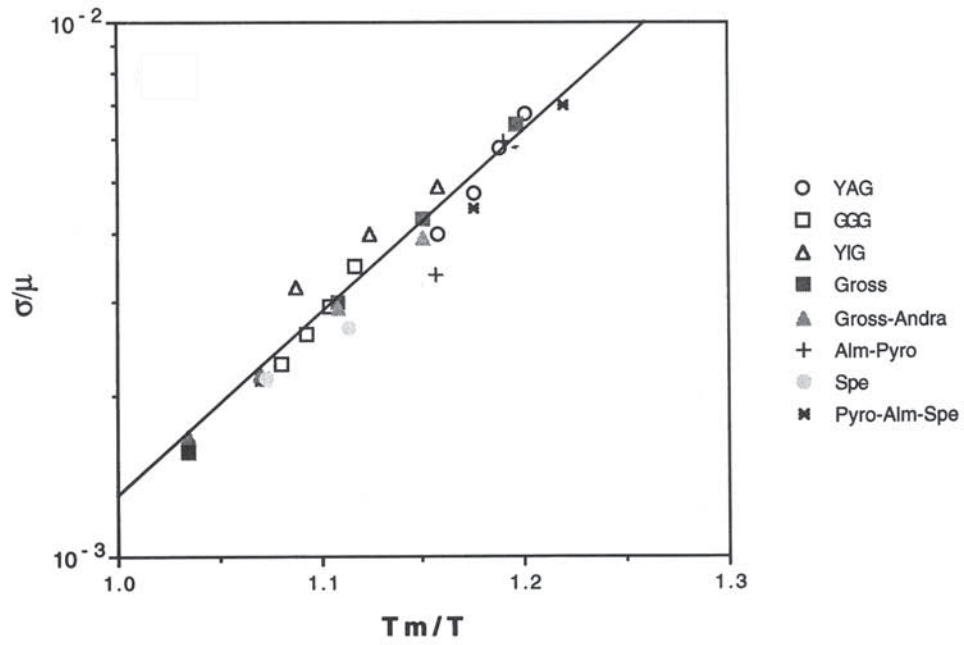


Fig. 15 (Karato-I)

(c)

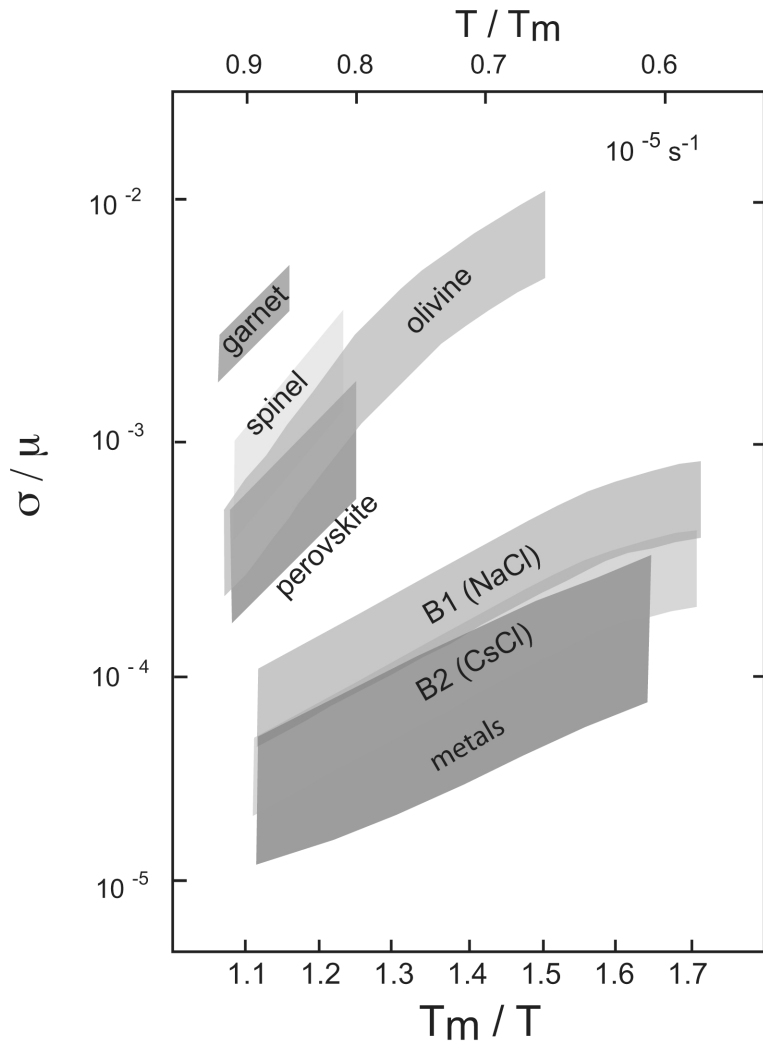


Fig. 15 (Karato)

olivine + basalt

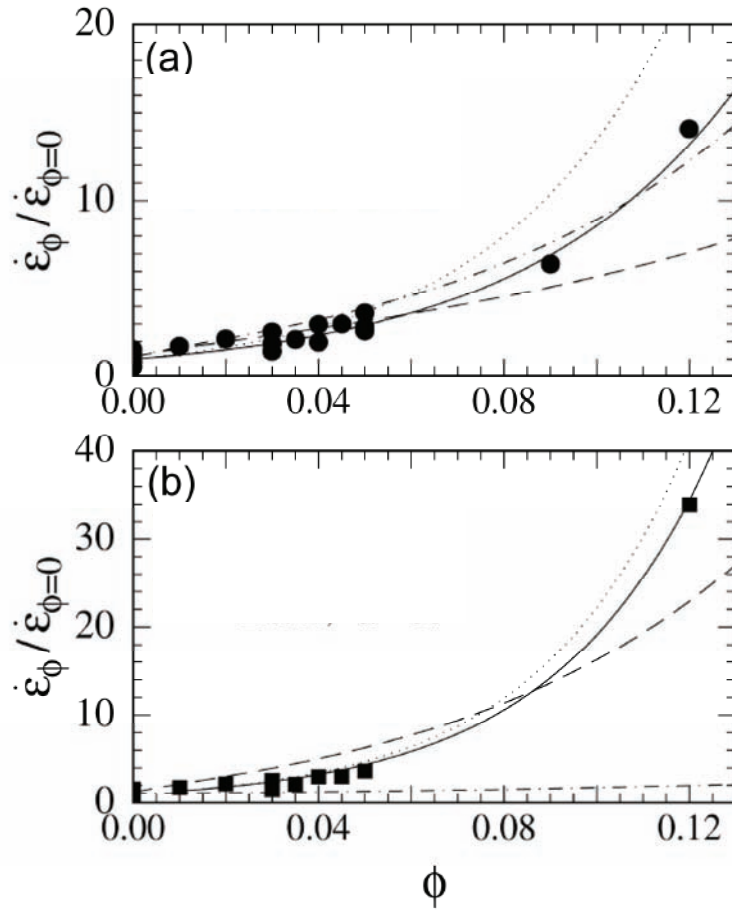
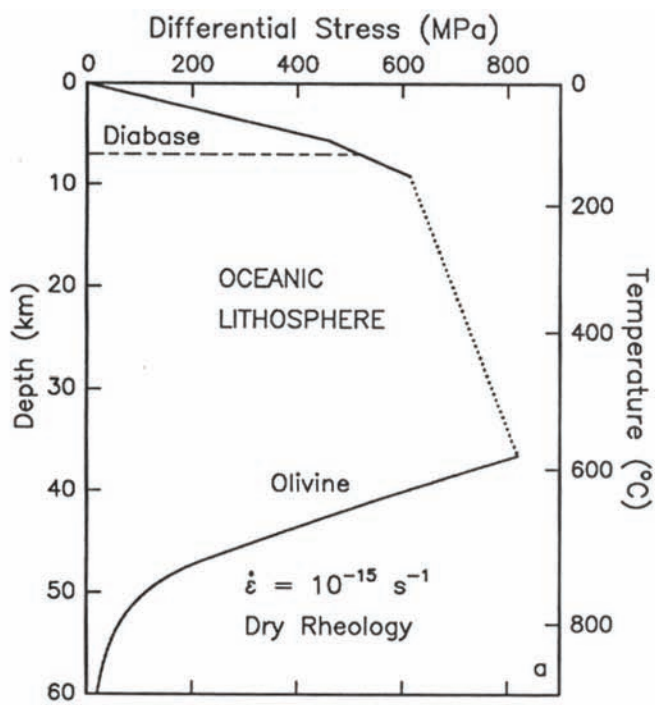


Fig. 16 (Karato-I)

(a)



(b)

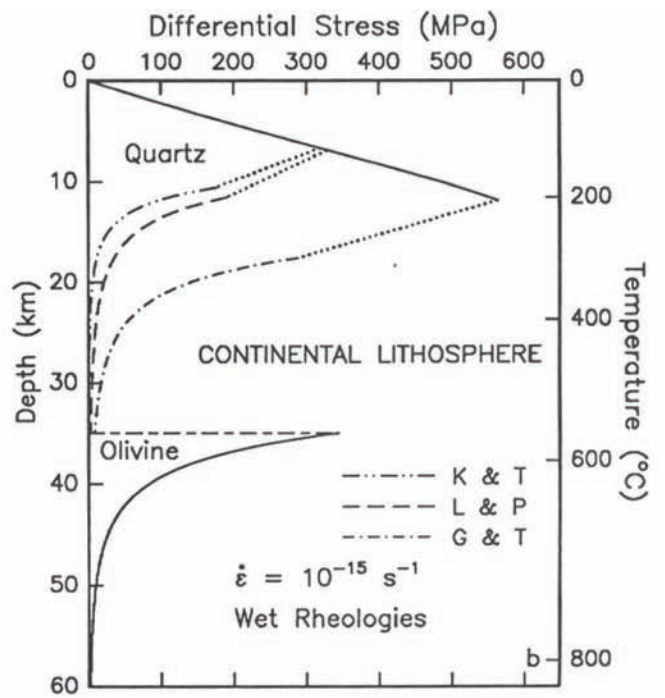


Fig. 17 (Karato-I)

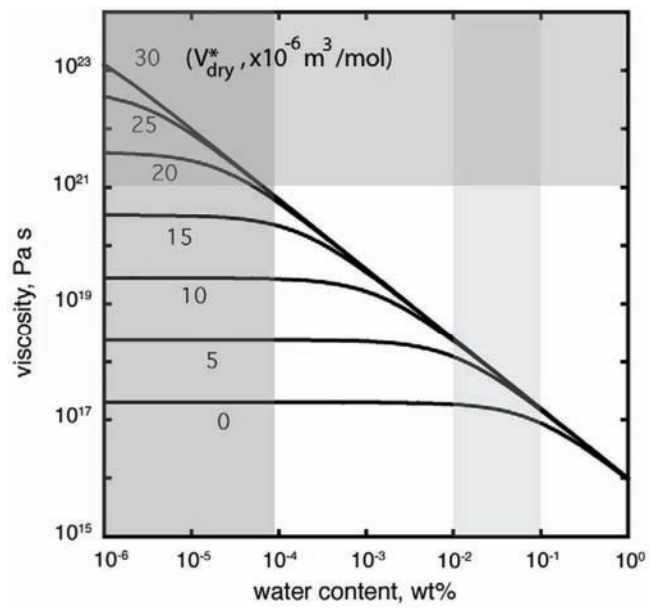


Fig. 18 (Karato-I)

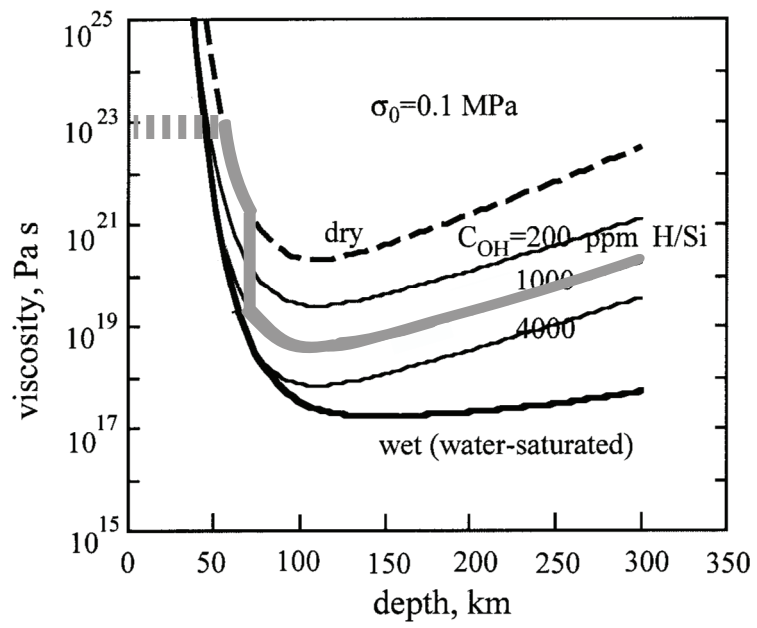


Fig. 19 (Karato-I)

ringwoodite

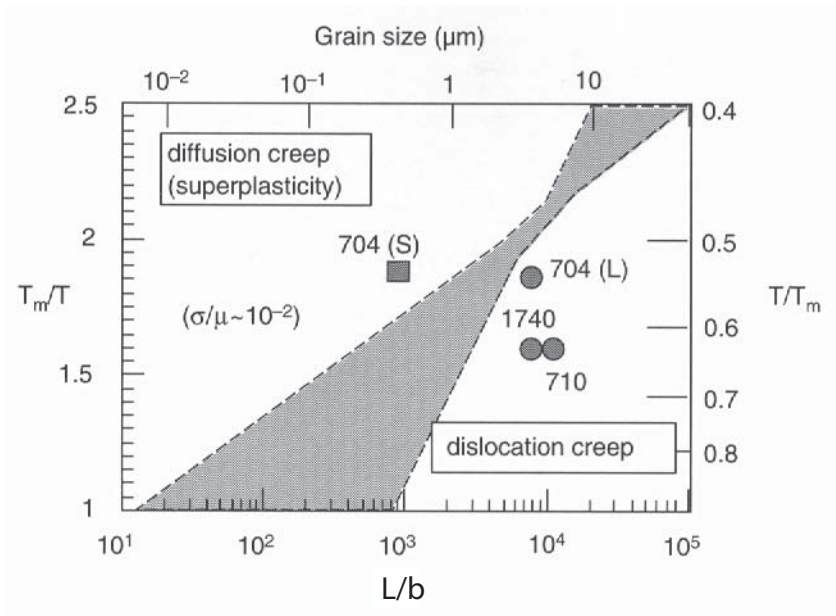


Fig. 20 (Karato

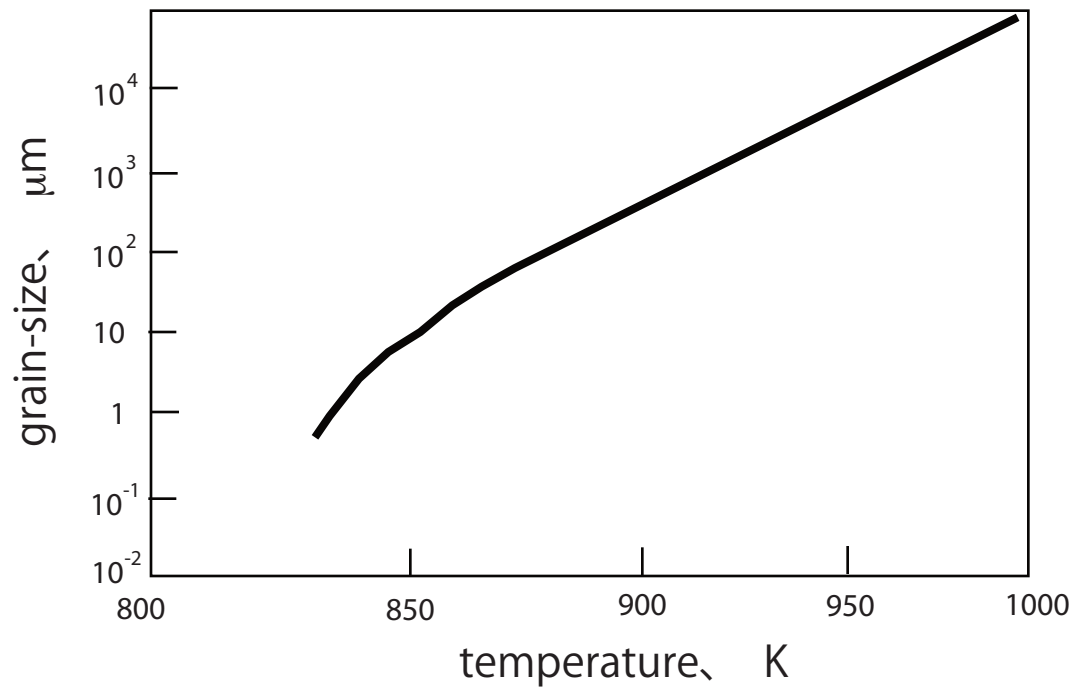
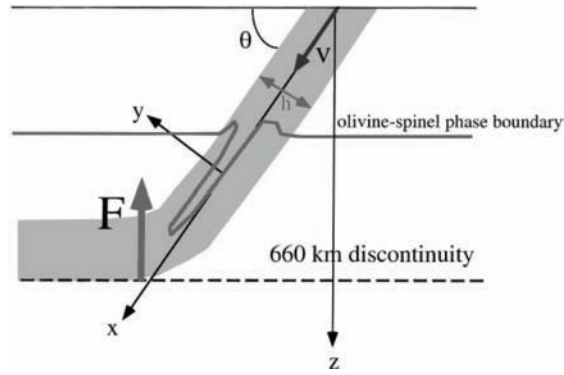
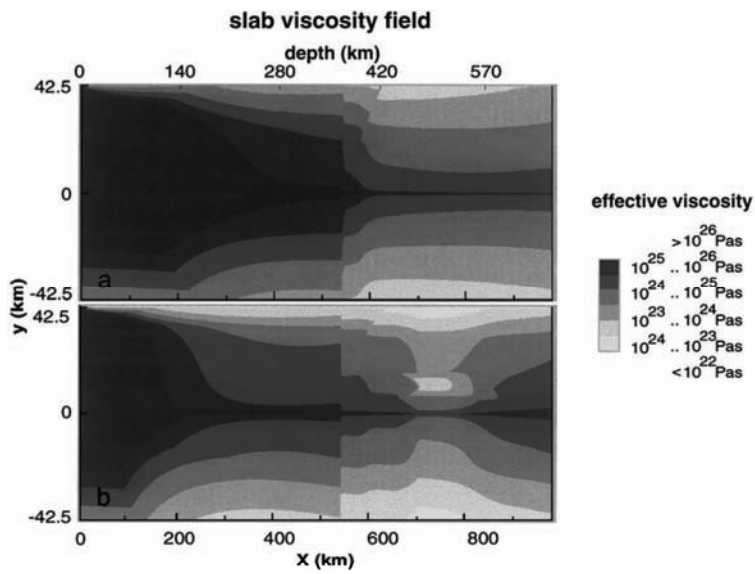


Fig. 21 (Katato-I)

(a)



(b)



(c)

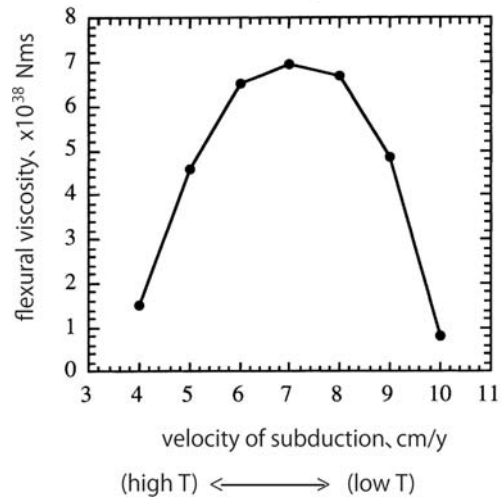


Fig. 22 (Karato-I)

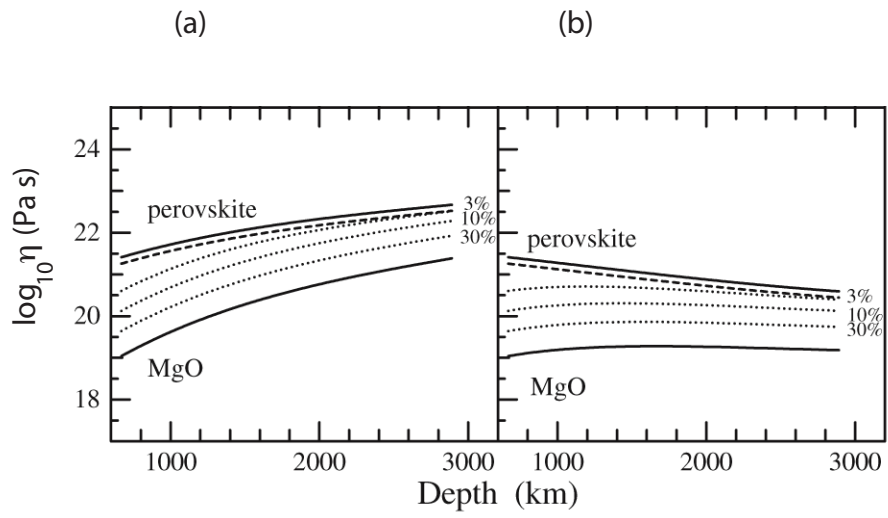


Fig. 23 (Karato-I)

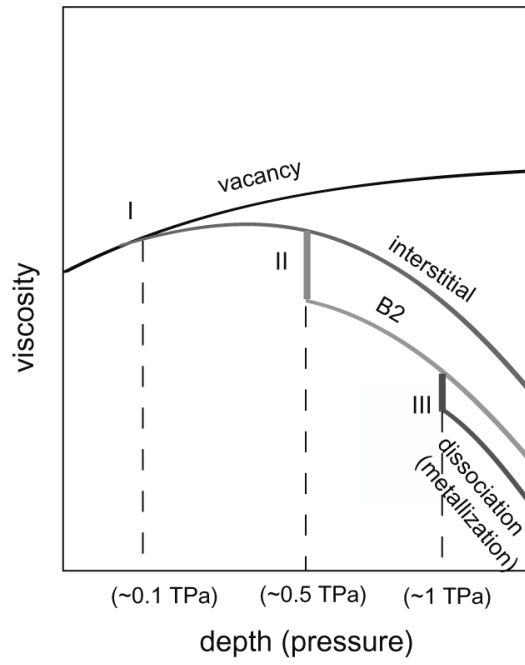


Fig. 24 (Karato-I)